ENGINEERING PROPERTIES OF TERNARY BLENDED GEOPOLYMER CONCRETE AND ROLE OF OXIDE COMPOSITION ON MORTAR

AFIA SHARMIN

FACULTY OF ENGINEERING
UNIVERSITY OF MALAYA
KUALA LUMPUR

2016

ENGINEERING PROPERTIES OF TERNARY BLENDED GEOPOLYMER CONCRETE AND ROLE OF OXIDE COMPOSITION ON MORTAR

AFIA SHARMIN

DISSERTATION SUBMITTED IN FULFILMENT OF THE REQUIREMENT FOR THE DEGREE OF MASTER OF ENGINEERING SCIENCE

FACULTY OF ENGINEERING
UNIVERSITY OF MALAYA
KUALA LUMPUR

2016

UNIVERSITY OF MALAYA

ORIGINAL LITERARY WORK DECLARATION

Name of the Candidate: **Afia Sharmin**

Registration /Metric No: **KGA130050**

Name of the degree: **Master of Engineering Science**

Title of Dissertation:

ENGINEERING PROPERTIES OF TERNARY BLENDED GEOPOLYMER CONCRETE AND ROLE OF OXIDE COMPOSITION ON MORTAR

Field of study: **Structural Engineering and Materials**

I do solemnly and sincerely declare that:

1. I am the sole author/writer of this work;
2. This work is original;
3. Any use of any work in which copy exists was done by way of fair dealing and for permitted purposes and any excerpt or extract from, or reference to or reproduction of any copyright work has been disclosed expressly and sufficiently and the title of the work and its authorship have been acknowledged;
4. I do not have any actual knowledge nor do I ought reasonably to know that the making of this work constitutes an infringement of any copyright work;
5. I hereby assign all and every rights in the copyright to this work to the University of Malaya (UM), who henceforth shall be owner of the copyright of this work and that any reproduction or use in any form or by any means whatsoever is prohibited without the written consent of UM having been first had and obtained;
6. I am fully aware that if in the course of making this work I have infringed any copyright whether intentionally or otherwise, I may be subject to legal action or any other action as may be determined by UM.

Candidate's Signature Date:

Subscribed and solemnly declared before,

Witness's Signature Date:

Name:

Designation:

ABSTRACT

The use of mineral admixtures has had positive effect in reducing carbon-di-oxide (CO_2) emission. However, the quantity of mineral admixtures being used in the cement or concrete production is small compared to the mineral admixtures or pozzolanic materials produced. Recent advances in concrete that include geopolymer concrete utilize more amount of mineral admixture. This has resulted in cement free concrete and effective use of more quantities of suitable mineral admixtures and pozzolanic materials. This research investigates the contribution of different oxides present in the rice husk ash (RHA), ground granulated blast furnace slag (GGBS) and metakaolin (MK) on the performance of geopolymer mortars.

Twenty-six mixes were designed with combined base materials and varied $NaOH_{aq}$ concentration used as one of the activators. RHA, GGBS and MK were varied between 15% and 70%, 0% and 75%, and 0% and 40%, respectively. The binder/fine aggregate, water/binder and alkaline activator/binder ratios were constant and the values were 0.5, 0.25 and 0.5 while all the samples were cured at 65^{o}C for 24 h. The mixture (ternary) that contained 25% RHA, 25% MK and 50% GGBS ($M_{25}R_{25}G_{50}$) gave the maximum compressive strength of 48 MPa, in addition to better flow rate and density than any binary combinations. Among the twenty six mixes, four mixes with $NaOH_{aq}$ concentration 14M were tested with scanning electron microscope (SEM) and energy dispersive X-ray spectroscopic analysis (EDS) and X-ray diffractometer to investigate the effect of oxide composition on mortar. The findings through microstructural and characterization tools show that regardless of the source, SiO_2 and CaO present in the base materials contributed to the strength, while Al_2O_3 influenced the amorphorsity of the products. The SiO_2 present in MK and GGBS were more reactive compared to the SiO_2 based RHA.

The use of oil palm shell (OPS) and palm oil clinker (POC) in construction material industry would enable the disposal of huge amount of wastes from palm oil industry and also reduce the negative effect of construction on the environment. Five concrete mixtures were prepared with POC as fine

aggregate with manufacture sand (M-sand) and rice husk ash (RHA), ground granulated blast furnace slag (GGBS), metakaolin (MK) as pozzolan or whole cement replacement materials. The mechanical properties of OPS light weight geopolymer concrete including compressive strength, flexural strength, ultrasonic pulse velocity and splitting tensile test were investigated and reported. OPS and granite (9 mm) were used in different percentages as coarse aggregates in five different mixes. As the volume of OPS increased, the resulting compressive strength decreased because the increase of OPS content reduced the density of concrete significantly due to more pores in this concrete. An increase in the replacement of OPS by granite led to an increase in UPV values. The test results showed that 20% OPS and 80% granite containing POC sand up to 50% with M-sand, a grade 35 OPS lightweight geopolymer concrete can be produced with 14% lighter than normal weight concrete.

The effect of micro-steel fiber on the fracture energy and toughness was also investigated; fracture test has been conducted on five mortar specimens prepared by using steel microfiber up to 3%, in addition to the control specimen. Fracture energy was increased up to 10 times due to the incorporation of microfiber at 3% compared to control specimen. In addition to the fracture energy, fracture toughness was also calculated using RILEM TC 50-FMC and it was found that the highest fracture toughness was achieved for the specimen with 1.5% steel microfiber.

ABSTRAK

Penggunaan bahan tambah mineral mempunyai kesan positif dalam mengurangkan karbon -di- oksida (CO_2). Walau bagaimanapun, kuantiti bahan tambah mineral digunakan dalam simen atau pengeluaran konkrit adalah kecil berbanding dengan bahan tambah mineral atau bahan pozzolanic dihasilkan. Kemajuan terkini dalam konkrit yang termasuk konkrit geopolimer menggunakan lebih banyak jumlah bahan tambah mineral. Ini telah menyebabkan simen penggunaan konkrit dan berkesan bebas lebih kuantiti bahan tambah mineral sesuai dan bahan-bahan pozzolanic. Kajian ini menyiasat sumbangan oksida yang berbeza di dalam abu sekam padi (RHA), tanah pasir sanga relau bagas (GGBS) dan metakaolin (MK) mengenai prestasi mortar geopolimer.

Dua puluh enam campuran telah direka dengan bahan-bahan asas gabungan dan NaOHaq kepekatan yang berbeza-beza digunakan sebagai salah satu daripada activators. RHA, GGBS dan MK telah berbeza di antara 15% dan 70%, 0% dan 75%, dan 0% dan 40% masing-masing. Pengikat / agregat halus, air / pengikat dan alkali pengaktif nisbah / pengikat tetap teguh dan nilai adalah 0.5, 0.25 dan 0.5 manakala semua sampel telah sembuh pada 65oC selama 24 jam. Campuran (pertigaan) yang mengandungi 25% RHA, 25% MK dan 50% GGBS (M25R25G50) memberikan kekuatan mampatan maksimum 48 MPa, sebagai tambahan kepada kadar aliran yang lebih baik dan kepadatan daripada mana-mana gabungan binari. Di antara dua puluh enam campuran, empat campuran dengan NaOHaq kepekatan 14M telah diuji dengan imbasan mikroskop elektron (SEM) dan tenaga serakan analisis X-ray spektroskopi (EDS) dan sinar-X diffractometer untuk mengkaji kesan komposisi oksida pada mortar. Hasil kajian melalui alat mikrostruktur dan pencirian menunjukkan bahawa tanpa mengira sumber, SiO_2 dan CaO yang terdapat di dalam bahan-bahan asas menyumbang kepada kekuatan, manakala Al_2O_3

mempengaruhi amorphorsity produk. The SiO_2 di dalam MK dan GGBS lebih reaktif berbanding dengan RHA SiO_2 berasaskan.

Penggunaan tempurung kelapa sawit (OPS) dan klinker minyak sawit (POC) dalam pembinaan industri bahan akan membolehkan penjualan sejumlah besar sisa daripada industri minyak sawit dan juga mengurangkan kesan negatif pembinaan terhadap alam sekitar. Lima campuran konkrit telah disediakan dengan POC agregat sebagai denda dengan pasir pembuatan (M-pasir) dan abu sekam padi (RHA), tanah pasir sanga relau bagas (GGBS), metakaolin (MK) sebagai pozolan atau keseluruhan bahan pengganti simen. Sifat-sifat mekanik OPS menyalakan berat konkrit geopolimer termasuk kekuatan mampatan, kekuatan lenturan, halaju denyut ultrasonik dan membelah ujian tegangan telah disiasat dan dilaporkan. OPS dan granit (9 mm) telah digunakan dalam peratusan yang berbeza sebagai agregat kasar dalam lima campuran yang berbeza. Sebagai jumlah OPS meningkat, kekuatan mampatan yang dihasilkan menurun kerana peningkatan kandungan OPS mengurangkan ketumpatan konkrit dengan tinggi kerana lebih liang dalam konkrit ini. Peningkatan dalam penggantian OPS oleh granit membawa kepada peningkatan dalam nilai-nilai UPV. Keputusan ujian menunjukkan bahawa 20% OPS dan 80% granit yang mengandungi pasir POC sehingga 50% dengan M-pasir, gred 35 OPS geopolimer konkrit ringan boleh dihasilkan dengan 14% lebih ringan daripada konkrit berat badan normal.

Kesan daripada serat mikro keluli pada tenaga patah dan keliatan juga disiasat; ujian patah telah dijalankan ke atas lima spesimen mortar disediakan dengan menggunakan microfiber keluli sehingga 3 %, sebagai tambahan kepada spesimen kawalan. Tenaga patah telah meningkat sehingga 10 kali kerana penubuhan microfiber pada 3% berbanding spesimen kawalan. Selain tenaga patah, patah juga dikira menggunakan

RILEM TC 50- FMC dan didapati bahawa patah tertinggi dicapai bagi spesimen dengan 1.5 % keluli microfiber.

ACKNOWLEDGEMENTS

I would like to thank Almighty Allah (SWT) for providing me the opportunity to pursue my studies as well as instilling the patience and persistence during my research work.

I would like to express my sincere thanks and deep appreciation to my supervisor, Dr. Ubagaram Johnson Alengaram for his guidance, encouragement and valuable time spent on the fruitful discussion throughout the work, which was extremely valuable in conducting this research work.

I would also like to express my gratefulness to my co-supervisor Prof. Ir. Dr. Mohd Zamin Bin Jumaat for his treasured and relevant advice throughout the study.

I would like to acknowledge the grant HIR (UM.C/625/1/HIR/206) provided by the University of Malaya to fulfil the study as well as the research works.

Finally, I would like to thanks my family members who always support me in my life.

TABLE OF CONTENTS

LIST OF FIGURES

LIST OF TABLES

LIST OF SYMBOLS AND ABBREVIATIONS

Symbols **Descriptions**

f_c'	compressive strength
f_r'	flexural strength
E	modulus of elasticity (Young's modulus)
Ø	diameter
P	Maximum applied load indicated by the testing machine

Abbreviations	**Descriptions**
GGBS	ground granulated blast furnace slag
MK	metakaolin
POFA	palm oil fuel ash
RHA	rice husk ash
LWC	lightweight concrete
LWA	lightweight aggregate
OPS	oil palm shell
MS	manufactured sand (MS)
ODD	oven-dry density
MOE	modulus of elasticity

CSH	calcium-silicate-hydrates
NaOH	sodium hydroxide
OPC	ordinary Portland cement
SSD	saturated surface dry
XRF	X-ray fluorescence
Al	aluminium
Al_2O_3	aluminium oxide (Alumina)
Ca	calcium
CaO	calcium oxide
$Ca(OH)_2$	calcium hydroxide
CO_2	carbon dioxide
Fe_2O_3	ferric oxide
H_2O	water
KOH	potassium hydroxide
K_2O	potassium oxide
LOI	loss on ignition
Na	sodium

Na_2SiO_3	sodium silicate
Si	silicon
SiO_2	silica or quartz
SO_3	sulphuric anhydride

CHAPTER 1: INTRODUCTION

1.1 Background

Greenhouse gas emission is an environmental concern for current world. Cement production is an energy-intensive process and each tonne of portland cement produced releases approximately 1 tonne of CO_2 (Rehan & Nehdi, 2005). During the manufacture of cement, fossil fuels are burnt and limestone is de-carbonized and most CO_2 is emitted from this source. Therefore, the use of alternative base materials instead of cement needs to focus and the cement industry is now under monitoring for dropping its greenhouse gas emissions.

International efforts on the reduction of greenhouse gas emissions started at the United Nations (UN) Conference on the Human Environment in 1972 and touched an important landmark with the adoption of the Kyoto Protocol in 1997. According to the Kyoto Protocol, technologically advanced nations made binding commitments to reduce their greenhouse gas emissions by 5.2% below 1990 levels around year 2008–2012 (Rehan & Nehdi, 2005).

The environmental effect of the production of concrete, is of significant importance due to ecological imbalance it caused. Concrete contribute to surface runoff by making rigid surfaces that may be the reason for flooding and water pollution. Conversely, the means of flood control such as damming, diversion, and deflection of flood waters is made from concrete. In spite of the harmful impact of concrete, its benefits have made it compulsory for our life. The harmful constituent material of concrete has been identified and planned to be replaced by other material possessing similar characteristics. The base material of concrete production is cement, which has its own environmental and social impact.

50% of all emissions from cement production (Damtoft, Lukasik, Herfort, Sorrentino, & Gartner, 2008) is caused by the direct emission of cement through a chemical process

called calcination. Calcination occurs when limestone ($CaCO_3$) is heated, breaking down into calcium oxide and CO_2. 40% of cement emissions (Damtoft et al., 2008) is caused by indirect emissions of burning fossil fuels to heat the kiln. Kilns are usually heated by coal, in producing electricity. Electricity is inevitable to power plant and machinery and rest of the emission by cement comes from this. Final transportation of cement also creates emissions (Damtoft et al., 2008).

The use of base materials which do not contain limestone can reduce the CO_2 emissions from cement. Blended cement with fly ash and blast furnace slag can be a better alternative of limestone-based clinker. 20% of CO_2 emissions could be reduced by blended cement, but there are some limitations of using blended cement such as substitutes of cement containing toxic heavy metals, lack of sufficient amount of substitute materials and longer setting time of blended cement (Rehan & Nehdi, 2005). The share of CaO in clinker amounts varies from 64%–67%. The remainder consists of silicon oxides, iron oxides, and aluminium oxides.

The utilization of industrial by-products such as rice husk ash (RHA), Metakaolin (MK) and ground granulated blast furnace slag (GGBS) as the cement replacement or as the additional cementitious materials has had a beneficial effect in reducing greenhouse gas emissions. An ideal solution possessing an environmentally friendly concrete could be achieved through the use of industrial waste materials.

Industrial waste materials can also be used as fine and coarse aggregates. There is a danger of depletion of natural aggregates for which alternative options are being researched to utilize industrial by-products. Natural sand assets are not sufficient and the extraction of natural sand is an expensive action due to metropolitan growth, local laws and environmental limitations. In many regions of the world, the extraction of sand is severely taxed or completely forbidden to try to preserve residual deposits. Use of crushed granite aggregates increases dead load of

the whole structure. Thus, the research focus is on to investigate the means of reducing dead load of structure using comparatively lightweight aggregate instead of crushed granite.

1.2 Geopolymers

Geopolymers are new materials for being used as bonding agent, new binders for fibre reinforced complexes and new cementing material for concrete. The geopolymer technology proposed by (Davidovit, 2002), has proved itself as a workable alternative binder to the Portland cement through its application in concrete industry. Regarding environmental issue the geopolymer technology could lessen the CO_2 emission to the air produced by cement industries. The wide variety of geopolymer concrete's potential applications includes: materials for safe casting of corrosive liquid blends, geopolymer mold and tooling in fighter plane, heat resistant, fire proof, storage of toxic and radioactive wastes, utilization in art and decoration, repairing corroded steel reinforced building with fiber reinforced geopolymer composites, bio-technologies (materials for medicinal applications) (Davidovits, 2005).

1.3 Local waste materials to produce geopolymer concrete

1.3.1 Industrial by-products as binders

Rice Husk Ash (RHA) is an agricultural waste product, and as a waste product, disposal of it is a concern for waste managers. As concrete is the most widely used building material and among all constituent materials of concrete, binder or cement is the most expensive part. If this part of cement can be fully or partially replaced by locally available waste material like RHA, it will help to reduce cost of construction. Here, environmental issues are also very important because RHA from the parboiling plants is posing serious environmental threat. Moreover, RHA possesses about 85% to 90% silica content which makes it very essential for producing geopolymer concrete. Naturally, RHA has fine particles and in the presence of moisture

chemically react with calcium hydroxide at ordinary temperatures to form compounds possessing cementite's properties. Many researchers ((Abu Bakar, Putrajaya, & Abdulaziz, 2010; Coutinho, 2003; Mahmud, Malik, Kahar, Zain, & Raman, 2009)) have already proved its properties of high workability and long term durability in the concrete. Rice husk is burnt for electricity generation and produces large amount of agricultural wastes known as RHA. Physical and chemical properties of RHA make its disposal unhealthy and harmful for the environment (Asavapisit & Ruengrit, 2005; Basha, Hashim, Mahmud, & Muntohar, 2005). Therefore, a new invention is compulsory to make the best use of RHA which will ensure green environment and low cost construction.

Kaolin, after suitable treatment, is the main source of Metakaolin (MK). Kaolin consists of alternate layers of silica and alumina in tetrahedral and octahedral coordination, respectively. Possessing of this electrically neutral crystalline structure is a common characteristic of clay minerals. The primary constituent of kaolin (40–70%) is hydrated aluminium disilicate, $Al_2SiO_5(OH)_4$. The structure of kaolin breaks down at temperature of 650–900°C and puckers the long chain of alumina and silica layers. MK is the result of dehydroxylation and disorder of kaoline which is suitable for use in cementing applications because of its (Yao, Zhang, Zhu, & Chen, 2009) properties of amorphorsity, pozzolanic and latent hydraulic reactivity.

Ground Granulated Blast Furnace Slag (GGBS) is a by-product of steel manufacturing process. It has already been used as sustainable construction material in construction industry all over the world since the mid 1800s. GGBS cement was discovered by Emil Langin after thirty-eight years of the invention of Portland Cement. Since then, many blast furnaces and steel industries of Europe has used GGBS widely in all aspects of structures. About 17.7 million tonnes of GGBS are now being used annually in Europe. GGBS cement concrete can produce higher strength than Portland cement concrete because GGBS based concrete produces a higher

amount of chemical compound calcium silicate hydrates (CSH) than Portland cement concrete and reduces the production of free lime, which produces CO_2.

1.3.2 Fine aggregates

Malaysia consumed 2.76 billion metric tonnes of natural aggregate (gravel and sand) worth USD14.4 billion in 2010 of which half of the total consumption was used in government funded projects (Ashraf, Maah, Yusoff, Wajid, & Mahmood, 2011). The more the particle size of sand will be finer, the less will be the voids in it. As cement has tendency to clog in the voids of sand particles, the requirement of cement or binder will be less for the finer particles of sand. For this reason, natural sand should be replaced by manufactured sand (M-sand), which is a derivative of quarry dust attained by centrifuging it using equipment known as the Vertical Shaft Impact (VSI). The shape and texture of M-sand provides improved strength due to the good interlocking between particles (Donza, Cabrera, & Irassar, 2002).

1.3.3 Oil palm shell as coarse aggregate

The aim behind the replacement of conventional crushed granite is to use low cost material like industrial by-product and to reduce the dead load of structure. All parameters of the materials such as specific gravity, water absorption, aggregate impact and aggregate crushing value have been tested so that granite replacement by industrial waste doesn't deteriorate the quality of structure. Serviceability, strength and durability of the members have also been examined. The wastes produced from the palm oil factories include empty fruit bunches (EFB), oil palm shells (OPS), palm oil clinker (POC) and palm oil fuel ash (POFA). OPS and POC have been used as coarse aggregates in the development of lightweight concrete. (Kupaei, Alengaram, & Jumaat, 2014; Kupaei, Alengaram, Jumaat, & Nikraz, 2013; Liu, Chua, Alengaram, & Jumaat, 2014) have produced OPS based lightweight concrete.

OPS is sustainable and firm and it does not convert to toxic substances after being bound in concrete. The density of OPS concrete is around 25% lower than normal weight concrete and it could be used to develop lightweight concrete.

1.4 Problem statement

The use of industrial by-products such as fly ash (FA), silica fume, ground granulated blast furnace slag (GGBS), and rice husk ash, as the cement replacement or as the additional cementitious materials has had a productive consequence in reducing greenhouse gas emissions. Throughout the world, much research is being conducted on the use of industrial by-products. The disposal of waste is the main problem faced by the industries.

Thus, landfill can be affected by toxic metals which cause ground water contamination. On the other hand, Malaysia is currently producing more than half of the world's total output of palm oil and palm oil fuel ash is commonly known as POFA. Another waste material produced from the palm oil industry, OPS, that could be an alternative to the conventional coarse aggregate other than landfilling and can reduce the cost of construction. Hence, this research has evaluated the performance of these waste materials to produce structural grade concrete.

1.5 Research Objectives

1. To develop appropriate mixture design for geopolymer mortar using ground granulated blastfurnace slag (GGBS), rice husk ash (RHA) and Metakaolin (MK) as ternary binder.

2. To investigate the microstructure of ternary blended geopolymer mortar and to synthesis its contribution on the development of geopolymer mortar.

3. To identify the role of oxide composition on the performance of ternary blended geopolymer mortar.

4. To calculate the fracture energy of the steel micro-fibre reinforced geopolymer mortar.

5. To study the effect of crushed oil palm shell (OPS) and conventional crushed granite as coarse aggregates and two types of sand as replacement for conventional sand (M-sand and POC-sand) on the mechanical properties of structural grade ternary blended geopolymer concrete.

1.6 Scope of research work

The scope of the research is based on the objectives set above and the details are given below:

- Test on binder:

The chemical and physical properties (particle size distribution) tests for RHA, GGBS and MK were conducted using X-Ray Fluorescence (XRF) and particle size analyser, respectively. Preparation and tests on mortar

A total of twenty mixes were performed for RHA-GGBS-MK based ternary mortar to obtain the optimum mix proportion. The local waste material and industrial by-products were used as binders. Manufactured sand (M-Sand) was used instead of conventional mining sand. Sodium hydroxide (NaOH) and Sodium Silicate (Na_2SiO_3) were used as alkaline activator for geopolymerization. Molarity of NaOH for these twenty mixes was 14M. Additional six mortar mixes were prepared with 12 M NaOH choosing six mix proportion from above mentioned twenty mixes.

- Micro-structural investigation on mortar

Microstructural analysis such as scanning electron microscopy coupled with energy dispersive X-ray spectroscopic analysis (SEM + EDS), and X-ray diffractometer tests have been done on four selected mortar mixes among twenty mortar mixes.

- Mortar specimens for fracture test

Another five mortar mixes have been prepared using the following:

- Binder/MS ratio: 1:2
- Four mixes with different percentages of fiber with respect to binder volume
- A control mix of without fibre
- Prisms of 50×50×250 mm^3 were prepared for fracture test

- Preparation and tests on concrete:

After obtaining the optimum mix from the mortar, concrete specimens were prepared using two types of fine and coarse aggregates. Six series of concrete mixes using the variables were prepared using the optimum mix proportion of RHA, MK and GGBS for binder contents.

The variables investigated include types of fine and coarse aggregates. –

Fine aggregate:

a) manufactured sand (M-Sand)

b) palm oil clinker sand (POC-sand) and

coarse aggregate – (i) crushed OPS and (ii) crushed Granite.

Table 1.1: Summary of mortar and concrete mixes

No. of mixes	Variables	Non-variables
Step 1: 26 mixes (mortar)	i) Contents of RHA,GGBS, and MK, ii) Molarity	Content of M-sand
Step 2: 6 mixes (concrete)	i) Fine aggregate contents: M-sand and POC-sand, ii) Coarse aggregate contents: Crushed OPS and crushed Granite	Contents of RHA,GGBS,and MK
Step 3: 5 mixes (mortar)	5 different weight ratios of micro steel fibers	Contents of RHA,GGBS,MK and M-sand

- Tests included:

- Flow test of fresh mortar, oven dry density (ODD) and compressive strength of mortar cube

- Scanning electron microscopy coupled with energy dispersive X-ray spectroscopic analysis (SEM + EDS), and X-ray diffractometer test.

- Mechanical properties of concrete– cube compressive strength, splitting tensile strength, flexural strength, Young's modulus.

- Fracture test for mortar prism using Three Point Bending test.

1.7 Structure of the dissertation

Chapter 1 provides a brief background and description of geopolymer concrete, the problem statement, and objectives of present study and scope of work.

Chapter 2 presents literature review on geopolymer, three binder materials, microstructural analysis of mortar, lightweight concrete (LWC), oil palm shell concrete (OPSC), fibre reinforced concrete (FRC), their mechanical properties and fracture energy of geopolymer

mortar. Materials used in this research such as RHA, GGBS, MK, M-Sand, POC sand, OPS, crushed granite and micro steel fibre are discussed.

Chapter 3 describes the physical and chemical properties of materials, preparation of specimen and test procedures done for the proper investigation of research. This chapter also represents the exact guidelines of research work done in laboratory and the details of mixture proportions and all other experimental parameters used to fulfil the objectives of the research.

Chapter 4 reports the results found from the tests and justification on the reasons of the results. It also discusses on the performance of the materials for achieving the research objectives.

Chapter 5 outlines the conclusions and recommendations for future works.

CHAPTER 2: LITERATURE REVIEW

2.1 General

This chapter represents the previous experiments and researches done by other researchers in the related field. A detailed review of past research articles on the mechanism of geopolymer matrix, a brief description of industrial by-product and alkali activators and microstructural investigation of mortar has been done and reported. Further, the development of geopolymer concrete along with compressive strength development and, binding materials and lightweight aggregate for geopolymer concrete, fracture properties and use of steel microfiber in mortar have been represented.

2.2 The necessity of using industrial by-product as binders

The cement industry is one of the major polluters as it contributes 5% of the total carbon dioxide (CO_2) worldwide; 50% of the emissions are from the chemical process, 40% from burning fuel and 5–10% from the industry's emissions (Klee & Coles, 2004). The production of one ton of concrete creates about 410 kg/m^3 CO_2; this could be reduced to 290 kg/m^3 with 30% fly ash as a cement replacement (Dhir & Jappy, 1999). The constructive solution in minimizing greenhouse gas emissions can be the utilization of industrial by-products, such as fly ash (FA), silica fume (SF), GGBS, palm oil fuel ash (POFA), MK and RHA as the cement replacement materials. The use of these waste materials as a cement replacement could also help reduce the problem concerning the storage and disposal of these wastes. In recent years, increasing consciousness concerning the amount and variety of hazardous solid waste generation and its influence on human health has forced many researchers to consider the potential use of such waste in the production of construction materials. One of the significant achievements is the development of geopolymer concrete using waste materials, such as FA, GGBS, RHA, MK and POFA, as binder materials.

2.3 Formation of the geopolymer matrix

RHA, MK, POFA and GGBS contain a large amount of alumina and silica and so they can be used as mineral admixtures in the development of geopolymer concrete. Caustic alkalis or alkaline salts are normally used as alkaline activators in alkali activated cement and concrete. A three-dimensional network of Si–O–Al–O bonds is formed when various alumina and silica containing materials react under highly alkaline conditions, which is called a geopolymer (Davidovits, 1991). The mechanism for geopolymerization is very complex. Figure 2.1 shows Poly(sialate) structures according to (Davidovits (2005)).

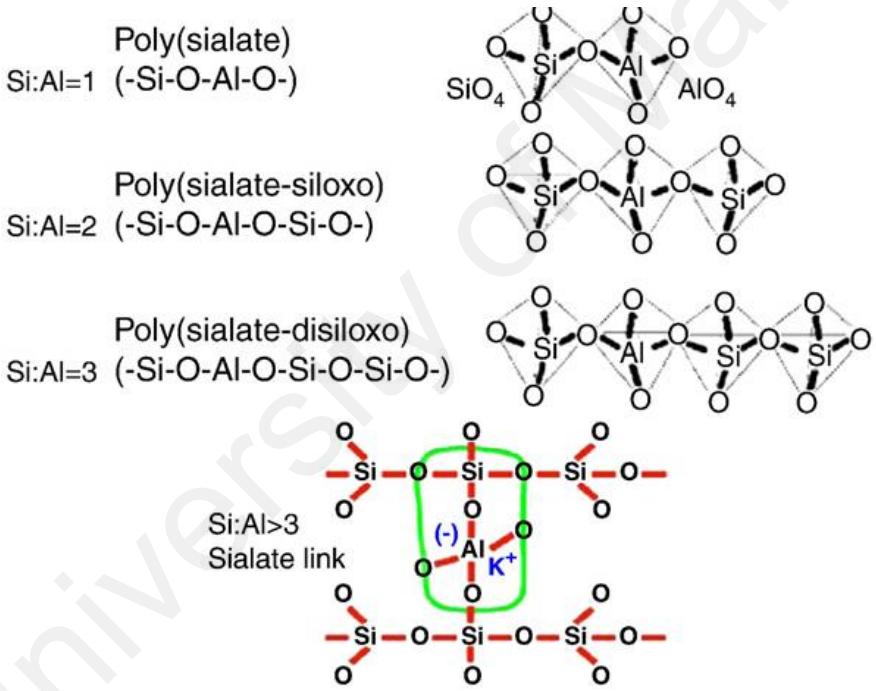

Figure 2.1: Poly(sialate) structures according to (Davidovits (2005))

2.4 Rice Husk Ash (RHA)

RHA has a silica content of about 85% to 90% (Yalçin and Sevinç, 2001). About 400 million metric tons of rice is produced annually of which more than 10% is husk (Conradt et al., 1992). Due to geographical position, climatic disorder and multiplicity of the rice, unusually rice husk contains about 20% ash content (Asavapisit and Ruengrit, 2005, Basha et al., 2005). Rice husk

ash being used as base material helps to break down of the cellular structure in geopolymer matrix, reduces fine pores and increases the strength and durability of the concrete (Manmohan and Mehta, 1981). The value of induction period for rice husk ash is smallest compared to many other mineral admixtures (e.g. silica fume, fly ash and strong furnace dross) (Manmohan and Mehta, 1981). RHA particles play significant role to make compacted gel structure, which is necessary for a load circulation system among geopolymer concrete frames (Kusbiantoro et al., 2012). The amorphous RHA particle is not strong enough and may affect the strength of the end products (He et al., 2013). RHA works better at an elelvated temperature in the formation of geopolymer matrix (Kusbiantoro et al., 2012). Figure 2.2 (left) shows that RHA has its cellular structure before grinding while the right figure shows very irregular-shaped particles of ground RHA and there are pores among the cellular surface of RHA (right).

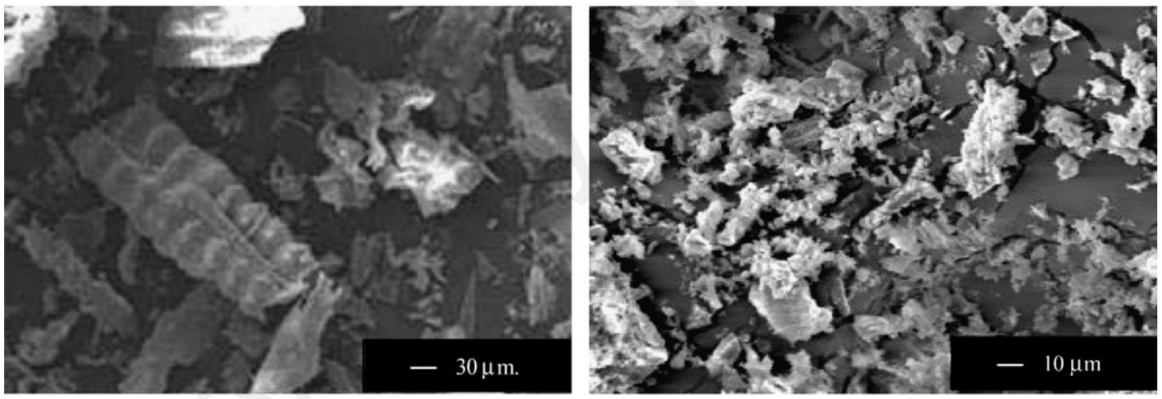

Figure 2.2: SEM images of Original RHA and ground RHA ((Chindaprasirt, Rukzon, & Sirivivatnanon, 2008))

2.5 Metakaolin

MK has been commercially used as a pozzolan since the mid-1990s. Kaolin, after suitable treatment, is the main source of MK. Kaolin is a phyllosilicate, consisting of alternate layers of silica and alumina in tetrahedral and octahedral coordination, respectively. Figure 2.3 shows the schematic structure of kaolinite (Caglar et al., 2013). MK has attracted a lot of attention

due to having both pozzolanic and micro filler features (Poon et al., 2001). Although MK is an inorganic material it is similar to organic materials because it reacts with solid polymers (Buchwald et al., 2007) and forms a strong alumina-silicate network by polycondensation. When MK mixes with slag under alkaline activation condition, both the calcium silicate hydrate system and geopolymer system interact at their contact surfaces and produce good strength performance (Buchwald et al., 2007). The MK structure in alkaline media consequently releases the silicate and aluminate species into the solution and converts 5- and 6-coordinated Alto 4-coordination upon dissolution (Duxson et al., 2005).

MK delivers a very good particle packing and strength of its pozzolanic property rises the resistance of the concrete to destructive environments also. It has also been used successfully for the development of high strength self-compacting concrete using mathematical modelling (Dvorkin et al., 2012). MK has proved itself as pozzolan on the development of high strength concrete and also shows good permeability and durability characteristics of concrete designed for a very low w/b ratio of 0.3.

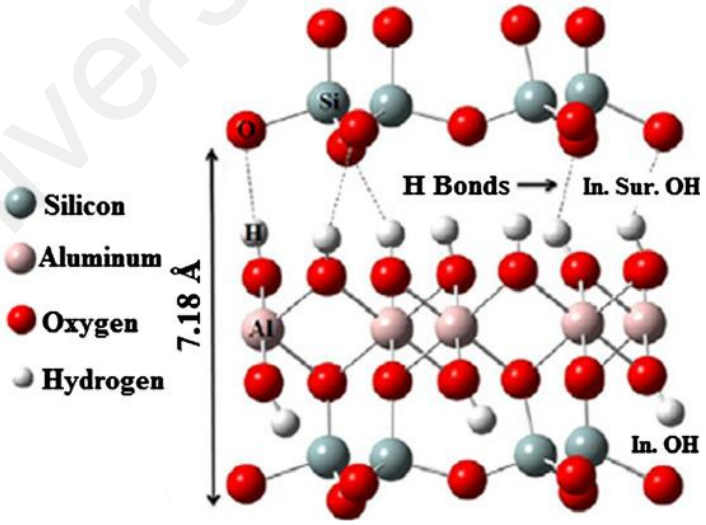

Figure 2.3: Schematic structure of kaolinite ((Caglar et al., 2013))

2.6 Ground Granulated Blast Furnace Slag (GGBS)

The use of GGBS has become reliable all over the world since the mid-1800s. Ordinary Portland cement and other pozzolanic materials have been combined with GGBS and have ensured the durability of concrete structures (Lothenbach et al., 2011). GGBS has been widely used in Europe, and increasingly in the United States and in Asia (particularly in Japan and Singapore) for its dominance in concrete stability (Malagavelli and Rao, 2010). GGBS cement is routinely specified in concrete to provide protection against both sulphate and chloride attacks. GGBS has been activated successfully by an alkaline medium for more than 40 years Talling and Brandstetr, 1989. The geopolymeric gel gets predominance upon CSH gel at higher concentrations of NaOH (> 7.5 M) but small amount of calcium precipitates are formed (Yip et al., 2005). The reaction mechanism starts with a demolition of the slag bonds Ca–O, Mg–O, Si–O–Si, Al–O–Al and Al–O–Si, and then the formation of a Si–Al layer, and, finally, the hydration products are formed (Li et al., 2010). A compressive strength of 30 MPa to 100 MPa can be developed at 28 days for self-compacting GGBS concrete by using various replacement levels ranging from 20% to 80% (Dinakar et al., 2013). Wang et al., (1995) concluded that GGBS-based alkali-activated mortar and OPC mortar both participate in the formation of CSH gels but the difference can be noticed in the patterns of pores. Gel pores are more dominant in GGBS mortar while capillary pores are more dominant in OPC mortar. Figure 2.4 shows SEM images of GGBS (left) and Ordinary Portland Cement (right).

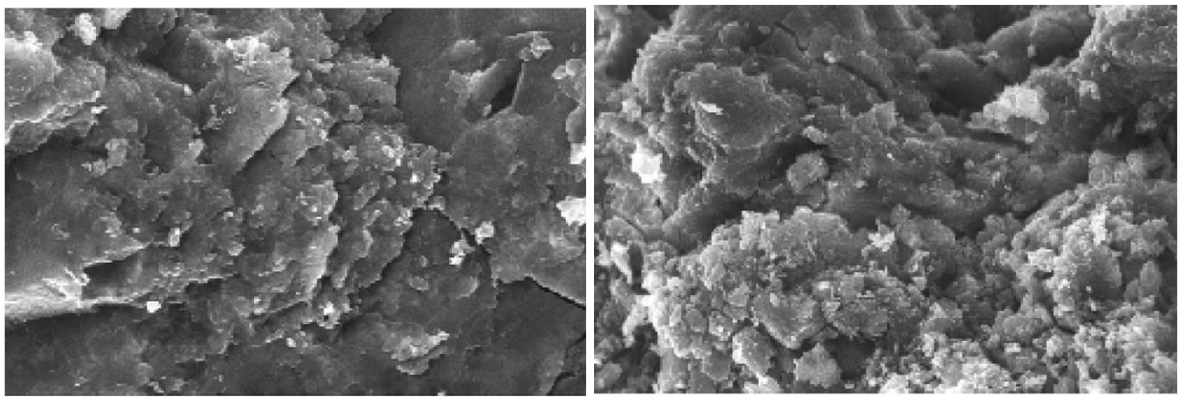

Figure 2.4: SEM images of GGBS (left) and Ordinary Portland Cement (right) ((Yang, Song, Ashour, & Lee, 2008))

2.7 Alkali Activators

The alkalis used in this study were sodium silicate (Na_2SiO_3) and sodium hydroxide (NaOH). Although there are many types of slag – granulated blast-furnace slag, electro thermal furnace phosphorous slag and steel slag – GGBS is generally used. Sodium silicate, sodium hydroxide activated slag mixes sets very quickly. Hardjito et al., (2004) also stated that alkali concentration plays a noteworthy role for geopolymerization and that a higher concentration of NaOH produces greater compressive strength. High reactivity is required for the source materials. This can be achieved by calcination at high temperatures, which converts the crystalline phases in the source materials to amorphous (Xu and van Deventer, 2003). It has been proven that when the value of pH is higher, the activator displays improved slag hydration capability (Chang, 2003). As the activator concentration increases, the polymer formation becomes delayed, which prevents faster setting (Alonso and Palomo, 2001). The temperature increases the energy of reactant particles so that they can overcome the difficulty of diffusion for ion species in the aqueous phase due to acceleration of the activator concentration (Alonso and Palomo, 2001). A higher alkalinity is not desirable sometimes because of the disturbance in the condensation of the geopolymeric gel by the surplus of free alkalis (Burciaga-Diaz et al., 2012).

2.8 Compressive strength of blended cement mortar

At first, researchers started to replace the cement with different percentages by pozzolanic materials or binders. The cement was replaced by not only single but also binary combination of binder. de Gutiérrez et al., (2005) reported that the addition of SF, GGBS, and MK at 15% of total binder increased the cube compressive strength by 23%, 19%, and 6%, respectively. RHA blended cement produced higher compressive strength compared to OPC cement and this phenomenon can be justified by the filler (physical) effect which was reported by Givi et al., (2010). Previously, ternary blended cement with Fly ash and RHA has been prepared and its strength has been found higher than binary combination of cement with fly ash or binary combination of cement with RHA (Chindaprasirt and Rukzon, 2008). When the replacement level is higher (40%), then the addition of binary blending of FA and RHA was found to have stronger performance than the single pozzolan due to the synergic effect (Chindaprasirt and Rukzon, 2008). According to Isaia's studies, in a ternary mixture, one less reactive pozzolan can work better with another one more reactive pozzolan where a synergy is created among ternary pozzolans. This is called synergic effect of ternary blended mortar (Isaia et al., 2003). The achievement of 7-day strength is 95-99% for blended pozzolan mortars compared to normal OPC mortar while this achievement is only 75–77% for single pozzolan mortars. The strength of blended concrete is improved due to synergic effect when the blend of fine pozzolans are incorporated (Chindaprasirt et al., 2008). Figure 2.5 shows total, filler and pozzolanic effects at ages of 28 day unitary compressive strength of mineral addition mixtures (Chindaprasirt and Rukzon, 2008).

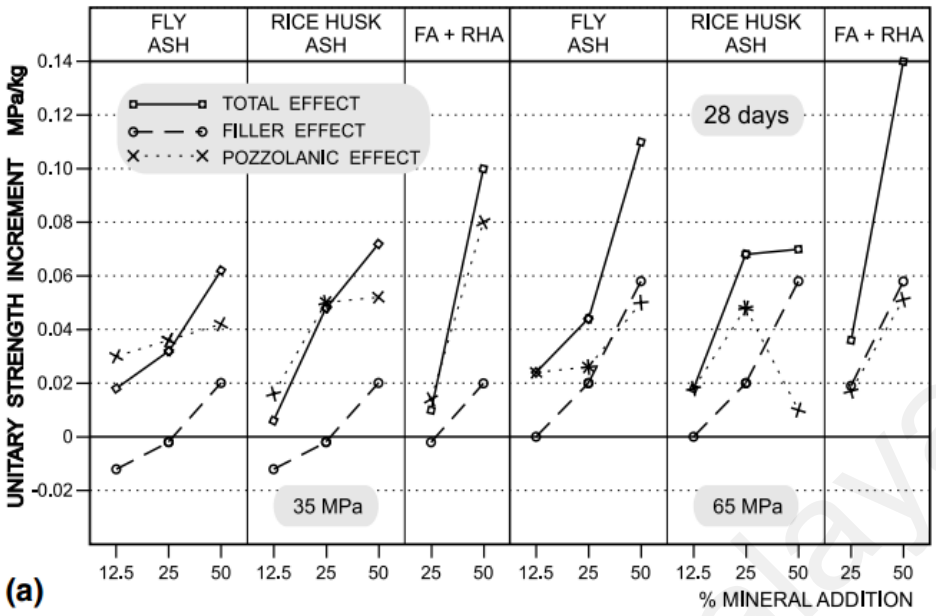

Figure 2.5: Total, filler and pozzolanic effects at ages of 28 day unitary compressive strength of mineral addition mixtures ((Chindaprasirt & Rukzon, 2008))

2.9 Compressive strength of geopolymer mortar

As the speciality of geopolymer mortar is the use of non-cement binder, compressive strength development of geopolymer mortar greatly depends on the combined effect of binary or ternary binders. Karim et al., (2013) reported that geopolymer mortar with ternary combination of RHA, GGBS and POFA produced higher compressive strength than the mortar with binary combination of GGBS and POFA due to having more silica. 28 day compressive strength of GGBS-based alkali activated mortars are much higher than that of Fly ash-based alkali activated mortars (Yang et al., 2008). Ng and Foster, (2013) reported that compressive strength of geopolymer mortar is greatly influenced by the strength of the geopolymer binder materials. He showed the ternary blending of binders such as GGBS and Fly ash from two different sources in geopolymer mortar. Kabir et al., (2015) produced 28-day compressive strength of 47 MPa with the addition of GGBS up to 35%, POFA up to 45% with 20% MK. Figure 2.6 shows effect of GGBS addition on compressive strength of geopolymer.

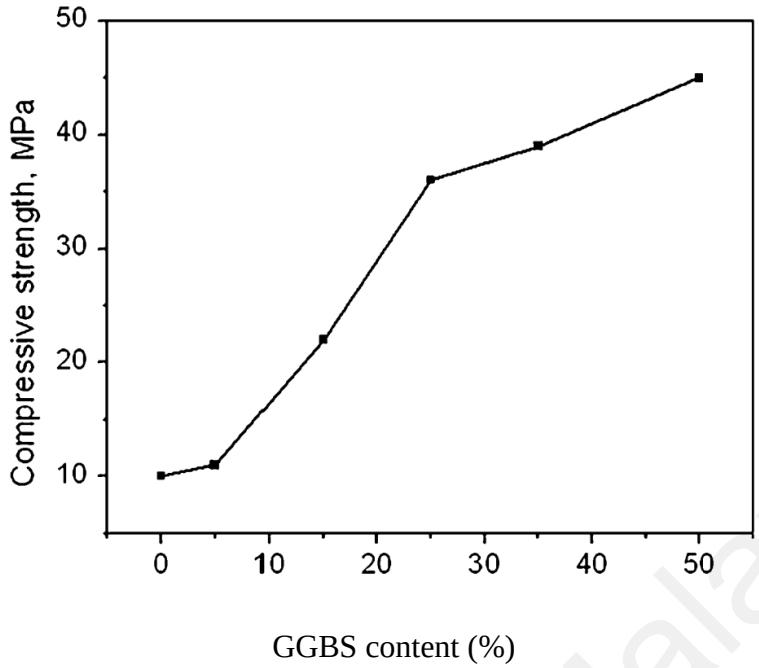

Figure 2.6: Effect of GGBS addition on compressive strength of geopolymer ((Kumar, Kumar, & Mehrotra, 2010))

2.10 Microstructural analysis of mortar

Ranjbar et al. (2014) reported on the compressive strength of POFA and FA using micro-structural analyses. In this investigation, they showed that SEM image of FA has lower pores than SEM image of POFA. Ranjbar et al. (2014) reported the effect of curing at elevated temperature on FA and POFA based geopolymer mortars in terms of microstructural investigation.

Yusuf et al. (2014) reported that GGBS is more amorphous than UPOFA. They justified from SEM micrograph that Ca does not only contribute to strength but also increase the density of microstructure through its capacity of filling pores. As geopolymer is the result of amorphous formation, using more amorphous material as binders is more effective for geopolymerization process. Kumar et al., 2010 reported that amorphorsity of geopolymer increased with the increased percentages of GGBS content as shown in figure 2.7.

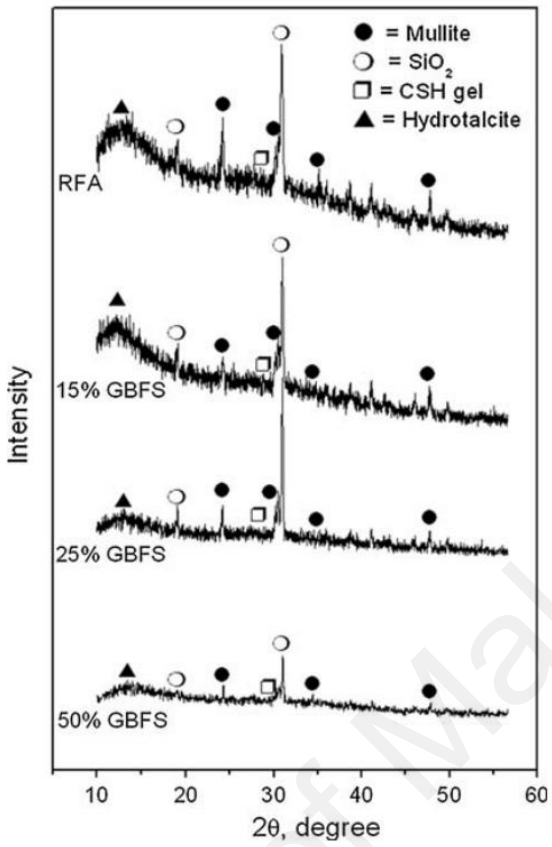

Figure 2.7: XRD results of geopolymer showing increased amorphorsity with increase in GGBS content ((Kumar et al., 2010))

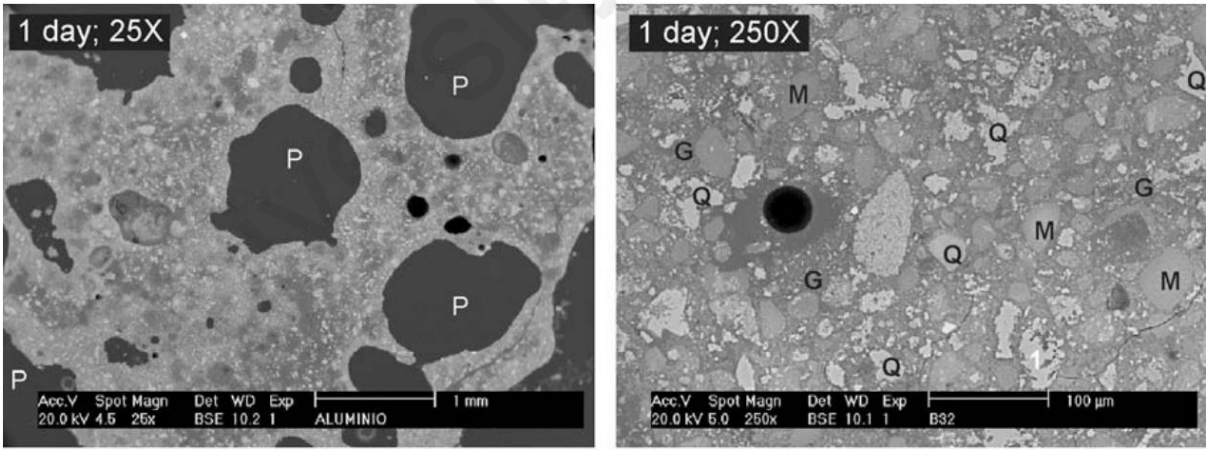

Figure 2.8: SEM images of 1 day concrete with 100% MK at two different magnification ((Arellano Aguilar, Burciaga Díaz, & Escalante García, 2010))

At low magnifications, pores are larger than 1 mm, resulting from the liberation of H_2. From EDS, particles were found rich in Al and Si which justifies the presence of unreacted MK

(Arellano Aguilar et al., 2010). Figure 2.8 shows SEM images of 1 day concrete with 100% MK.

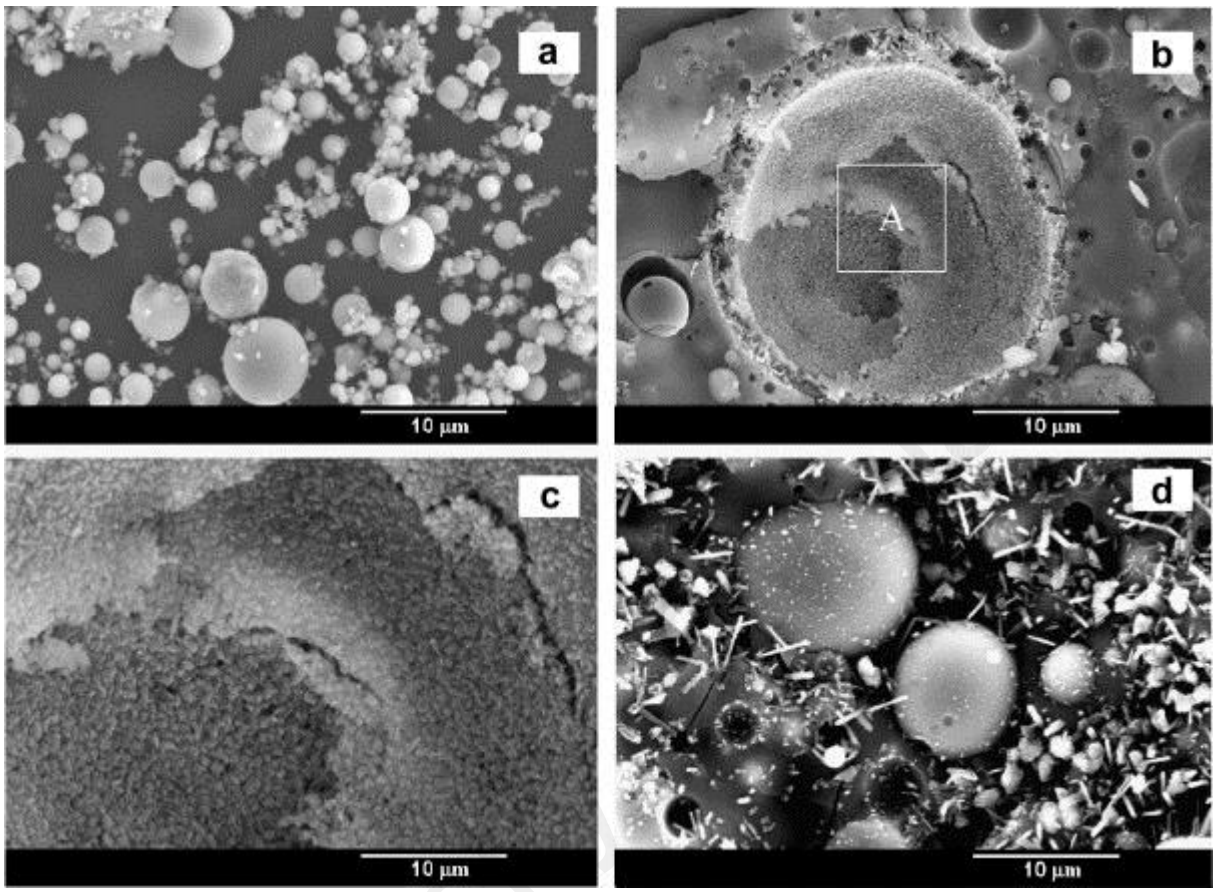

Figure 2.9: Scanning electron microscope (SEM) of (a) the original class C fly ash (CFA), (b) the reactive CFA sphere, (c) the reactive "A" area of CFA sphere in graph (b), and (d) CFA geopolymer (CFAG) cured at 75 °C for 8 h followed by curing at 23 °C for 28 d ((Guo, Shi, & Dick, 2010))

Compressive strength and micro structural characteristics of a class C fly ash geopolymer (CFAG) were studied by researchers (Guo et al., 2010). Škvára et al., (2006) reported that SEM micrograph of fly ash based geopolymer represents the porous characteristics of fly ash. Figure 2.9 shows SEM images of different states of class C fly ash.

2.11 The demand of Geopolymer Concrete

The most demandable material in construction industry is concrete which is generally produced by the combination of binding material, aggregate, admixtures and water. Ordinary Portland

cement (OPC), granite and mining sand are generally used as binding material, coarse aggregate and fine aggregate, respectively. The production of OPC, processing of granite and mining sand cause CO_2 emission and also liable for the ecological imbalance due to continuous depletion of natural resources. Besides the environmental disaster by the construction material, the generation of huge amount of wastes and industrial by-product have made concern due to the shortage of storage and creating environmental issues by earth, water and air pollution at the vicinity of the industrial area.

A lot of research efforts have been carried on in the last few decades and reveals few solutions to mitigate the CO_2 emission and the source of construction material by geopolymer technology and utilising the wastes and industrial by-products in construction industry (Bashar et al., (2014), Kanadasan and Razak, 2013, Khana et al., 2014, Safiuddin et al., 2011, Shafigh et al., 2013, Wood and Marek, 1995, Yap et al., 2014).

Davidovits (2008) as known as the pioneer of the term "geopolymer", describes it as the inorganic aluminosilicate polymers which can be produced by synthesizing of pozzolanic materials in an alkaline activated environment. Geopolymer could be an alternative to OPC (Feng et al., 2015) due to its environmentally sustainable green characteristics (Duxson et al., 2007, Nematollahi and Sanjayan, 2014) high compressive strength, low shrinkage, high temperature resistance (Barbosa and MacKenzie, 2003) and acid & fire resistance (Duxson et al., 2007, Wu and Sun, 2007).

2.12 Binding materials for Geopolymer Concrete

Some of the industrial waste and by-product materials like palm oil fuel ash (POFA) (Bamaga et al., 2013, Galau and Ismail, 2010, Pui, 2011, Warid Hussin and Abdul Awal A. S, 1997), fly

as (FA) (Halstead, 1986, Hardjito et al., 2005, Tamim et al., 2013) and rice husk ash (RHA) (Della et al., 2002, Khana et al., 2014, Sharma and Chand, 2013) consist of pozzolanic characteristics which lead to develop geopolymer concrete due to high percent of alumina and silica content. RHA is one of the biggest source of pozzolanic material. Huge amount of rice is cultivated in whole world. The husk from the paddy is separated in the paddy industry and generally, is treated as the waste part of the rice. A big volume of rice husk is dumped or used for landfilling which causes environmental and water pollution. The utilization of RHA in concrete production will ensure the usage of an agro-industrial waste material and a good source of pozzolans for geopolymer concrete development.

Two types of silica is available in RHA; one is amorphous form and another is crystalline form (Khana et al., 2014). By proper incineration, about 90% amorphous silica can be found in RHA which performs pozzolanic reaction. The development of geopolymer concrete depends on the proportion of alumina and silica. The right proportion of alumina/ silica gives the higher strength (Davidovits, (2008)). RHA consists of low quantity of alumina which demands the insertion of alumina or a source of alumina like MK to reach a proper proportion to develop silica based geopolymer binder. Figure 2.10 shows compressive strength of RHA and MK blended cement concrete.

There is another abundant waste material in Malaysia is ground granulated blast furnace slag (GGBS) which is a by-product of iron industry. A lot of research work on GGBS has been carried out since 1939 to evaluate its performance as cementitious material in concrete (Li et al., 2010). Bakharev et al. (2001) found that alkali activated GGBS had lower resistance of carbonation than similar grade of OPC concrete. Davidovits (2008) introduced calcium based geopolymer which is developed by GGBS.

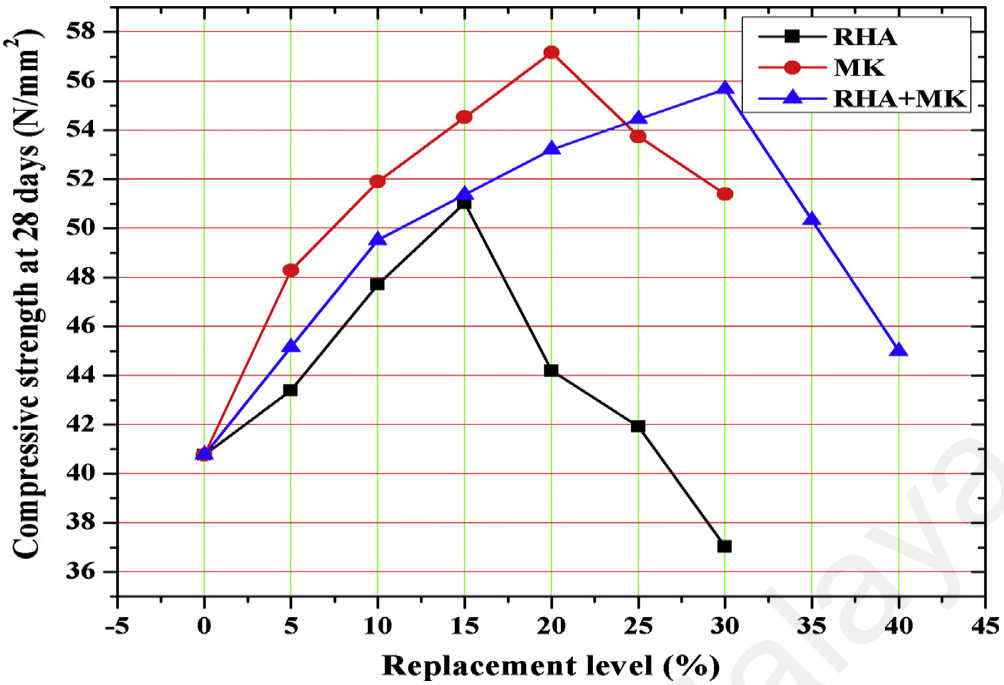

Figure 2.10: Compressive strength of RHA and MK blended cement concrete ((Kannan & Ganesan, 2014))

2.13 Lightweight Aggregate for Geopolymer Concrete

The aggregates in concrete are also replaceable by industrial by-product like manufactured sand (M-sand) and ago-industrial by-product like oil palm shell (OPS) and palm oil clinker (POC). M-sand is the end product from the granite/ quarry industry.

Millions of tons of quarry dust are produced from the quarry industry during the crushing of granite. About 25% of quarry dust is generated during granite crushing Appukutty and Murugesan, 2009. These wastes are generally used for dumping or landfilling. The flacky and sharp edges from Quarry dust are removed by a sophisticated technology, known as vertical shaft impact (VSI) crusher system and thus the end product, M-sand is prepared for a replacement fine aggregate in concrete.

Researchers (Liu et al., 2014, Yap et al., 2014) explored the suitability of OPS as lightweight aggregate and found structural grade lightweight concrete could be produced using OPS as coarse aggregate. During the last three decades, many research works have been carried out

using OPS in OPC concrete as lightweight aggregate to replace conventional granite aggregate (Abdullah, 1996, Alengaram et al., 2008, Alengaram et al., 2011, Alengaram et al., 2013, Liu et al., 2014, Mo et al., 2014, Okpala, 1990); Yap et al. (2014) reported the possibility of significant cost saving production of OPS based concrete.

POC is produced through the incineration process of oil palm shell (OPS) and mesocarp fibre (Kanadasan and Abdul Razak, (2015)). The huge production of POC is generally dumped to the landfill that causes ecological imbalance. The proper utilization of POC in the construction industry may promote the environmental sustainability. The low specific gravity and high aggregate crushing value have made the potentiality of usage of POC as an alternative source of aggregate which has not required any pre-treatment or modification (Kanadasan and Abdul Razak, (2015)) and this could lead to reduce the depletion of natural resources.

POC based lightweight aggregate (LWA) concrete (POCC), in terms of ductility, was reported as slightly lower ductile material than normal weight aggregate (NWA) concrete (NWAC). Ahmmad et al. (2014) found 1.26 and 1.54 times lower displacement and torsional ductility index of POCC than that of NWAC. Similarly, the modulus of elasticity, modulus of resilience, modulus of toughness and strain were reported to lower value; however the compressive strength of POCC was comparatively lean to that of NWAC (Ahmmad et al., (2014)).

Mohammed et al. (2014) reported that POCC concrete beams meet the maximum tolerable deflection criteria. Kanadasan and Abdul Razak (2015) proposed a mix design of POC for self-consolidated concrete.

2.14 Fracture properties of mortar and concrete

The observation on the propagation of cracks in specimen is the main part of fracture test. The specimen's resistance to fracture means the torturous path of crack propagation. The tolerance

to any damage can be increased by the improvement of fracture properties of the mortar and concrete composites. The damage can be minimized by the prediction of crack growth through the experimental studies of fracture mechanics. Fracture properties of cement paste and mortar depend strongly on both specimen size and strength. When strength become higher, the ultimate load, fracture toughness and fracture energy of cement paste and mortar increase. But for cement paste, with the increase of compressive strength, the brittleness of cement paste increases which is unfavorable to the fracture properties of cement paste. It also can be found that fracture properties of the matrix can't be improved by only increasing compressive strength and though the grain size of the aggregate in matrix used was very small, is very helpful for improving fracture properties of the matrix (Zhu and Xu). Silva and Thaumaturgo 2003 reported that the difference of fracture toughness between geopolymer concrete and Portland cement concrete (0% of fiber) is about 80%. This justifies the role of geopolymeric materials on the fracture properties of concrete. Susan et al., (2006) also stated that slag based geopolymer concrete reinforced with steel fiber exhibits a three times higher toughness than ordinary Portland cement concretes to early ages of curing. The strengthening and toughening mechanisms in steel microfiber reinforced composites through in-situ crack propagation measurements during load application are described by Yi and Ostertag, (2001). Crack growth resistance behavior of mortar reinforced with steel microfibers have been narrated by Ostertag and Yi, 2007.

2.15 Use of steel micro-fibers to interprete Fracture properties

Fibers are called microfibers when they have diameter in the range of μm unit. The benefit of their small diameter is the ability of interaction with micro-cracks. Another beneficiary aspect of it is that it can occupy small volume with large density due to thinner shape of it. It can make bridging among micro-cracks so that the formation of macro-cracks become delay (Ostertag

and Yi, 2007). Aggregate bridging was only observed in the reinforced mortar specimens, not in mortar without fiber. Furthermore, aggregate bridging was more dominant in steel microfiber reinforced mortar compared to polymer fiber reinforced mortar due to the lower crack velocity, stable crack extension and crack pinning action in steel microfiber reinforced composites (Ostertag and Yi, 2007). Yoo et al. (2014) investigated the effect of fiber content on the material and interfacial bond properties of ultra high performance fiber reinforced concrete (UHPFRC), using four different volume ratios of micro steel fibers (Vf = 1%, 2%, 3%, and 4%). It was shown that fracture parameters including cohesive stress and fracture energy are significantly influenced by the fiber content: higher cohesive stress and fracture energy were achieved with higher fiber content. Pierre et al. 1999 investigated to assess the mechanical properties of high performance pastes and mortars with steel microfibers (0, 2.5 and 5% of the paste volume). He reported that the addition of microfibers significantly improves the mechanical properties of cement pastes. Figure 2.11 shows SEM image of steel microfibers (Ostertag and Yi, 2007). Figure 2.12 shows crack formation in a fiber bridging site.

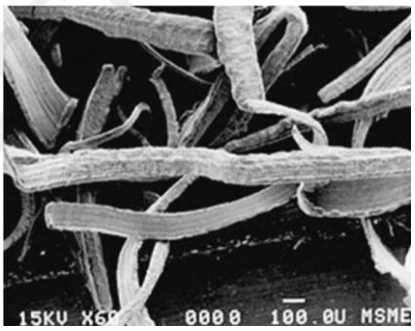

Figure 2.11: SEM image of steel microfibers ((Ostertag & Yi, 2007))

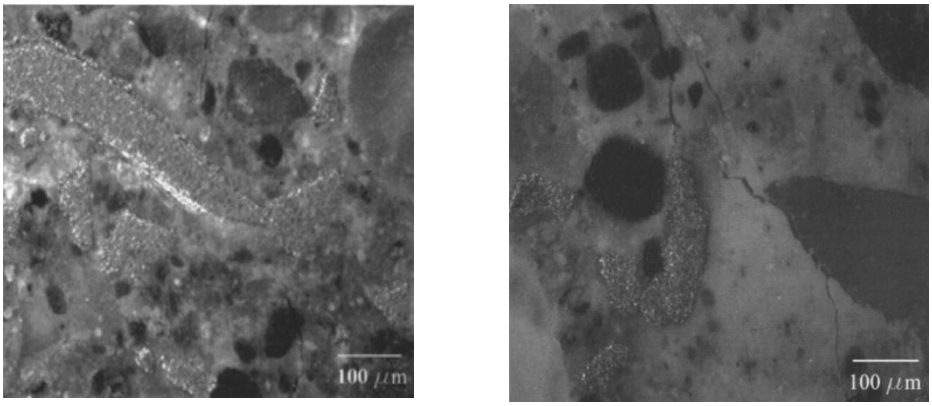

Figure 2.12: Secondary crack formation to the right of a fiber bridging site observed prior to peak load (left) and Fiber bridging site located close to the notch tip at 90% of peak load (right) ((Ostertag & Yi, 2007))

2.16 Research gap

Author	Previous research works	Significance of current research
M.R. Karim et al.(2013)	3 day compressive strength of 23.12 MPa was produced with non-cement binder GGBS(42%), RHA(28%) and POFA(30%) under 48 hours water curing when water/binder ratio was 0.5 and sand/binder ratio was 3.	It was observed from literature review that there is only one paper with ternary blended non-cement binder. This work focusses on using alumina based MK instead of silica based POFA and the combined oxide composition found from ternary blending of GGBS, RHA and MK. Here, the significance of this research is that the necessity of amorphous property for base materials in geopolymer was investigated through microstructural analysis. It has been well established that the combination of RHA and MK works better in cement concrete, but no literature is available on these binders in geopolymer concrete. According to previous literature, local waste material, POC sand has been used only in cement concrete; however, this research focusses on the use of POC sand in geopolymer concrete. Moreover, another significance of this research is the reduction of oven dry density of crushed granite aggregate concrete by using POC sand as fine aggregate. There is no literature available on ternary blended OPS lightweight geopolymer concrete. This work focusses on five local waste materials to produce OPS light weight geopolymer concrete. There are no works carried out on microstructural investigation of ternary blended geopolymer mortar and mechanical properties of ternary blended geopolymer concrete. Also, to the knowledge of the author, there is no literature available on the effect of micro-steel fibers on fracture properties of geopolymer mortar.
V. Kannan and K. Ganesan et al.(2014)	The highest compressive strength produced in blended cement concrete when cement was replaced by the binary combination of RHA and MK at 30%.	
Payam Shafig et al.(2014)	Two waste materials from the palm oil industry were used as coarse and fine aggregates in ordinary Portland cement concrete. Using OPS as coarse aggregate and POC sand and local mining sand as fine aggregates, they reported that the use of more than 37.5% POC sand is not recommended.	
RH Kupaei et al.(2013), MYJ Liu, , UJ Alengaram et al. (2014)	Fly ash based and POFA based OPS lightweight geopolymer concrete was produced.	
Doo-Yeol Yooa et al. (2014)	The effect of micro steel fibers content on the material and interfacial bond properties of ultra high performance micro steel fiber reinforced cement mortar was investigated.	

CHAPTER 3: MATERIALS AND METHODS

3.1 Introduction

This chapter explains the name and properties of materials and procedures according to the code of practice for various types of tests. Materials were used including ground granulated blastfurnace slag (GGBS), rice husk ash (RHA), Metakaolin (MK), manufactured sand (M-Sand), palm oil clinker sand (POC-sand), oil palm shell (OPS), crushed granite and micro steel fibre. Materials tests include water absorption, specific gravity, bulk density, particle size distribution etc. Further, the X-ray fluorescence (XRF) test was conducted to investigate the oxide composition of raw materials. The main points of specimens and tests are following at Table 3.1.

3.2 Experimental Programme

3.2.1 Characterisation of binders

Tables 3.2 and 3.3 show the chemical composition (wt%) and physical properties of all three binders, respectively. The carbon content was estimated as the percent loss on fire. The LOI value of RHA was 7.76 and it is of grey black colour. Its specific gravity and specific surface area were 2.30 and 2981 m^2/kg, respectively. MK typically contains 50–55% SiO_2 and 40–45% Al_2O_3. Other oxides present in small amounts include Fe_2O_3, TiO_2, CaO and MgO (Table 3). MK is an off-white powder and its specific gravity of 2.5 is slightly higher than that of RHA; due to its fineness, its specific surface area of 4315.8 m^2/kg is higher than RHA. . GGBS was obtained from YTL Cement Marketing Sdn. Bhd., Malaysia. GGBS is a glassy, granular material essentially consisting of oxides, such as SiO_2, CaO, Al_2O_3, and MgO. GGBS is an off-white powder. Its relative density is 2.85 to 2.95 and its surface area 400–500 m^2/kg. The specific gravity is 2.89 g/cm^3. The particle size distributions of GGBS, MK and RHA are shown in Figure 3.1. GGBS contains

almost 75% CaO and SiO_2 together whereas Portland cement possesses about 85% CaO and SiO_2 together. GGBS contains more Al_2O_3 than OPC. The total binder content is 766 kg/m^3 for mortar.

Table 3.1 Details of specimens and tests accomplished including code of practice

Test		Code of practice	Shape and nature of Specimen	Measurement of Specimen (mm)	Age of test (day)
Physical properties of materials	Specific gravity & water absorption	BS EN 1097-6:2013	N/A	N/A	N/A
	Bulk density	BS 3N: 1097-3:1998	N/A	N/A	
	Sieve analysis	BS EN 933-1:2012	N/A	N/A	
	Moisture content	BS EN 1097-5:2008	N/A	N/A	
	Workability	BS EN 12350-2:2009	N/A	N/A	
	Oven-dry density	BS EN 12390-7:2009	N/A	N/A	28
Compressive strength		BS EN 12390-3:2009	Cube (mortar and Concrete)	50 & 100	3, 7, 28
Splitting tensile strength		BS EN 12390-6:2009	Cylinder	100Ø×200h	28
Flexural strength		BS EN 12390-5:2009	Prism	100×100×500	28
Young's modulus		BS EN 12390-5:2009	Cylinder	150Ø×300h	28
Fracture test		RILEM TC 50-FMC	Prism (mortar)	50×50×250	28
Ultrasonic pulse velocity (UPV)		BS EN 12390-5:2009	Cube	100	28

3.3 Manufactured Sand

Manufactured sand (M-sand) is more angular and has a rougher surface texture than naturally weathered sand particles. Its specific gravity and fineness modulus (FM) were 2.78 and 3.19, respectively. The M-sand has a wide range of particles as shown in the distribution curve (Figure 3.2). Hence, the M-sand is well graded and falls under zone-C [BS 882:1992]. With a well-designed screening system, the required grading (Zone II) and fineness modulus (2.4 to 3.1) can also be achieved consistently in the case of M-sand.

Table 3.2: Chemical composition (wt%) of the raw materials, X-ray Fluorescence (XRF) analysis

Oxide composition	CaO	SiO_2	Al_2O_3	MgO	Na_2O	SO_3	P_2O_5	K_2O	TiO_2	MnO	Fe_2O_3	SrO	Cl	CuO	LOI
RHA	1.03	93.46	0.58	0.51	0.08	0.6	1.6	1.82	0.0	-	0.52	-	-	-	7.76
MK	0.71	51.7	40.6	0.96	0.31	0.1	0.2	2	3	0.08	0.64	0.03	-	-	1.19
GGBS	45.8	32.5	13.7	3.3	0.3	1.8	0.0	0.5	0.7	0.4	0.8	0.1	0.0	-	0.6

Table 3.3: Physical properties of constituent materials

Properties	Materials			
	RHA	GGBS	MK	M-Sand
Specific gravity	2.3	2.89	2.5	2.78
Specific surface area (m^2/kg)	2981	405	4315	-
Colour	Grey black	Off-white	Off-white	-

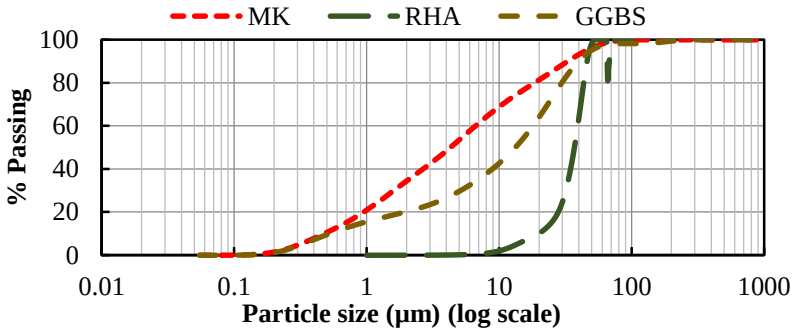

Figure 3.1: Particle size distribution of RHA, MK and GGBS

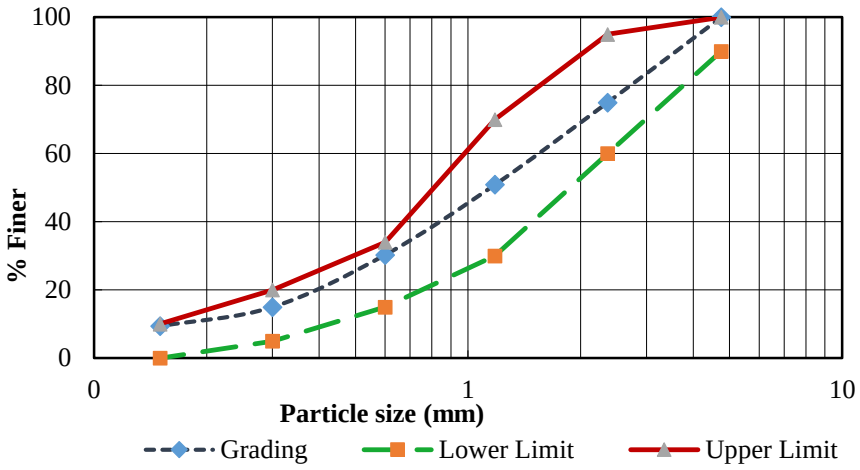

Figure 3.2: Particle size distribution of M-sand (BS 882:1992)

3.4 Aggregates used for concrete

POC sand and M-sand were used in two different proportions as composite fine aggregate. OPS was used as full and partial replacement of conventional crushed granite as coarse aggregate. The above-said aggregate materials were collected from the local industry in Malaysia.

The raw POC (Figure 3.3a) which is a by-product through incineration of OPS in the palm oil industry for generating heat, was crushed and sieved through 5 mm sieve. The particles between 5 mm and 300 µm of crushed POC were used as fine aggregate. Figure 3.3b shows the surface texture of POC of size lower than 4 mm.

The second type of aggregate used in this investigation is M-sand which is end product of quarry dust. M-sand was dried and sieved before being used as fine aggregate (Figure 3.3c). Figures 3.3b and 3.3d show the particle shapes of POC sand and M-sand. It was noticed that POC sand had sharp angular edge and M-sand had rounded shape due to its centrifugal processing through VSI crusher. POC sand particles contained a lot of pores with rough surface. The physical properties of POC sand and M-sand are shown in Table 3.4. The specific gravity of POC sand is lower than M-sand and this could be useful in

the development of lightweight concrete. Due to porous in nature, the water absorption rate of POC sand was found 1.76 times higher than M-sand.

OPS was collected from the palm oil industry; the raw OPS was washed, dried, crushed, sieved, soaked in water for 24 hours and dried to saturated surface dry condition before using for casting. The sizes of crushed OPS were controlled between 2.36 and 14 mm. The physical properties of OPS and granite are shown in Table 3.4. Due to its low specific gravity, it exhibits lightweight and high water absorption property of OPS. The crushed OPS and crushed granite aggregates are shown in Figure 3.3e and Figure 3.3f respectively. Figures 3.3g and 3.3h show the concave and convex surface texture, respectively.

Table 3.4: Physical properties of aggregates

Properties	Materials			
	POC sand	M-sand	OPS	Granite (mm)
Size	<5 mm to 300 µm			9
Specific gravity	1.97	2.78	1.3	2.67
Water absorption (%)	9.88	5.6	20.25	1.25
Fineness modulus	3.37	2.68	5.63	5.98

a. POC< 4mm,

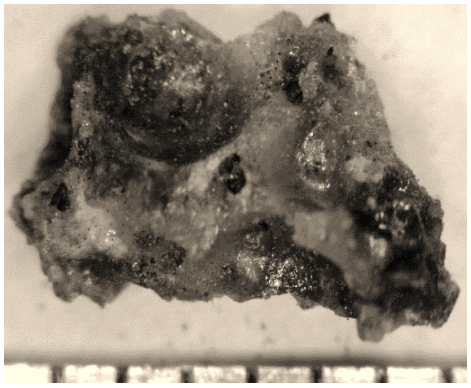

b. Surface texture of POC<4mm

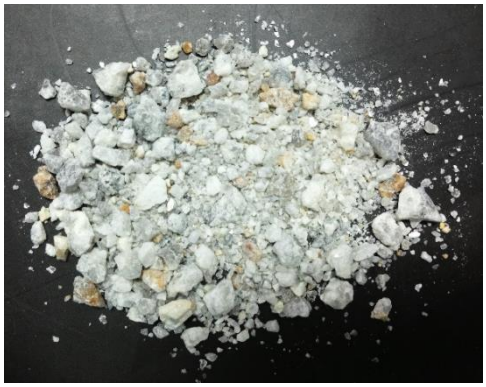

c. M-sand,

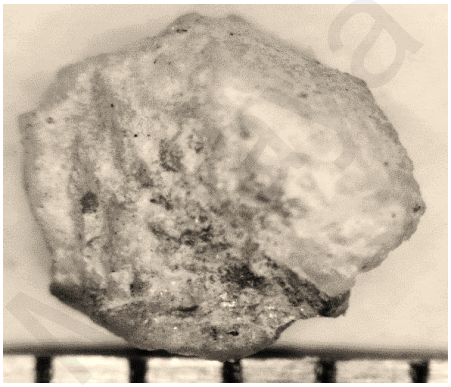

d. Rounded shape of M-sand

e. Oil palm shell (OPS)

f. Crushed granite aggregate (9mm)

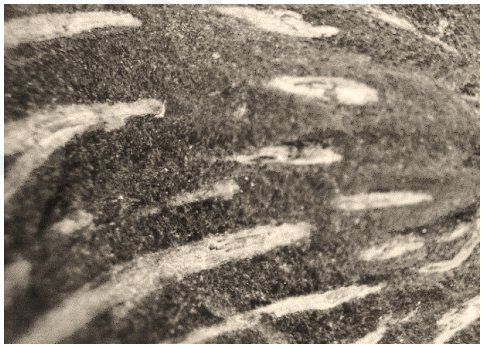

g. OPS-concave surface

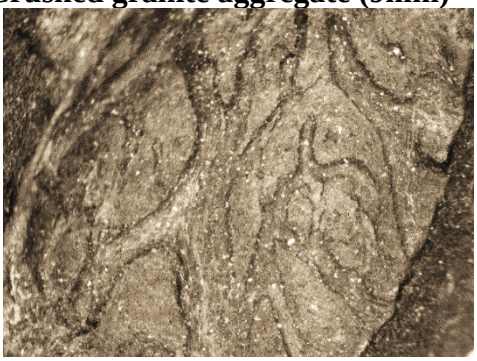

h. OPS-convex surface

Figure 3.3 a. POC< 4mm, b. Surface texture of POC<4, c. M-sand, d. Surface texture of M-sand e. OPS f. Gravel (9mm) g. OPS-concave surface texture, h. OPS-convex surface texture

3.5 Alkaline activators

The geopolymerization of pozzolanic materials takes place in the presence of alkaline activator. Commonly used alkaline activators are the hydroxide, silicate, carbonate and sulphate forms of sodium and potassium ions. (Hardjito et al., (2004)) reported that alkaline solution prepared by sodium hydroxide and liquid sodium silicate could be a better choice of activator for geopolymer material. 14 and 12 molarity (M) of NaOH solutions were prepared 24 hours before casting and was mixed with liquid sodium silicate in a weight proportion of 1:2.5 just before the casting. The alkaline activator to binder ratio was kept constant as 0.5 for all the mixes.

3.6 Preparation and curing for mortar

3.6.1 Mixing, casting and curing of mortar

GGBS, RHA, MK and M-sand were first mixed together in a pan mixer for about three minutes. Figure 3.4 shows casting of mortar. The aggregate to binder ratio was kept at 2:1. Binders were mixed in twenty different proportions and molarity of NaOH solution was fixed 14M for these mixes. Among the 20 mixes, six mixes were chosen for additional casting. These additional six mixes were mixed with 12M of NaOH for comparison between two different molarities of NaOH. The compressive strength of the mortars decreased with the increasing aggregate to binder ratio. It has been described that the accumulation of aggregate in some cases may reinforce the geopolymer matrix (Joseph & Mathew, 2012). The sodium hydroxide and the sodium silicate solutions were mixed together and the solution and the additional water were then added to the dry materials and mixed for about four minutes. The additional water to binder ratio was kept at 0.25. Table 3.5 shows all the experimental parameters. The fresh concrete was cast into the moulds immediately after mixing, in three layers and compacted using a vibrating

table. After casting, the specimens were cured in heat curing chamber at 65°C for 24 hours. Figure 3.5 shows the photograph of curing chamber at open and close condition. The heat-cured specimens were left to air-dry in the laboratory for three days before testing 3- 7-, 14- and 28-day compressive strengths.

Figure 3.4: Casting of mortar

Figure 3.5: Curing chamber open (left) and close (right)

3.7 Testing for mortar

In accordance with ASTM C 230, the flow test was conducted using a flow table, flow mould and tamping rod, and the percentage of flow was measured using a measuring tape. Figure 3.6 shows flow table and flow test of fresh mortar.

The oven-dry density was measured for all specimens. The cubes were tested in compression in accordance with ASTM: C109/C109M-13. The average of compressive

strength for three specimens were taken for the determination of appropriate compressive strength. Figure 3.7 shows the specimens prepared for testing.

Figure 3.6: Flow table and flow test of fresh mortar

Figure 3.7: Specimen prepared for testing

Table 3.5: Experimental Parameters for mortar

Binder: M-Sand	Binder	M-Sand	Activators (1:2.5) (kg/m^3)		Added Water	s/b	w/b	Curing temp
	(kg/m^3)	(kg/m^3)	NaOH solution(14M)	Na_2SiO_3	(kg/m^3)	(wt/wt)	(wt/wt)	^{o}C
1:2	766	1532	109	274	191	0.5	0.25	65

s/b: solution to binder weight ratio, w/b: water to binder weight ratio

Table 3.6: Mixture Proportions (kg/m^3) for mortar

Mix No.	Binders						Solution
	MK		RHA		GGBS		NaOH
	%	Weight (kg/m^3)	%	Weight (kg/m^3)	%	Weight (kg/m^3)	Molarity (M)
M1	0	0	40	345	60	422	14
M2	5	30	35	240	60	422	14
M3	10	77	30	230	60	460	14
M4	15	115	25	192	60	460	14
M5	20	153	20	153	60	460	14
M6	20	153	17	130	63	483	14
M7	20	153	15	115	65	498	14
M8	20	153	25	192	55	422	14
M9	20	153	30	230	50	383	14
M10	25	192	20	153	55	422	14
M11	25	192	25	192	50	383	14
M12	25	192	30	230	45	345	14
M13	25	192	40	307	35	268	14
M14	30	230	20	153	50	383	14
M15	30	180	25	150	45	270	14
M16	30	230	30	230	40	307	14
M17	30	230	40	307	30	230	14
M18	30	230	70	537	0	0	14
M19	40	307	40	307	20	153	14
M20	0	0	25	150	75	450	14
M5 B	20	153	20	153	60	460	12
M6 B	20	153	17	130	63	483	12
M7 B	20	153	15	115	65	498	12
M10 B	25	192	20	153	55	422	12
M11 B	25	192	25	192	50	383	12
M12 B	25	192	30	230	45	345	12

Table 3.7: Experimental Parameters for concrete

Binder: FA: CA	Binder	FA	CA	Activators(1:2.5)(kg/m^3)		Added Water	s/b	w/b	Curing temp
	(kg/m^3)	(kg/m^3)	(kg/m^3)	NaOH solution(14M)	Na_2SiO_3	(kg/m^3)	(wt/wt)	(wt/wt)	^{0}C
1:2.5:0.6	463.42	1158.54	278.05	109	274	191	0.5	0.25	65

s/b: solution to binder weight ratio, w/b: water to binder weight ratio

Table 3.8: Mix Proportion for concrete

Mixes	**Fine aggregate**				**Coarse aggregate**			
	M-Sand		**POC sand**		**OPS**		**Granite (9 mm)**	
	%	**kg/m^3**	**%**	**kg/m^3**	**%**	**kg/m^3**	**%**	**kg/m^3**
C1	50	579.27	50	579.27	100	278.05	0	0
C2	50	579.27	50	579.27	80	222.44	20	55.61
C3	50	579.27	50	579.27	60	166.83	40	111.22
C4	50	579.27	50	579.27	20	55.61	80	222.44
C5	50	579.27	50	579.27	0	0	100	278.05

3.8 Mix proportion, casting and curing for concrete

Five geopolymer concrete mixes were prepared with the variable of coarse aggregates, OPS and crushed granite of size (5 to 9 mm). The binder content and the proportion of RHA, GGBS and MK were kept constant as 463.41 kg/m^3 and 1:2:1, respectively. The alkaline activators to binder ratio was kept consistent as 0.5 whereas water to binder ratio was 0.25. Details of all experimental parameters for the casting of concrete are shown in Table 3.7 while Table 3.8 shows the mix proportions of all the mixes for concrete.

The coarse and fine aggregates were mixed in the rotary drum mixer for about 3 min, followed by the addition of all binder (RHS.MK and GGBS) for another 6 min. After the addition of mixing alkaline activators and then water, the mixing was continued for another 8 min. Figure 3.8 shows casting of concrete. The concrete was then poured into molds and compacted. To remove the entrained air and bubbles the samples were vibrated

with standard compaction using a rod and vibrating table. Figure 3.9 shows concrete being cast on the vibration table.

Immediately after casting, the specimens along with the moulds were covered using plastic film to reduce water loss and were kept in a curing chamber for 24h at 65^0C. Afterwards, the specimens were taken out of the curing chamber and kept at ambient condition with an average temperature 28°C and relative humidity 70%.

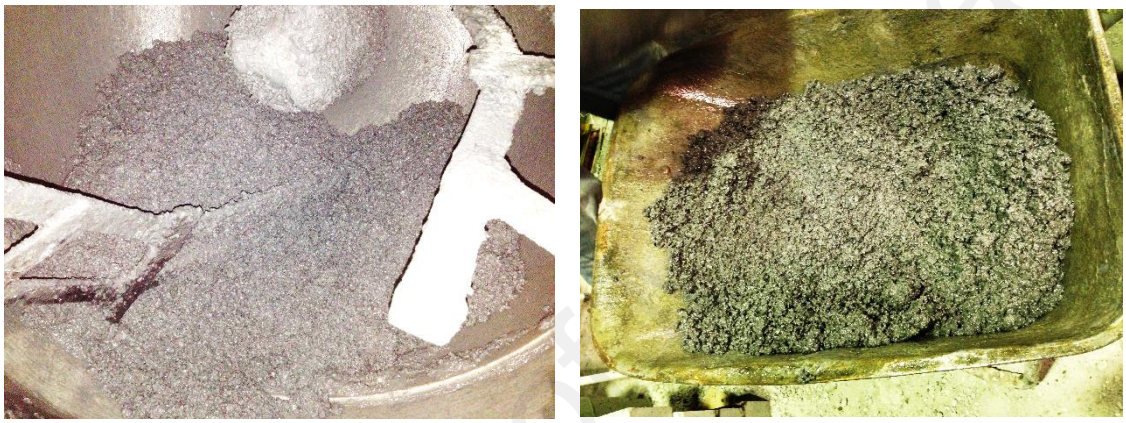

Figure 3.8: Casting of concrete

Figure 3.9: Concrete being cast on the vibration table

3.9 Test methods for concrete

3.9.1 Mechanical properties test

The compressive strength, flexure, splitting and static modulus of elasticity tests were carried out in accordance with BS EN codes. The specimen dimensions, quantity and testing methods are shown in **Table 3.9**.

Table 3.9 Tests

Tests	Specimen type	Specimen dimensions	No. of specimen	Standards
Compressive strength	Cube	100	3	BS EN 12390-3:2009
Splitting tensile strength	Small cylinder	100-ϕ, 200 h	3	BS EN 12390-6:2009
Flexural strength	Prism	100, 100, 500	3	BS EN 12390-5:2009
Modulus of elasticity	Big cylinder	150 Ø, 300 h	3	BS EN 12390-5:2009
Ultrasonic pulse velocity	Cube	100	3	BS EN 12390-5:2009
Fracture	Prism	50, 50, 250	3	RILEM TC 50-FMC

3.10 Ultrasonic pulse velocity (UPV)

The quality of concrete based on the compaction of matrixes could be analysed by the propagation variations of ultrasonic pulse velocity (UPV) wave. The UPV was measured following BS EN 12390-5:2009 code. A portable ultrasonic non-destructive digital indicating tester with adjoining transducers was used to measure the travelling time for pulse between the ends of specimens. The UPV was calculated by dividing the length of pulse travel with the time measured.

3.11 Scanning electron microscopy coupled with energy dispersive X-ray spectroscopic analysis (SEM + EDS), and X-ray diffractometer test for mortar

The fragmented binder surface of the specimens tested for compressive strength was used for SEM micrographs and the EDS of the specific areas within the microstructure was then obtained. The pulverized or finely divided samples passing through 45 µm sieve were used for XRD test. Sample was put on sample holder and it was ensured that the level of sample was same with the level of sample holder. Each sample holder was placed in each row of the column. Figure 3.10 shows material preparation for XRD tests. Figures 3.11-3.14 show SEM Micrograph and EDS of MK, RHA, GGBS and M-sand respectively. Table 3.10 shows element percentages from EDS results.

Figure 3.10: Material preparation for XRD tests

3.11.1 Casting of test specimens

To determine the fracture properties of steel microfiber reinforced geopolymer mortar, prism specimens were prepared for three-point bending test. The ratio of the span to the depth of the beam (S/D) was 5 for all the specimens. The ratio of the notch length to the beam depth was 0.3 for all the specimens. For the casting of geopolymer mortar specimens, steel moulds were used. At the same time, cube of 50x50x50 mm and prisms of 50×50×250 mm were cast for the test of 28 days compressive strength and 28 days fracture test respectively. All the experimental parameters are as same as Table 3.5. The only variable was fiber content as percentage (wt%) of binder content. Table 3.11 shows mixture proportions for fracture test and details of fibers. Figure 3.15 shows the photographs of steel fibers. After casting, the specimens were cured in heat curing chamber at 65°C for 24 hours. The heat-cured specimens were left to air-dry in the laboratory before testing 28-day compressive strengths and fracture tests.

Table 3.10 Mixture proportions for fracture test and details of fibers

Mixes	Steel microfiber (wt % of binder)	Weight of steel fibers (kg/m^3)	Length of steel fibers(mm)	Dia of steel fibers (mm)
F0	0	0	18	0.16
F1	1	7.66	18	0.16
F1.5	1.5	11.49	18	0.16
F2.5	2.5	19.15	18	0.16
F3	3	22.98	18	0.16

Figure 3.11: Steel fibers

3.12 Procedure of Fracture test for mortar specimen

The fracture test specimens were 50 mm, 50 mm section and 250 mm long beams with a 15 mm deep notch in the middle of the beam. A ratio of notch depth and beam depth was 0.3 in the specimens of this study so that the crack propagation can be observed in the mortar. The notch was generated during casting of the specimens. If the notch is cut after drying of the specimen, fine cracks form in the ligament during the cutting process. Three point bending tests were performed in deflection controlled mode by using a very stiff closed loop Instron Servo Control machine. The ends of the test specimen were placed on the supporting rollers at a span of 200 mm with the notch on tension side, as shown in Figure 3.16. The Instron machine had a built in digital data acquisition system. It was incorporated with a load cell to record the load with an accuracy of 0.001 KN and a digital strain gauge measuring the vertical displacement with an accuracy of 0.001 mm. The data acquisition system had the ability to record up to 1000 data per second. Two identical specimens were tested for each mixture. Figure 3.17 shows specimen of F0 mix without fiber content at the time of breaking the specimen.

Figure 3.12: Machine arrangement of fracture test

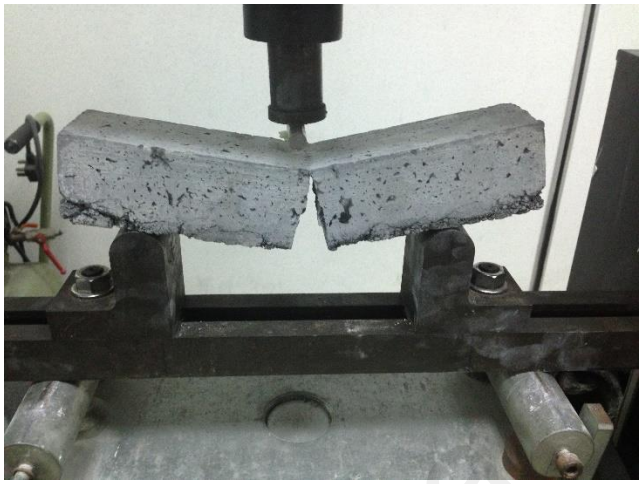

Figure 3.13: At the time of breaking the specimen of without fiber content

CHAPTER 4: : RESULTS AND DISCUSSIONS

4.1 Introduction

This chapter details the results of tests carried out on fresh and hardened mortar, fragmented mortar, powder form of mortar and hardened concrete; the interpretation and justification on analysis of materials, mortar, chemical composition, etc. are provided. The results of all trial mixes done for mortar and concrete are also discussed and selection of the appropriate mixes for further work is justified. The results include the material characteristics, flowability and density of fresh mortar, compressive strength of geopolymer mortar, microstructural investigation of geopolymer mortar, fracture toughness of steel microfiber reinforced geopolymer mortar, mechanical properties of geopolymer concrete and the effect of two different coarse aggregates on the mechanical properties of geopolymer concrete.

This chapter is divided into four sections:

Section 4.2: This section represents results of compressive strength of different trial mixes and discussions on the role of ternary binders on the development of compressive strength.

Section 4.3: This section provides the findings of microstructural investigation for few mixes of geopolymer mortar and discussions on the role of oxide composition of ternary blended mortar for the development of compressive strength.

Section 4.4: This section shows the results of fracture energy of steel microfiber reinforced geopolymer mortar and discussions about the significance of steel microfiber on the fracture properties of geopolymer mortar.

Section 4.5: This section represents the results and discussions of the engineering properties of geopolymer concrete.

4.2 Development of geopolymer mortar compressive strength

4.2.1 General

The use of ternary binders has been justified from the combined oxide composition of mortar. Here, the roles of binders have also been revealed on the development of geopolymer mortar.

4.2.2 Effect of binders on workability by flow test on mortar

Table 5 shows that the highest and the lowest flows of 76% and 10% were achieved for the mixes M7 (20% MK, 15% RHA, 65%GGBS) and M18 (30%MK, 70%RHA, 0%GGBS), respectively. These two mixes have different percentages of RHA, the former with a low amount of 15%, and the latter with 70%. Thus, the effect of RHA on the workability is evident, as the use of a large amount of RHA reduces the ability of the mortar to flow. The water requirement in concrete is usually less for ash with low LOI. Table 1 shows that RHA, MK and GGBS have LOI values of 7.76, 1.19 and 0.6, respectively. As the LOI of RHA is higher, the RHA needs more water for mixing. Moreover, RHA has amorphous silica and a larger surface area, which increases its water demand. MK has greater surface area than RHA as shown in Table 2 which justifies the low flow rate of 15% for the mix M19 with MK of 40%. Due to its lowest specific surface area and LOI among the three binders, GGBS produced the highest flow rate for mix M7 containing GGBS of 65%. Figure 4.1 shows the measurement of the flow of fresh mortar and Figure 4.2 shows the percentages of the flow with the varying percentages of GGBS, MK and RHA.

Figure 4.1: Measurement of flow of fresh mortar

Table 4.1: Flow(%) and Density of different mixes

Mixes	M1	M2	M3	M4	M5	M6	M7	M8	M9	M10	M11	M12	M13	M14	M15	M16	M17	M18	M19	M20
Flow %	35	40	55	70	75	75	76	70	55	65	60	52	40	58	55	45	40	10	15	60
3 day ODD (kg/m^3)	1914	2155	2169	2176	2188	2195	2210	2128	2038	2146	2070	1980	1933	2084	1957	1943	1868	1617	1685	2018

4.2.3 Oven-dry density

The oven dry densities (ODD) of all twenty mixes are shown in Table 4.1. It can be seen that the varying percentages of binders along with the ODD are given and that all the ODD were compared. The highest ODD of 2210 kg/m^3 was obtained for mix M7 with a high content of GGBS (20%MK, 15%RHA, 65%GGBS). The lowest density was measured at 1617 kg/m^3 for M18 (30%MK, 70% RHA, 0%GGBS). The density of M18 was 27% lower than the highest density of M7. It is noticeable that the highest density achieved for the mix with 65% GGBS due to its higher specific gravity compared to the other binders; similarly, mix M18 with 70% RHA produced the lowest density, which could be attributed to the low specific gravity of RHA and it should be noted that no GGBS was used in this mix. The shape of GGBS is mostly spherical and its surface is relatively smooth. Particles with spherical shape generally have higher packing density compared to crushed particles, resulting in higher density (Sakai, Hoshino, Ohba, & Daimon, 1997). Thus, the mixes with a large quantity of GGBS produced high density. It is also evident that the use of high percentages of RHA in the mortar showed lower

density due to its low specific gravity. In mixes M1 (0%MK, 40% RHA, 60%GGBS) and M19 (40%MK, 40%RHA, 20% GGBS), the ODD was found to be 1914 kg/m^3 and 1685 kg/m^3 respectively, which shows that density of mortar reduces about 12% due to the lower specific gravity of MK than GGBS. From the mix M1 and M5, it was evident that density of mortar reduces 12.5% due to the lower specific gravity of RHA compared to MK.

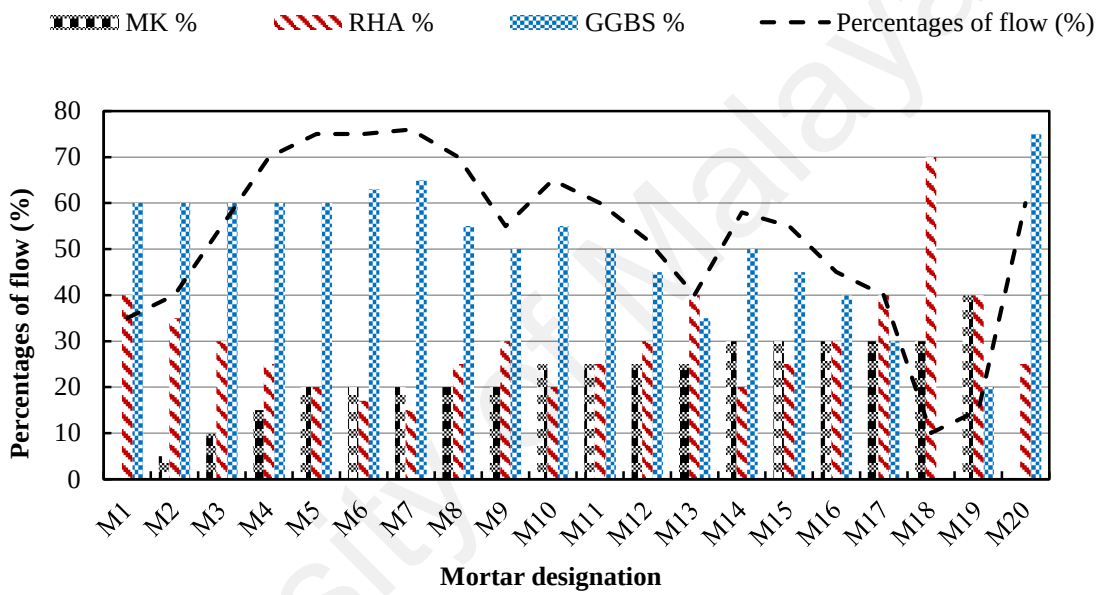

Figure 4.2: Percentages of flow and percent reduction of density from the peak with the varying percentages of RHA, MK and GGBS

4.2.4 Development of the compressive strength of the mortars

The development of the compressive strength of the mortars is shown in Figure 4.3. The achievement of 70% to 95% of the respective 28-day compressive strength at the age of 3 days is shown in Table 4.2. The early age strength development due to the fast geopolymerization at high temperature curing is reported by (Azizul Islam, U Johnson Alengaram, Mohd Zamin Jumaat, & Iftekhair Ibnul Bashar, 2014b). The mortar M7 gained the maximum rate of 95% of 28-day compressive strength development at the age of 3 days. The mortar mixes, M5, M6, M7 and M10, containing GGBS (>60%) but with less than 20% RHA developed a 3-day strength of about 90% of the 28-day strength. This

could be attributed to the higher apparent activation energy of GGBS, which makes it sensitive to the increased temperature for the development of strength ((Barnett, Soutsos, Millard, & Bungey, 2006)). The mortars containing a large proportion of GGBS produced early age strength for even a 10ºC increase in temperature from the standard curing temperature ((Barnett et al., 2006)). Therefore, oven curing at 65ºC influenced the early age strength development of the mortars containing a high level (>45%) of GGBS with a combination of MK.

Researchers (Susan A. Bernal, Ruby Mejía de Gutiérrez, & John L. Provis, 2012),(Azizul Islam, U. Johnson Alengaram, Mohd Zamin Jumaat, & Iftekhair Ibnul Bashar, 2014a) have reported that the incorporation of a high quantity of GGBS improved the strength in the geopolymer concrete and the 3-day strength development of mortar mix M20 with 75% of GGBS showed a slightly lower rate of strength development of 85%, which could be due to the absence of MK. Moreover, mix M1 containing 60% of GGBS developed a 3-day strength of about 76% of the 28-day strength and the low rate of compressive strength development could be due to the high volume of RHA (40%). The mortar mixes containing 40–70% of RHA only produced 70–80% of the 3-day compressive strength of their respective 28-day compressive strength. The mortars containing 5–15% MK, 30% RHA produced 80–90% of 28-day compressive strength at the age of 3 days. However, the ternary effect of mixes with 20–30% MK, 15–25% RHA and 45–65% GGBS produced a high 3-day strength of about 90–95% of the corresponding 28-day compressive strength. It has been reported that Al_2O_3 dissolves faster than SiO_2 and the reaction between aluminate and silicate species is faster than the reaction between only silicate species (P. D. Silva, Sagoe-Crenstil, & Sirivivatnanon, 2007). Thus, the mixes containing high percentages of GGBS with MK and lower percentages of RHA achieved early strength.

The strength development of the mixes, as shown in Figure 4.3, showed a very steep increase up to the age of 3 days and then there is a slight fall in the curve at the age of 7-days.This could be due to the ratio of SiO_2/Al_2O_3, which affects the geopolymerization process (Guo et al., 2010). As aluminium dissolves earlier, after 3 days, the SiO_2/Al_2O_3 ratio becomes higher and the rate of geopolymerization becomes slower. Another possible explanation could be the incomplete hydration of CaO that may occur in high Ca based geopolymer as undesirable precipitation is produced between 3 and 7 days, which might slow the rate of geopolymerization (Lee & Van Deventer, 2002). However, mortars M1, M17, M18 showed a 13% strength increment from 3 to 7 days with the exception of mixes M1 and M18, which contained no MK or GGBS, respectively. As mortars M1, M17, M18 had a3.7–6.8 SiO_2/Al_2O_3ratio, their rate of geopolymerization gradually increased up to 7 days. The rate of geopolymerization was very low (4–19%) between 7and28 days. The mortars containing 40–70% RHA showed a slightly higher rate of geopolymerization between 7and 28 days due to the higher amount of SiO_2 content (P. D. Silva et al., 2007).

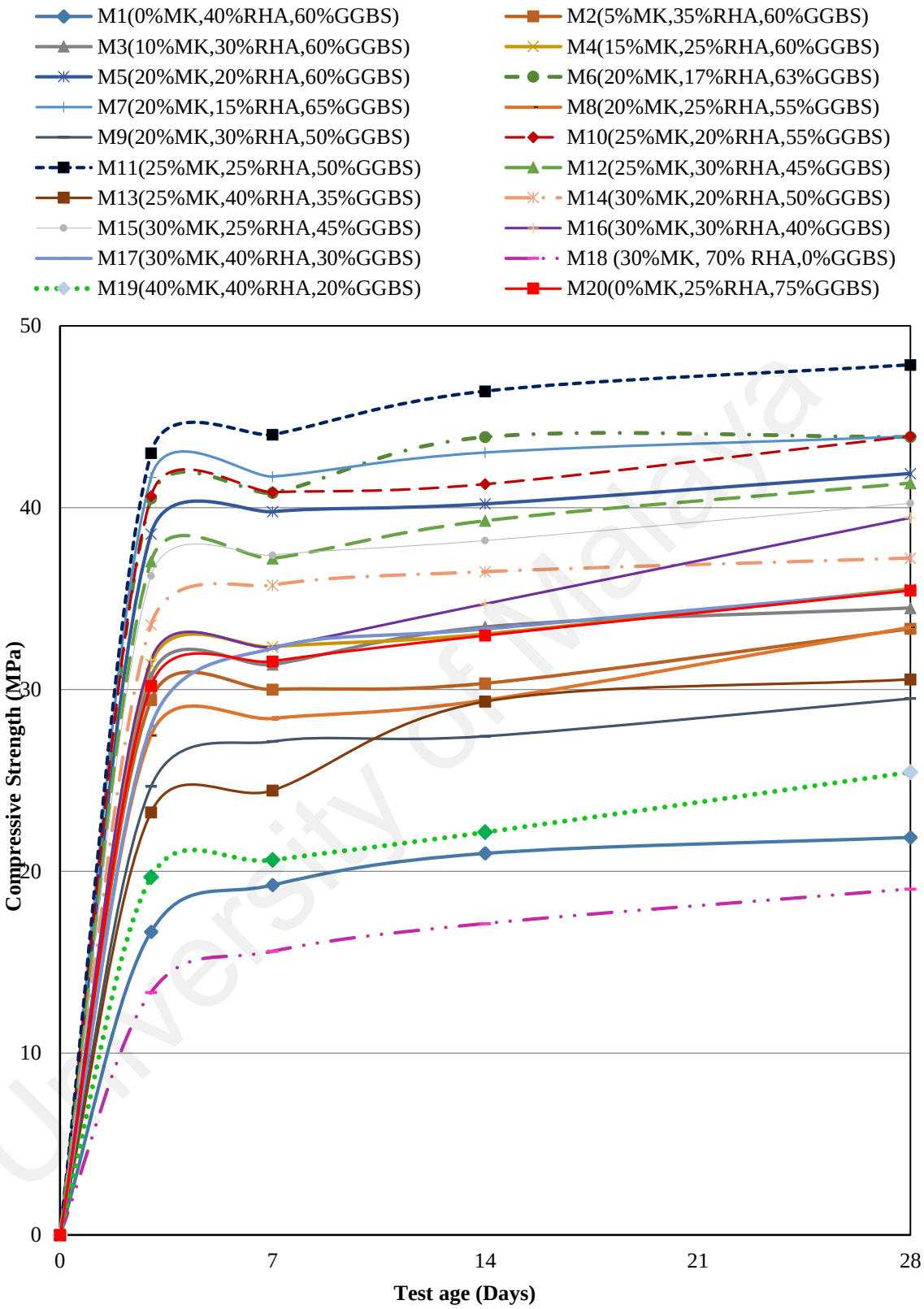

Figure 4.3: Development of compressive strength of mortar

Table 4.2: Increase of compressive strength with reference to 28-day strength (%)

Mixes	M1	M2	M3	M4	M5	M6	M7	M8	M9	M10	M11	M12	M13	M14	M15	M16	M17	M18	M19	M20
3 day	76	88	89	88	92	92	95	89	84	92.5	90	89.5	76	90	90	89	71	70	77	85
3 to 7 day	12	2	2	3	3	1	0	4.5	8	0.5	2	0.5	5	6	3	2	13	12	4	4
7 to 14 day	8	1	6	2	1	7	3	6.2	1	1	5	5	15	2	2	3	7	8	6	4
14 to 28 day	4	9	3	7	4	0	2	0.3	7	6	3	5	4	2	5	6	9	10	13	7

4.2.5 Analysis of Oxide Composition

As the oxide compounds of the binders participate in the geopolymerization reaction in the presence of an alkali activator, the development of the compressive strength greatly depends on the oxide composition of the ternary binders. Mixes M11 and M18 produced the highest and the lowest 28-day compressive strengths of 48MPa and 19 MPa, respectively, as shown in Table 4.3. Interestingly, these two mixes had different chemical oxide compositions, which could have affected the development of the compressive strength. As shown in Table 4.3, mixes M11 and M18 contained 23.34% of CaO, 52.54% SiO_2 and 17.15% Al_2O_3;and 0.93% CaO, 80.93% SiO_2 and 12.59% Al_2O_3, respectively. The difference in the quantity of CaO and Al_2O_3 in these mixes showed their influence on the development of the compressive strength. Mix M1, which contained 27.89% CaO, 56.88% SiO_2 and 8.45% Al_2O_3, also achieved a low compressive strength of about 22 MPa. The comparison between the oxide compositions of the mixes M1 and M11 proves that Al_2O_3 plays a significant role in the development of compressive strength in high-Ca based geopolymers. It is reported that Al_2O_3 produces crystalline sodium aluminate silicate (Zeolite), which has a negative effect on the development of the compressive strength; however, the presence of Ca^{2+} ion from the CaO hinders the formation of zeolite ((Chindaprasirt, De Silva, Sagoe-Crentsil, & Hanjitsuwan, 2012)). Also, in high Ca based geopolymers, the increase in SiO_2 content reduces the compressive strength ((Chindaprasirt et al., 2012)). This is noticeable in mixes M1 and M11, as these mixes

contained the same amount of SiO_2 but the former mix had more CaO content than the latter; in addition, it should be noted that mix M1 had a lower Al_2O_3 content than mix M11.

The role of SiO_2 in mixes M5 to M7 is obvious as these mixes have the same amounts of Al_2O_3 (17%) and CaO (28–30%); but the gradual reduction of SiO_2 content increased the compressive strength in these mixes. Almost all the mixes that contained SiO_2, Al_2O_3 and CaO of about 45–55%, 16–18% and 20–30%, respectively, produced high 28-day compressive strengths in the range of 40–48MPa.It was also noticed that although some of the mixes had adequate SiO_2, with Al_2O_3 below 16% they produced low compressive strength. The Al_2O_3 particles may also work as 'micro-aggregate' being unreacted/ undissolved in the geopolymer phase, as described by J Davidovits ((2008)), and increase the strength of the mortar.

Mix M19 contained 19.21% of Al_2O_3, but due to the lack of CaO content (9.86%), its influence on the development of compressive strength was low. Thus, the CaO content is vital for the appropriate activation of Al_2O_3. As half of the oxide composition of the mixes was comprised of SiO_2, its effect on the development of the compressive strength cannot be ignored. Further, an increase in the SiO_2 content increases the strength of geopolymers by providing low porosity to the whole structure (P. D. Silva et al., 2007). The increase in Al_2O_3 tends to hasten the setting of geopolymers, while the addition of SiO_2 hinders the setting (P. D. Silva et al., 2007) because the rate of condensation is reduced by the SiO_2 content (Ranjbar, Mehrali, Behnia, Alengaram, & Jumaat, 2014). As the Al_2O_3 content needs a high Ca based geopolymer to neutralize its harmful effect on the compressive strength, a certain amount of SiO_2 content is essential to delay the setting time (P. D. Silva et al., 2007). This is the combined role of oxide composition of ternary binders on the development of compressive strength of ternary blended geopolymer

mortars. Most of the mixes contained MgO of (1–2.5%),which was less than 5%. It should be noted that MgO exceeding 5% causes fissures in the hardened concrete (Islam et al., 2014b). Figure 4.4 shows the variation in the compressive strength with different percentages of oxide composition of ternary binders.

Table 4.3: Oxide compositions of ternary binders and results of compressive strength test

Mix No.	CaO (%)	SiO_2 (%)	Al_2O_3 (%)	MgO (%)	Fe_2O_3 (%)	Na_2O (%)	K_2O (%)	28-d Comp. Strength (MPa)	SiO_2/Al_2O_3 ratio
M1	27.89	56.88	8.45	2.18	0.69	0.21	1.03	21.87	6.73
M2	27.88	54.80	10.45	2.21	0.69	0.22	1.04	33.34	5.24
M3	27.86	52.71	12.45	2.23	0.70	0.24	1.05	34.48	4.23
M4	27.84	50.62	14.46	2.25	0.71	0.25	1.06	35.54	3.50
M5	27.83	48.53	16.46	2.27	0.71	0.26	1.06	41.88	2.95
M6	29.17	46.70	16.85	2.36	0.72	0.26	1.02	43.89	2.77
M7	30.07	45.48	17.11	2.41	0.73	0.27	1.00	43.91	2.66
M8	25.59	51.58	15.80	2.13	0.70	0.25	1.13	30.89	3.26
M9	23.35	54.63	15.14	2.00	0.68	0.24	1.20	29.5	3.61
M10	25.57	49.49	17.80	2.16	0.70	0.26	1.14	43.94	2.78
M11	23.34	52.54	17.15	2.02	0.69	0.25	1.21	47.85	3.06
M12	21.10	55.59	16.49	1.88	0.68	0.24	1.27	41.35	3.37
M13	16.62	61.68	15.18	1.60	0.65	0.21	1.40	30.56	4.06
M14	23.32	50.45	19.15	2.04	0.70	0.26	1.21	37.23	2.64
M15	21.08	53.50	18.49	1.90	0.68	0.25	1.28	40.20	2.89
M16	18.84	56.55	17.83	1.76	0.67	0.24	1.35	35.46	3.17
M17	14.37	62.64	16.52	1.48	0.64	0.22	1.48	39.44	3.79
M18	0.93	80.93	12.59	0.65	0.56	0.15	1.87	19.03	6.43
M19	9.86	64.56	19.21	1.25	0.62	0.22	1.63	25.46	3.36
M20	34.61	47.74	10.42	2.60	0.73	0.25	0.83	35.45	4.58

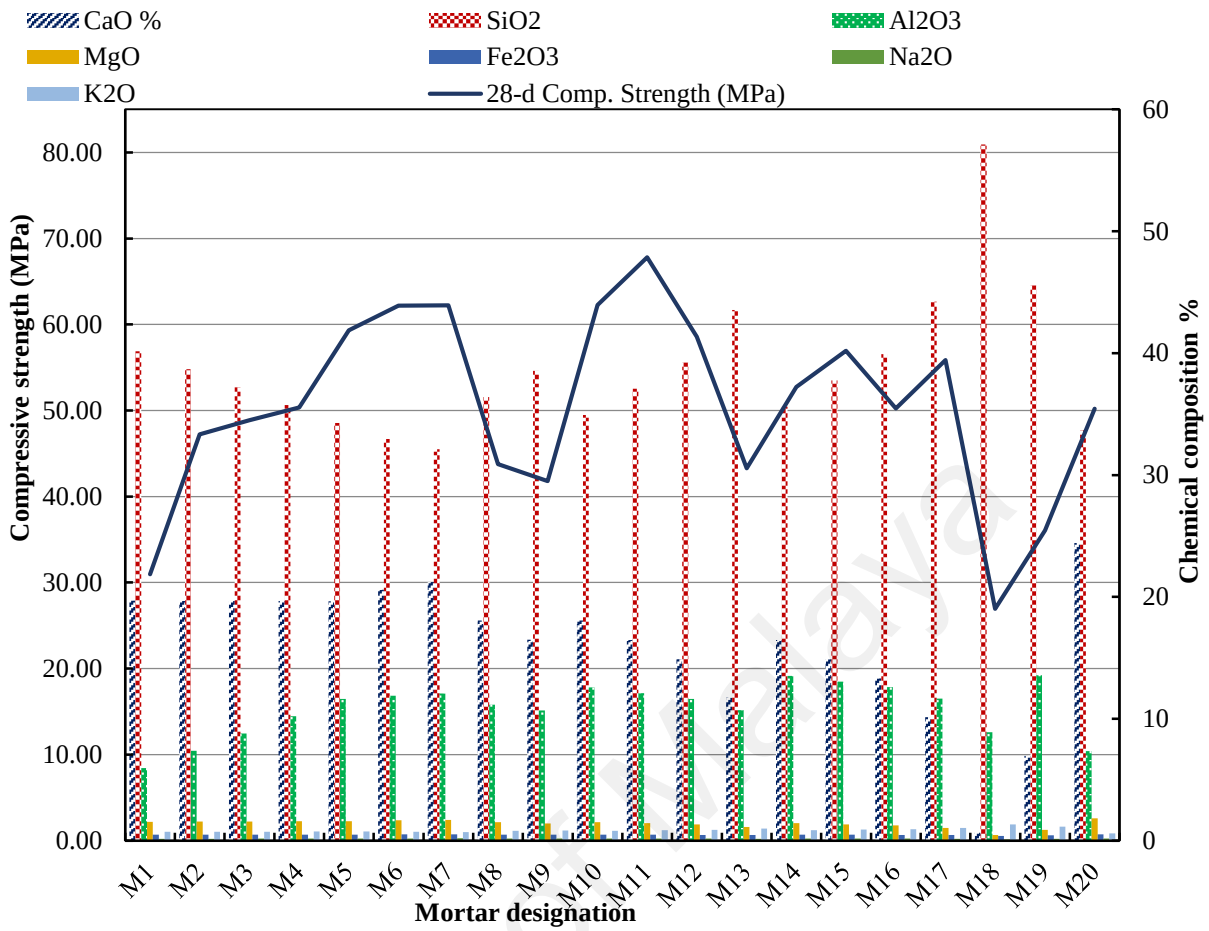

Figure 4.4: Variation of compressive strength with different percentages of chemical composition

4.2.6 Effect of Silica to alumina ratio

Table 4.3 shows that for the mixes M1 to M7, the SiO_2/Al_2O_3 ratio decreased from 6.73 to 2.66, and, as a consequence, the compressive strength increased from 21 to 44 MPa. As RHA contains about 90% SiO_2 content, the increase of SiO_2/Al_2O_3 ratio meant an increase in RHA content, which had a negative effect on the compressive strength. Table 4.3 shows that the highest 28-day compressive strength was achieved with a silica to alumina ratio of 3.06. At the highest silica/ alumina ratio 6.73, the 28-day compressive strength was only 21.87 MPa. In this experiment, as sodium hydroxide and sodium silicate were used as alkali activators, sodium provided an ordered structure and a strong

framework at a low Si/Al ratio. It is vital to note that in a given mix of this research work, the silica and alumina contents change as these undergo geopolymerization and hence SiO_2/Al_2O_3 ratio does not remain constant (Guo et al., 2010). Therefore, the rate of geopolymerization is affected by the SiO_2/Al_2O_3 ratio at different ages. The range of Si/Al ratio within 2.5 to 3.5 was found satisfactory in the compressive strength development.

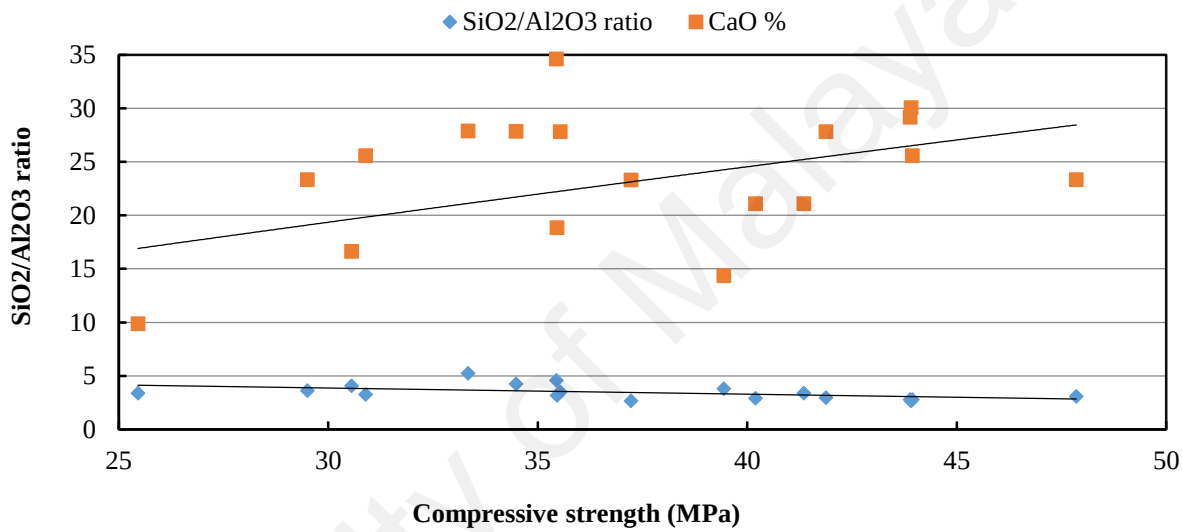

Figure 4.5: Combined effect of SiO_2/Al_2O_3 ratio and percentages of CaO on the development of compressive strength

4.2.7 Binary/ternary effect of binder on the strength of mortar

The influence of binary/ternary combination of the binder on the strength development could be seen from the oxide composition. The binary combination of RHA and GGBS produced a slightly lower 28-day compressive strength than the ternary combinations as seen from the cube compressive strengths of the mixes M1(40% RHA, 60%GGBS) and M20 (25% RHA, 75%GGBS) of 22 MPa and 36 MPa, respectively; and these were 54% and 25%, respectively lower than the highest compressive strength produced with the ternary combination of RHA, MK and GGBS, as shown in Table 4.3. This could be attributed to the fact that GGBS performs better in ternary combination of geopolymer

mortar. It has been reported previously that the optimum combination of cementitious materials for high strength depends upon the fineness of the siliceous materials and the C/S ratio (Alhozaimy, Al-Negheimish, Alawad, Jaafar, & Noorzaei, 2012). In this investigation, the fineness of GGBS and MK was higher than RHA and this was a good combination for synergic effect of ternary combination. (J. Wang et al., 2012) produced compressive strength of 80 MPa with the ternary combination of GGBS, MK and Fly ash and noticed that compressive strength increased with the addition of GGBS in the ternary combination. Another binary combination of the mix M18 containing 70% of RHA and 30% of MK produced compressive strength of about 19 MPa.

However, Susan A Bernal, Ruby Mejía de Gutiérrez, and John L Provis (2012) reported a 7-day compressive strength of about 40 MPa with a binary combination of 90% GGBS and 10% MK. In comparison, the ternary combination of RHA, GGBS and MK in mixes M5, M6, M7, M10, M11, and M12 produced a 28-day compressive strength in the range of 40-48 MPa and this could be attributed to different percentages of oxide composition of SiO_2, Al_2O_3 and CaO present in the ternary binders. The effect of a binary/ternary combination of binder has been reported by (M. R. Karim et al., (2013)). M. Karim, Zain, Jamil, and Lai (2013) reported a 28-day compressive strength of 18 MPa with 60%GGBS and 40% POFA; however, the use of ternary binders produced a 28-day compressive strength of 41MPa with a combination of 42% GGBS, 28%POFA and 30% RHA as binders. Sayed and Zeedan (2012) obtained a higher compressive strength of 18.0 MPa with a combination of 75% GGBS with 25% silica fume rather than the use of 100% GGBS. Chi and Huang (2013) also reported that the binary combination of GGBS with fly ash produced better strength than that of each individually in alkali activated mortar for the same conditions.

4.2.8 Effect of RHA on the development of compressive strength

The Si–O–Si bonds are produced from the oxide composition of silicon contributed by RHA which increase compressive strength and provide stiffness to the geopolymer. High specific surface area of RHA improves the property of ductility and its finer particle sizes make it more reactive for increasing the degree of geopolymerization (Chindaprasirt, Jaturapitakkul, Chalee, & Rattanasak, 2009). In the geopolymerization process, both the Si/Al ratio and the particle size of the binder materials greatly influence the performance of the final geopolymer products.

Different values of 28-day compressive strength were obtained for different percentages of RHA for three cases with constant contents of MK at 20%, 25% and 30% while the variation of GGBS for these mixes is in the range of 45–60%. It was observed that the addition of 15–30 % RHA with 20–25% MK and GGBS of up to 45–60% produced compressive strength in the range of 40-48 MPa. An increase in MK beyond 25% did not produce the desired compressive strength for any mix combination. Although 15% of RHA produced a comparable strength to that of 20% RHA, (Table 4.3), the use of 25% RHA is recommended, as it produced the highest 28-day compressive strength of about 48 MPa. Further, the optimum use of RHA to produce sustainable concrete is vital in the development of geopolymer concrete. The use of large amount of RHA with relatively larger RHA solid particles and low specific gravity of RHA produce weaker and less ductile geopolymeric mortar (Chindaprasirt et al., 2009). Hence, mortar with a large amount of RHA cannot be compacted properly and the strength of the mortar reduces. 28 day compressive strength of mix M18 containing RHA of 70% was found 19 MPa which was far lower than the highest 28 day compressive strength. The compressive strength of this mix may also be reduced for using RHA at 70% because more unreacted RHA may be present in the end products (Chindaprasirt et al., 2009). Moreover, the density of the

geopolymer binders is reduced when the organization of Si and Al is disturbed because of the higher concentration of soluble Si (Peter Duxson et al., 2005) and as a consequence compressive strength of geopolymer binder is also reduced. Larger quantities of alumina quicken the setting but weaken the cement (Punmia, Jain, & Jain, 2003). In the mix M7, M10, M11, M14, M15, M19, the presence of high amount of alumina (17 to 19%) due to large proportions of MK and GGBS could lead to increase of aluminate species. This increased aluminate ($Al(OH)_{4-}$) species become available for the reaction leading to a faster rate of condensation between $Al(OH)_{4-}$ and the silicate species with shorter setting times. Sometimes, casting becomes difficult due to the quick setting times. Hence, it is required to use a source high in SiO_2, which provides more silicate species available for condensation. The rate of condensation between the silicate species is slow, which normally leads to longer setting times.

4.2.9 Effect of Metakaolin on the development of compressive strength

MK reacts with alkaline solutions, which forms amorphous to semi-crystalline three-dimensional networks by polycondensation (Maragkos, Giannopoulou, & Panias, 2009) and this polycondensation forms an alumina-silicate network (Buchwald et al., 2007). It was observed from the compressive strength results of mixes M1 to M5 that the compressive strength increased with the increment of MK. Figure 4.6 shows that effect of MK on the 28-day compressive strength development while maintaining GGBS constant at 60%; however, the RHA content was varied to adjust the variation in MK content. It can be seen that the 28-day compressive strength of the mix with 5% of MK showed an increase of about 35% compared to binary mix M1 without MK. However, from the oxide composition as shown in Table 4.3, it is evident that there is no significant changes in the oxide composition when MK was varied between 5 and 15%. Among the mixes M2–M5, the mix with 20% MK (20% RHA and 60% GGBS) produced the highest

28-day compressive strength of 42MPa. The inclusion of small amounts (10–20%) of MK on the alkali-activation system provides additional aluminium to the responding system (Bernal, Provis, Rose, & Mejía de Gutierrez, 2011), which leads to the formation of a more polymerized structure. This polymerized structure enhances the rigidity of the binder and hence the compressive strength.

The effect of variation of MK between 20 and 30% has been shown while keeping RHA constant at 20%, 25% and 30%; however, GGBS content was adjusted to keep MK and GGBS in proportion with RHA content. The mix with 25% MK, 25% RHA and 50% GGBS produced the highest 28-day compressive strength of about 48MPa. As MK provides more Si–O–Al and Al–O–Al bonds rather than stronger Si–O–Si bonds, a large amount of MK is not desirable (Peter Duxson et al., 2005). Moreover, a large amount of MK creates sodium alumina silicate (zeolite) due to the excess alumina present, which has a negative effect on the development of strength (Bernal et al., 2011). Mixes M14 and M19 both contain about 19.20% Al_2O_3 and they possess 30% and 40% MK respectively with NaOH concentration of 14M which provide satisfactory alkalinity to stimulate the dissolution of MK (Susan A Bernal et al., 2012). At this high activator concentration of NaOH, the polymer formation is delayed due to the decrease of the mobility of ions (Alonso & Palomo, 2001). Moreover, MK produces massive precipitation of the alkaline alumina silicate while activated with higher activator concentration (Alonso & Palomo, 2001). A large proportion of MK needs an activator content with a very high concentration for dissolution resulting in huge undesirable precipitation and overall hampering of the polymerization process. Therefore, the increase of only 10% MK reduces the compressive strength about 32%. Thus, the inclusion of MK over 25% reduces the compressive strength. Hence, there should be an optimum MK replacement in geopolymer concrete.

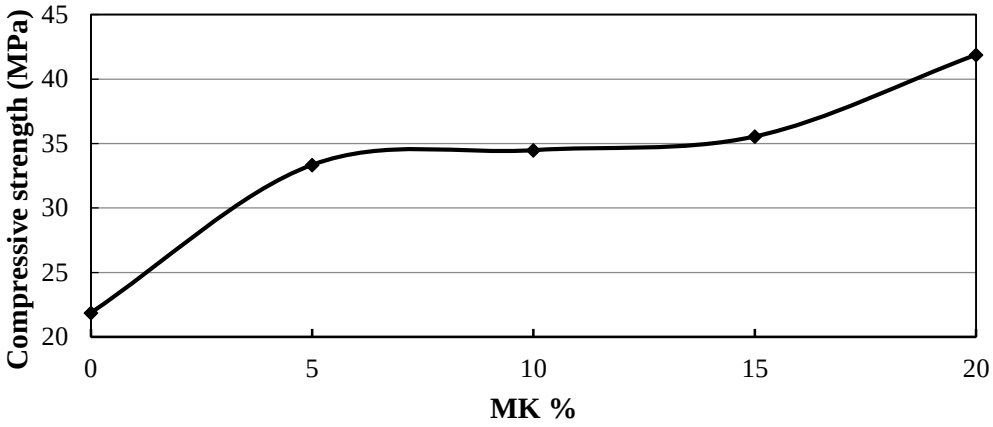

Figure 4.6: Variation of compressive strength with different percentages of MK for fixed 60% GGBS and variable RHA%

4.2.10 Effect of GGBS on the development of compressive strength

The addition of GGBS improves the compactness as well as the compressive strength, and the development of strong calcium based gel structure is the unique property of alkali-activated slag concrete (Shi, Jiménez, & Palomo, 2011). The increased activator concentrations are necessary to sustain a high pH and to help the dissolution of silica and alumina from the GGBS (Teoreanu, Volceanov, & Stoleriu, 2005). Figure 4.3 shows that the mixtures M18 (30% MK, 70% RHA & 0% GGBS) and M19 (40% MK, 40% RHA & 20% GGBS) produced a 28-day compressive strength of about 19 MPa and 25 MPa, respectively. These strengths were 60% and 48% lower, respectively, than the highest compressive strength produced for the mix M11 with 50% GGBS. As highest 28-day compressive strength is produced for mix M11 where GGBS content is 50% of the total binder content, GGBS contributes the most among the ternary binders for the increase of compressive strength in ternary blended geopolymer mortar. This can be attributed to the fact that GGBS produces calcium silicate hydrate and calcium aluminium hydrate which contributes to the hydroxylation of geopolymerization (J. Wang et al., 2012). The role of

GGBS in the development of strength can be seen from the results of the compressive strengths for the mixes M7 to M18; as the amount of replacement of GGBS with RHA increased, the strength decreased. In contrast, a reduction in RHA and subsequent increase in GGBS enhanced the strength. Another significant finding is that when the GGBS was reduced to below 45%, there was a reduction in the compressive strength and a 28-day strength of less than 40 MPa was obtained. GGBS is one of the most favourable raw materials that can be used to enhance the compressive strength as the geopolymerization process can be greatly influenced by the addition of high-calcium slag (Z. Li & Liu, 2007). About 60% of the oxide composition of GGBS consists of CaO and Al_2O_3 which play a significant role in the geopolymerization process during the development of the tetrahedral aluminium and a charge balancing cation Ca^{2+} provides electroneutrality to the geopolymer structure (Davidovit, 2002). The studies (Ch K Yip et al., 2005; Christina K Yip, Lukey, Provis, & van Deventer, 2008)) have reported about the positive effect of Ca on the compressive strength of geopolymer mortar. GGBS has higher apparent activation energy and it can develop early age strength at a slightly higher temperature than the standard curing temperature (Barnett et al., 2006). The early-age reactions are mainly associated with dissolution and precipitation mechanisms by the alkali activated solution (Fernández-Jiménez, Puertas, & Arteaga, 1998). Mixes M11 and M7, with 50% and 65% GGBS, respectively, produced a 28-day compressive strength of about 48 MPa and 44 MPa, respectively, which could be attributed to the combined effect of RHA and MK; the use of a higher percentage of both RHA and MK (25% each) performed strongly compared to 20% of MK and 15% of RHA in mix M7. Kannan and Ganesan (2014) reported that the replacement of OPC with a combination of 15% RHA and 15% MK produced a 28-day compressive strength of 56 MPa. To keep the balance in the Si/Al ratio, it is necessary to use the maximum amount of RHA, and, hence, the mix with the combination of 25% MK, 25% RHA and 50% GGBS produced the highest 28-day

compressive strength of about 48 MPa. As seen from Table 3.6 and Table 4.3, the use of GGBS were from 0–75% in the mixes; however, the mixes with 45–65% of GGBS produced satisfactory results of about 40–48 MPa. (Islam et al., 2014a) reported that the compressive strength of mortar with 70% GGBS produced the highest strength while a greater increase in the GGBS content decreased the compressive strength.

4.2.11 Effect of Molarity of Alkaline Activated Solution on Development of Compressive Strength

Table 4.4 shows the difference between 28-day compressive strength of the mixes with 14M and 12M. The compressive strengths at the age of 28-day for the mixes with 12M were found 10 to 28% lower than the corresponding strengths of the mixes with 14M. Another noticeable feature was that the mixes with 12M and 20% MK, 15-20% RHA and 60-65% GGBS produced 10-12% lower 28-day compressive strength than the corresponding mixes with 14M; however, the increase of MK (25%) and RHA (20-30%) and respective decrease in GGBS (45-55%) in the mixes with 12M produced about 28% lower 28-day compressive strength than the mixes with 14M. This phenomena could be attributed to the fact that high Ca-based geopolymer (GGBS>60%) can produce desired compressive strength under the concentration of 12M ((Islam et al., 2014b)). The bonding of solid particles is the most significant part of the geopolymeric system and the concentration of sodium hydroxide plays very important role to make this bonding stronger (Pierre et al., 1999). The greater dissolution of the initial solid materials is possible with the use of high concentration of sodium hydroxide and geopolymerization reaction becomes faster (Soroushian, Khan, & Hsu, 1992). Hardjito et al. (2001) reported that higher concentration of sodium hydroxide solution produced a higher compressive strength. (Bashar et al., (2014)) also showed that the mortar mixes produced higher compressive strength with 14M than the mixes with 12M.

Table 4.4: The difference between 28-day compressive strength of the mixes with 14M and 12M

Mortar designation	Mix proportion of binder MK: RHA: GGBS (%)	Binder: M-Sand	Molarity of Alkali activator	28-Day compressive strength (MPa)
M5	20:20:60	1:2	14	41.88
M6	20:17:63	1:2	14	43.89
M7	20:15:65	1:2	14	43.91
M10	25:20:55	1:2	14	43.94
M11	25:25:50	1:2	14	47.85
M12	25:30:45	1:2	14	41.35
M5 B	20:20:60	1:2	12	37.50
M6 B	20:17:63	1:2	12	38.88
M7 B	20:15:65	1:2	12	39.20
M10 B	25:20:55	1:2	12	32.00
M11 B	25:25:50	1:2	12	34.50
M12 B	25:30:45	1:2	12	30.00

Note: RHA-Rice husk ash; Mk-Metakaolin; GGBS-Ground granulated blast furnace slag

4.3 Microstructural investigation of ternary blended geopolymer mortar

4.3.1 General

Microstructural investigation helps to find the role of oxide composition on the development of compressive strength for ternary blended geopolymer mortar. This section represents the results from different microstructural test such as XRD, SEM and EDS and the explanations regarding how oxide composition of ternary binders help to increase the compressive strength of geopolymer mortar. The role of oxide composition needs to be investigated because in ternary combination of cementless binder, oxide

composition of each source material produces a new oxide composition of ternary blended mortar and the main source of alumina-silicate network for geopolymer consists of two oxides of silica and alumina. Therefore, the investigation on role of oxide composition of geopolymer mortar is noteworthy.

Table 4.5: Mix proportion of the mixes with microstructural tests

Mix No.	MK	RHA	GGBS	NaOH (Molarity)
MRG1/M11	25	25	50	14
MRG2/M10	25	20	55	14
MRG3/M16	30	30	40	14
MRG4/M2	5	35	60	14

4.3.2. SEM and EDS analysis of raw materials

Figures 4.7.1-4.7.3 show SEM micrograph and EDS analysis results of source materials. SEM image of RHA shows larger solid particles and porous structure compared to that of MK and GGBS. Figure 4.7.4 shows the SEM image of M-sand. It is observed from the EDS elemental analysis, that RHA, MK and GGBS contained the pozzolans of silicon, aluminium and calcium, respectively. SEM and EDS analyses of these three source materials justified the necessity of using these materials. Geopolymer is formed through alumina-silicate network and from EDS analysis, it is seen that MK has around 11 times higher aluminium content than RHA and GGBS.

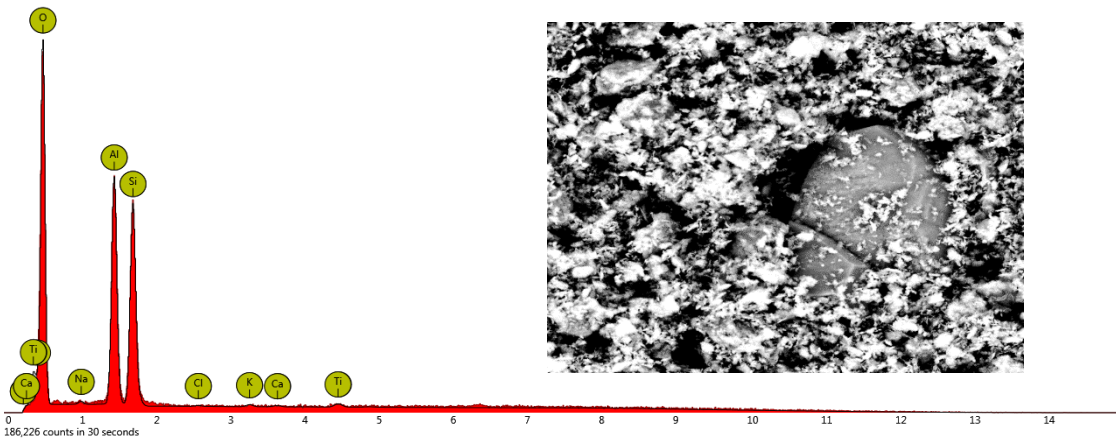

Figure 4.7.1: SEM Micrograph and EDS of MK

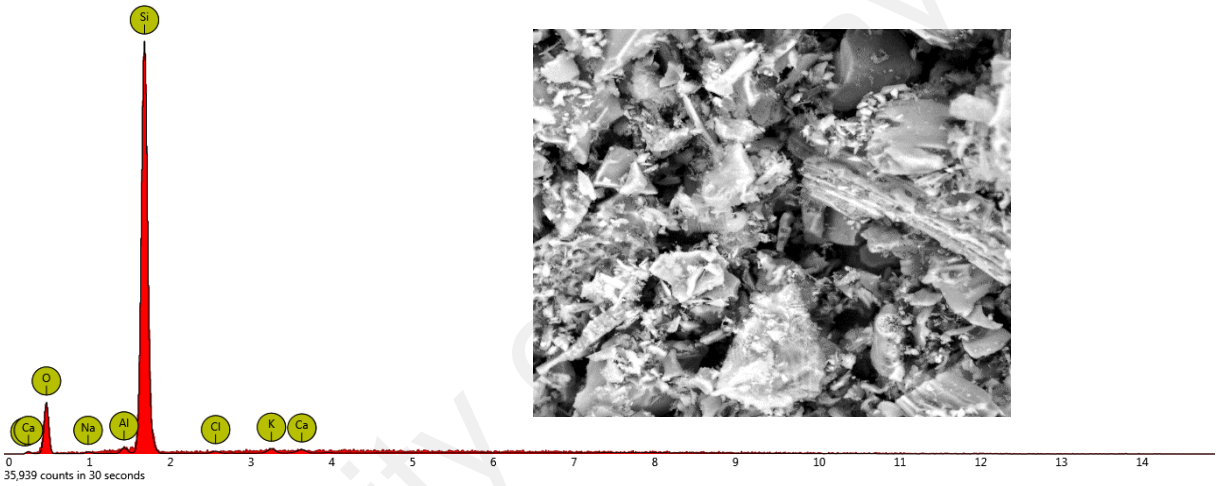

Figure 4.7.2: SEM Micrograph and EDS of RHA

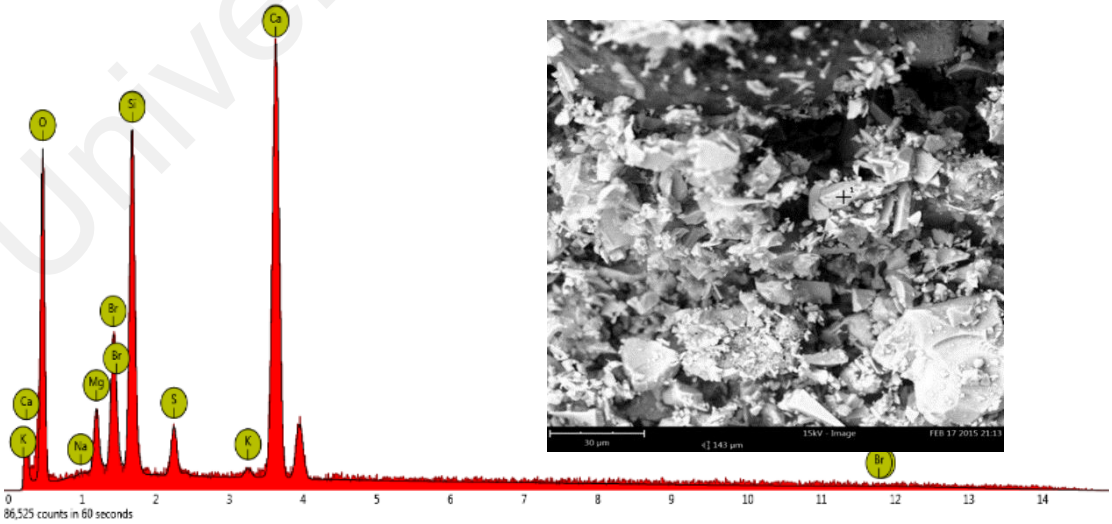

Figure 4.7.3: SEM Micrograph and EDS of GGBS

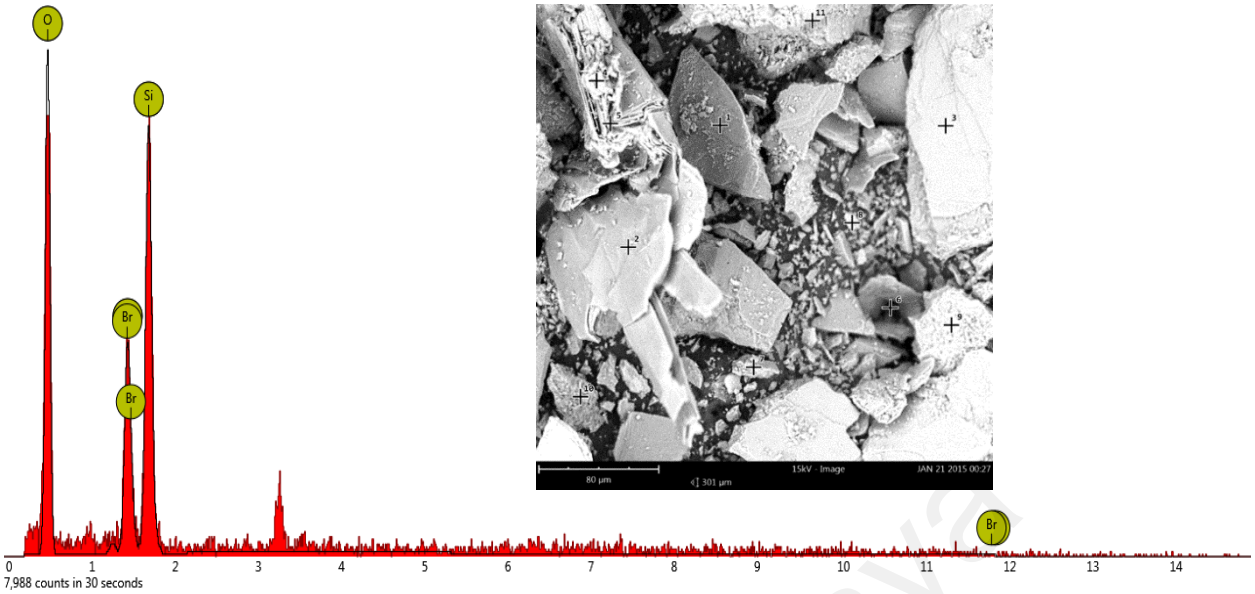

Figure 4.7.4: SEM Micrograph and EDS of M-sand

Table 4.6: Element percentages from EDS results are given below:

Element Symbol	O	Si	Al	Ca	Na	K	Cl	Br	Mg
MK (atom conc.)	77.8	9.6	11.7	0.1	0.5	0.1	0.1	0.1	
RHA (atom conc.)	54.8	42	0.7	0.7	0.6	0.8	0.4		
GGBS (atom conc.)	71.5	8.6	1.2	13.2	0.1	0.3		2.3	2.8

4.3.2 XRD Analysis of Mortar

The amorphorsity of the different products changed with the composition of the base materials present in the binders as shown in Figure 4.8. MK has the highest composition of Al_2O_3, and it appeared that the amorphorsity of the samples decreased as the alumina composition decreased. MRG3 sample that was composed of the highest quantity of MK showed a conspicuous diffractive halo within the 2-theta angle of 20-40 deg, whereas, such attribute was found to be gentle in the case of MRG4 that contained the least MK. The similitude of the diffractive halo of MRG1 and MRG2 could be traced to their equal quantities of MK. Furthermore, MRG3 also displayed the formation of calcium silicate

aluminium hydrate (C-A-S-H). This was caused by the excessive presence of tetrahedral alumina in IV fold coordination in that sample compared to the others. Alumina is capable of reacting with the lime (CaO) in GGBS and the silicic acid formed silica emanated from

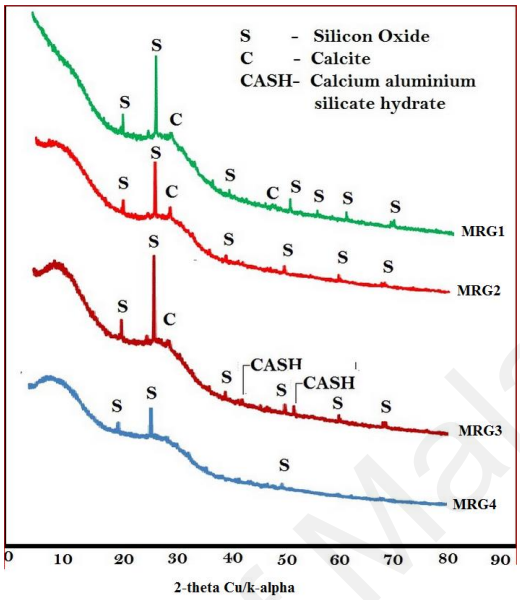

Figure 4.8: XRD diffractogram of different MK-RHA-GGBS mortars

RHA in the hydroxylation process to form geopolymer gel of calcium alumina-silicate hydrates as shown in Eq. 1 (Yusuf, Johari, Ahmad, & Maslehuddin, 2014). (Yusuf, Megat Johari, Ahmad, & Maslehuddin, (2014)-a) reported that calcium would always react preferentially to sodium in such reaction.

$CaO+H\text{-}Si\text{-}O\text{-}Al\text{-}OHCa+OH^{-} \rightarrow OH\text{-}Si\text{-}O\text{-}AlCaOH+Ca(OH)_2$ ……. (1)

From the MRG1 product, it is evident that the formation of calcite was connected to the reaction of lime (CaO) in the GGBS with the ambient CO_2 thereby leading to the formation of $CaCO_3$ as shown below.

$CaO+CO_2 \rightarrow CaCO_3$…….. (2)

The formation of calcite ($CaCO_3$) in the diffractogram of MRG1 and MRG2 could have contributed to the compressive strengths of 47 MPa and 45 MPa that were obtained in the

mortars, respectively as these peaks were absent in the XRD of MRG3 and MRG4 , which had the strengths of 35.46 and 33.34 MPa, respectively. In other words, there seems to be a relationship between the formation of calcite and SiO_2/Al_2O_3 (molar ratio) of the products. Table 4.6 shows the variation in 28-d compressive strength with the variation in molar ratio of different oxides found from XRF analysis. The calcite was formed when the molar ratio was within 4.7 to 5.2 as noted in the MRG1 and MRG2, whereas the ratio became 5.30 and 8.91 in the MRG3 and MRG4, respectively.

Further, upon examining the $CaO/(SiO_2+Al_2O_3)$ relationships with the strength in the products, it is evident that the values was 0.399 and 0.45 for MRG1 and MRG2, respectively. Excess MK in MRG3 at the expense of GGBS and shortage of MK in MRG4 in favour of GGBS caused this to become 0.301 and 0.49, respectively. Similarly, the $SiO_2/(CaO +Al_2O_3)$ ratio could also be used as an indicator for geopolymer strength prediction. For instance, the ratio became 1.307 and 1.497 for MRG1 and MRG2, respectively, whereas it increased to 1.84 and 1.52, respectively in MRG3 and MRG4. Thus, excessiveness in any of the base materials at the expense of others might affect the mineral composition substantially as reflected by the indices and the compressive strength values.

Therefore, for ternary blending geopolymer the SiO_2/Al_2O_3, $CaO/(SiO_2+Al_2O_3)$ and $SiO_2/(CaO +Al_2O_3)$ could be the best indicators to predict the compressive strength values of the synthesized binder. Thus, attention should be paid to the mineral composition of base materials in the synthesis of geopolymer binder as the agglomeration of monomers from these material precursors determines the alumina-silicate framework and its solid skeletons.

Table 4.7: Variation in 28-d compressive strength with the variation in molar ratio of different oxides found from XRF analysis

Mix No.	CaO %	SiO_2	Al_2O_3	SiO_2/Al_2O_3 molar ratio	$SiO_2/(CaO+Al_2O_3)$ molar ratio	$CaO/(SiO_2+Al_2O_3)$ molar ratio	28-d Comp. Strength (MPa)
MRG1(M11)	23.34	52.54	17.15	5.21	1.49	0.39	47.85
MRG2(M10)	25.57	49.49	17.8	4.73	1.31	0.45	43.94
MRG3(M16)	18.84	56.55	17.83	5.39	1.84	0.30	35.46
MRG4(M2)	27.88	54.8	10.45	8.91	1.52	0.49	33.34

4.3.3 Microstructural impacts of the products due to variation in the base materials

Element	Ca	Si	O	Al	Na	K	Mg	Total
Concentration (wt)	32	10.8	43.6	4.1	7.3	1	1.2	100
Concentration (atom)	18	8.6	61.2	3.4	7.1	0.6	1.1	100

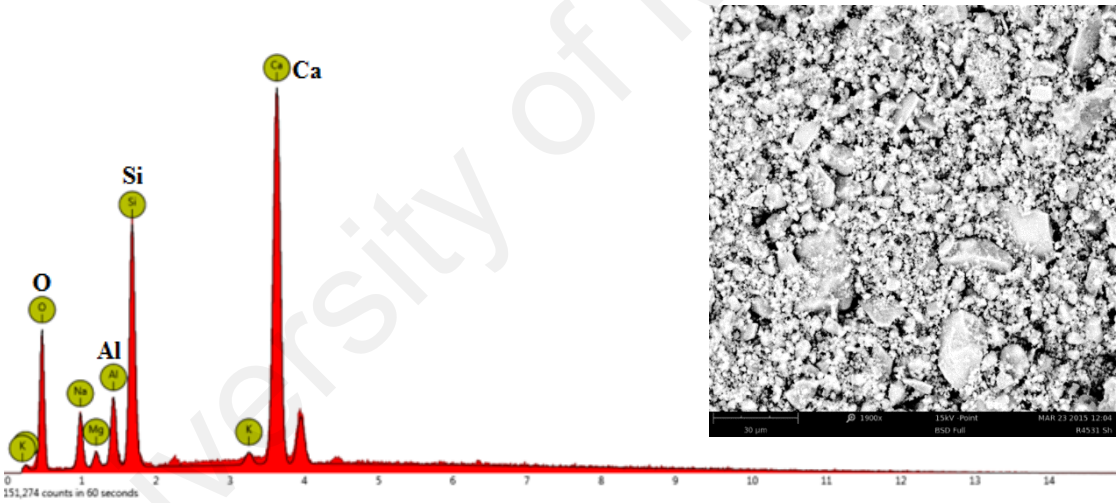

Figure 4.9: SEM micrograph of MRG1 and wt and atom percentage of element

The textures of the micrographs of MRG1 show a continuous dense microstructure with uniformly distributed pores in figure 4.9. This reveals the reason for its maximum compressive strength (48 MPa). The percentage composition of the product elements - Ca (32%), Si(10.8%), Al(4.1%) and O(43.6%) as given by the EDS – can be combined such that the CaO/SiO_2, $CaO/(SiO_2+Al_2O_3)$ and $SiO_2/(CaO+Al_2O_3)$ were varied as 0.630.77, 0.25-0.32 and 0.46-0.48, respectively.

Conversely, the micrograph of MRG2 shows a localized microstructural crack within the matrix in figure 4.10. This implies that there exists a weak zone with the microstructure thereby explaining the reason why the strength obtained in the MRG1 exceeded that of MRG2. The closer observation of EDS of MRG2 points to the fact as the CaO/SiO_2, $CaO/(SiO_2+Al_2O_3)$ and $SiO_2/(CaO+Al_2O_3)$ values were in the range of 0.21-0.51, 0.17-0.21 and 0.367-0.44, respectively. The wide range of these values indicate the less uniformity and density of the microstructure of MRG2 compared to MRG1.

Element	Ca	Si	O	Al	Na	S	Mg	Total
Concentration (wt)	11.6	10.9	57	7.2	6.7	0.5	6.1	100
Concentration (atom)	5.7	7.7	70.3	5.3	5.7	0.3	5	100

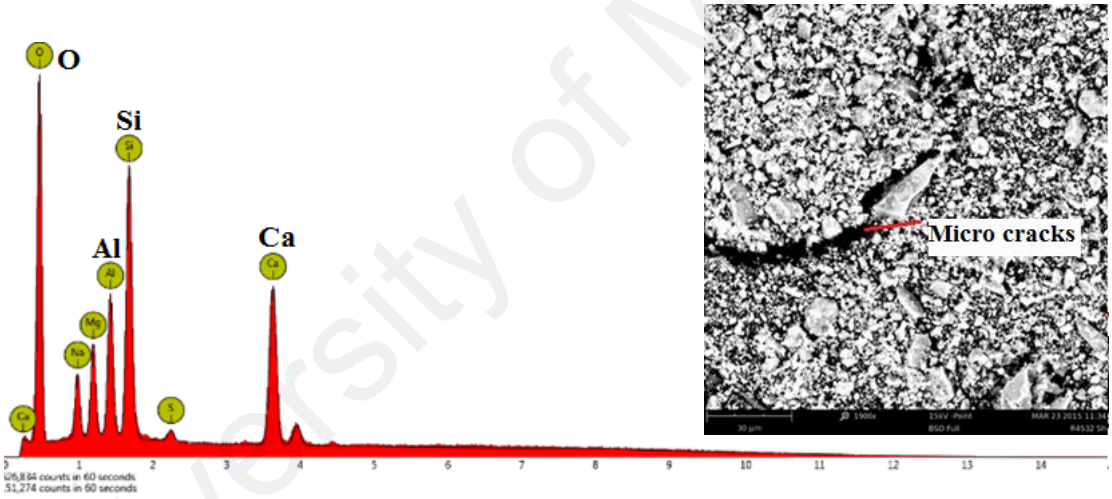

Figure 4.10: SEM micrograph of MRG2 and wt and atom percentage of element

The sample MRG3 that had a substantial amount of MK with lesser CaO compared to MRG1 and MRG2. This is reflected in the disparity of the micrographs with that of MRG1 and MRG2. The CaO/SiO_2, $CaO/(SIO_2+Al_2O_3)$ and $SiO_2/(CaO+Al_2O_3)$ in MRG3 of region A of figure 4.11 were in close proximity with MRG2 such as 0.46-0.52, 0.19-0.21 and 0.50-0.52 respectively. But this region A is only circle area in the micrograph. However, the micrograph shows a very low Ca content (0.7-10.1%) with an increase in the Al content (4.2-7.4%) when compared to MRG1 that had a high Ca (21.3-31.2%) and

moderate Al content of in the range of 4.1-7.9%. Excess and non-uniform alumina composition and the reduced Ca content caused the reduction in the compressive strength of MRG3 (35.46 MPa) when compared to MRG1 (47.85 MPa).

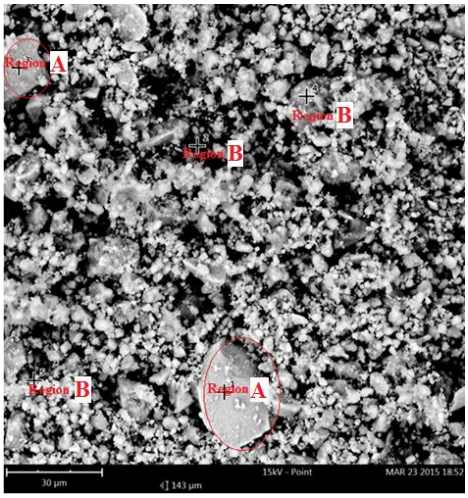

Element (Region A)	Ca	Si	O	Al	Na	S	Mg	Total
Concentration (wt)	11.3	10.5	41.1	5.5	26.4	0.4	4.8	100
Concentration (atom)	5.9	7.8	53.7	4.2	24	0.3	4.1	100

Element (Region B)	Ca	Si	O	Al	Na	K	Mg	Total
Concentration (wt)	1.5	19.4	57.4	10.3	9.5	1.1	0.8	100
Concentration (atom)	0.7	13.4	69.3	7.4	8	0.6	0.6	100

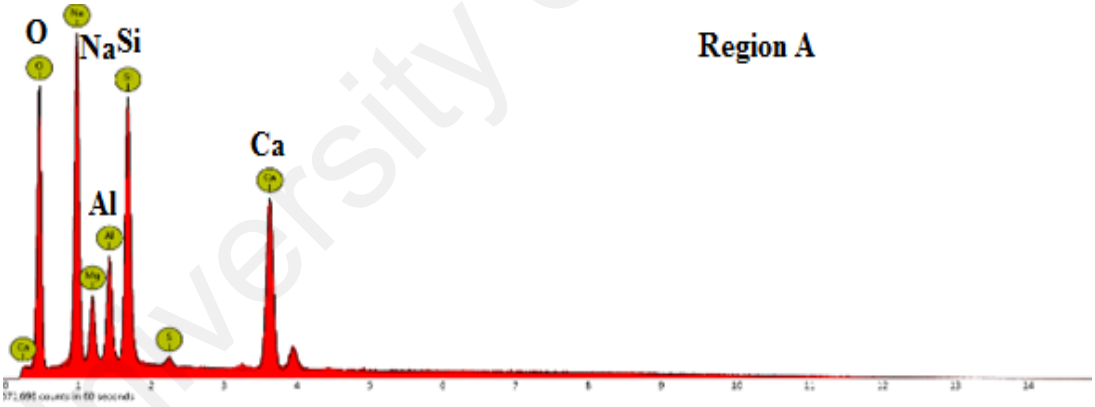

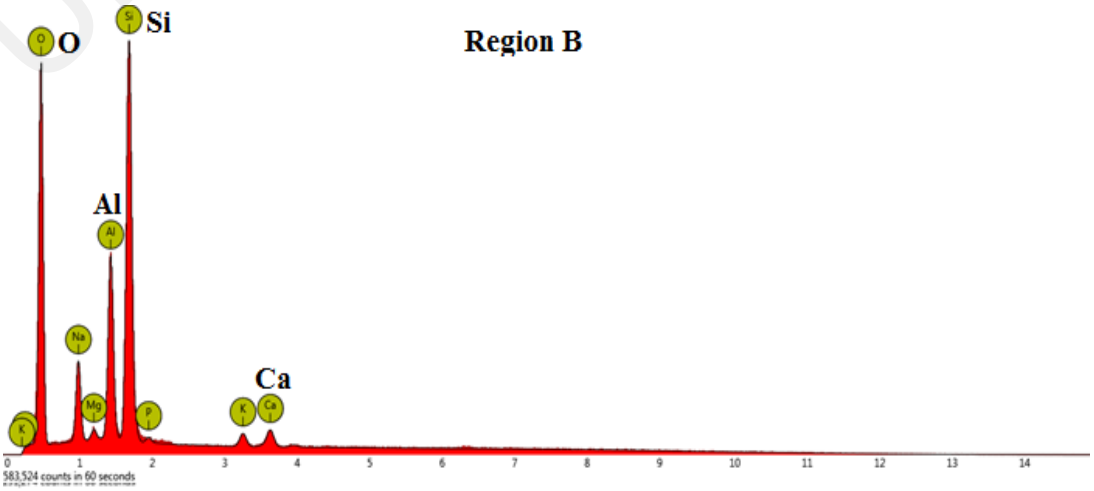

Figure 4.11: SEM micrograph of MRG3 and wt and atom percentage of element for Region A (top) and Region B (bottom)

The micrograph of MRG4 shows the formation of two different products as shown in the region A and B of Figure 4.12 with the distinctive the CaO/SiO_2, $CaO/(SiO_2+Al_2O_3)$ and $SiO_2/(CaO+Al_2O_3)$ of 0.695, 0.29 0.482 (region A), and 0.45, 0.19 and 0.58 (region B), respectively. Similarly, the Ca/Si ratios were 0.19 and 2.11 while the Ca/Al were 1.4 and 9.37 in the regions A and B. respectively.

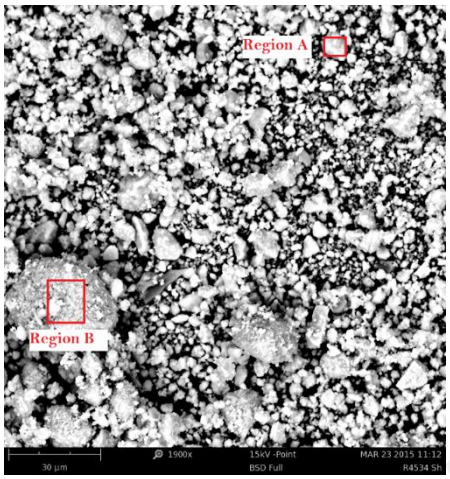

Element (Region A)	Ca	Si	O	Al	Na	K	Mg	P	Total
Concentration (wt)	4.2	21.6	60.8	3	7.8	0.7	1.2	0.7	100
Concentration (atom)	2	14.8	72.9	2.2	6.5	0.3	0.9	0.4	100

Element (Region B)	Ca	Si	O	Al	Na	K	Mg	Total
Concentration (wt)	28.1	13.3	48.4	3.4	4.2	1.6	1	100
Concentration (atom)	15.3	10.3	65.9	2.8	4	0.9	0.8	100

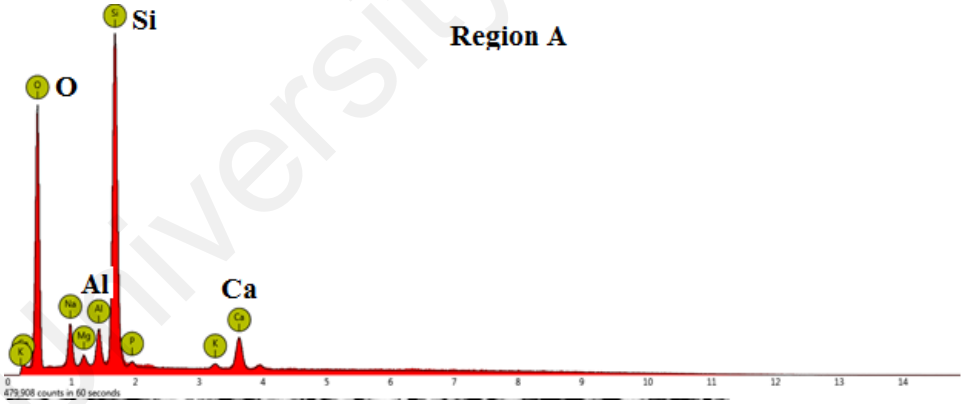

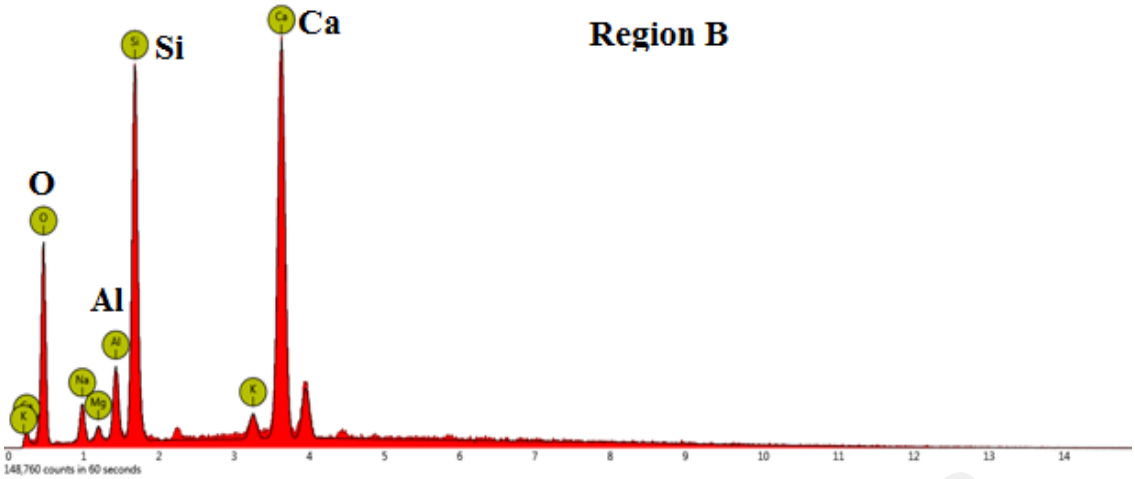

Figure 4.12: SEM micrograph of MRG4 and wt and atom percentage of element for Region A (top) and Region B (bottom)

This suggests that region A is dominated by C-A-S-H while B is controlled by C-S-H due to preponderance of Ca relative to Al in that region. The pocket of C-S-H products formed with the C-A-S-H could be responsible for the decreased in the strength recorded when compared to MRG1 and MRG2 whose products appeared to be dominated by C-A-S-H formations.

4.4 Fracture properties of steel microfiber reinforced mortar

4.4.1 General

Investigation on fracture properties of geopolymer concrete is important because fracture test can measure ductility of concrete and ductility of concrete is one of the vital characteristics of structural elements for serviceability requirement. This section represents the results of fracture energy from load-deflection curve of steel microfiber reinforced mortar and the discussions about the effect of steel microfiber on the fracture properties of mortar.

4.4.2 Load deflection curve

The load–deflection curve for the prism mortar specimens investigated in this study is shown in Figure 4.13. One of the noteworthy outputs of using steel microfiber in mortar is to create a torturous path of crack propagation. The control mortar mix F0 produced the lowest load of 382 N and as expected it produced the lowest final deflection of about 1.1 mm. Also the post-peak curve was drastic and hence the area under this curve was found very narrow. The effect of steel microfiber in the mortar can be seen through the increase in the flexural load, low crack width, wider post-peak curve, fracture energy and fracture toughness. The value of peak load was 815 N for the mix F1 with 1 % steel microfiber and its post-peak deflection continued beyond 10 mm. The load deflection curve shows enhancement with the increased percentages of microfiber gradually. This phenomenon could be attributed to the interaction between approaching crack and microfiber (Ostertag & Yi, 2007). Another aspect of the fibre is its crack bridging mechanism. Crack starts from the notch and propagate along the width of the prism. The possibility of placing microfibers is along the length of the prism. During the propagation, when crack faces the microfiber at lower angle or parallel to the direction of crack propagation, then the path of crack propagation becomes easy. On the contrary, when crack finds the microfiber at larger angle or perpendicular to the direction of crack propagation, then a torturous path of crack propagation occurs. This is called fiber bridging as shown in Figure 4.14 for which load releases very slowly from the maximum load capacity and specimens take long time to break after the initiation of crack (Ostertag & Yi, 2007). This provides the safety to the structure. Figure 4.15 shows that with the increase of fiber percentages, crack width decreases from 1.56 mm to 1.13 mm. In mortar with fibers, generally the crack path is torturous. At low water/cement ratio, the density of the matrix increases and crack path becomes more torturous (Ostertag & Yi, 2007). Here, as w/c ratio was lower and kept same for all mixes, difference in tortuosity of crack

path was mostly influenced by percentages of microfibers used. Multiple micro cracking is observed along the length of the fibre. Debonding, sliding and pulling-out of the fibers are the local mechanisms that control bridging action. The use of 3% microfiber provided proper bridging action and abruptly reduced crack width (Ostertag & Yi, 2007).

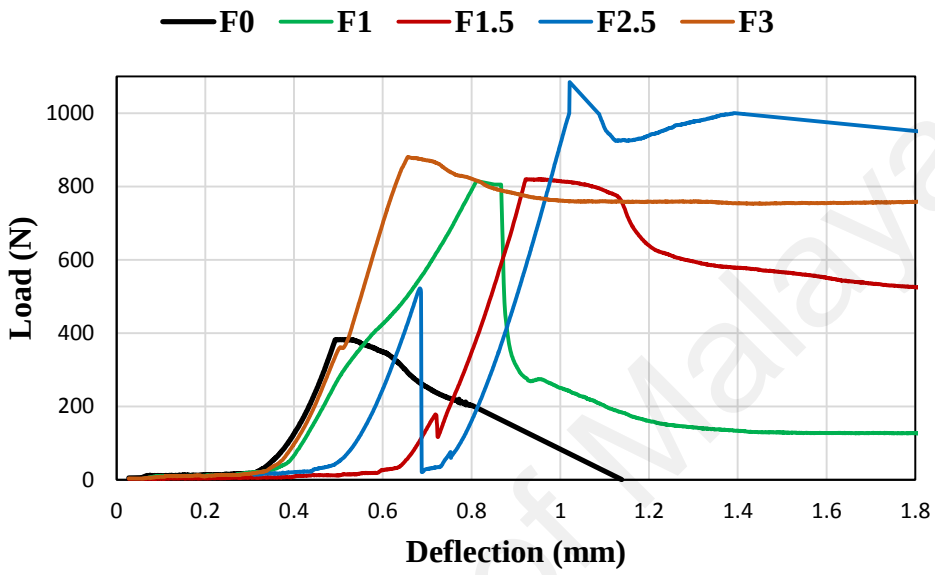

Figure 4.13: Influence of fiber on load-deflection curve

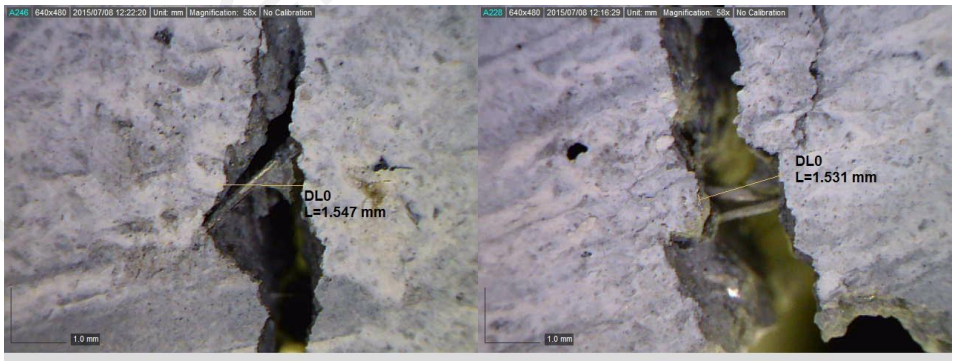

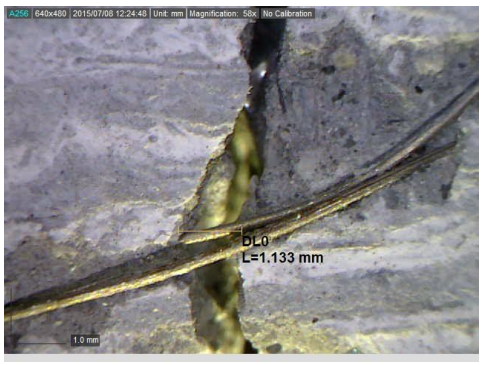

Figure 4.14: Fiber bridging along the path of crack propagation a) Mix F1.5 (above left), b) Mix F2.5 (above right) c) Mix F3 (below)

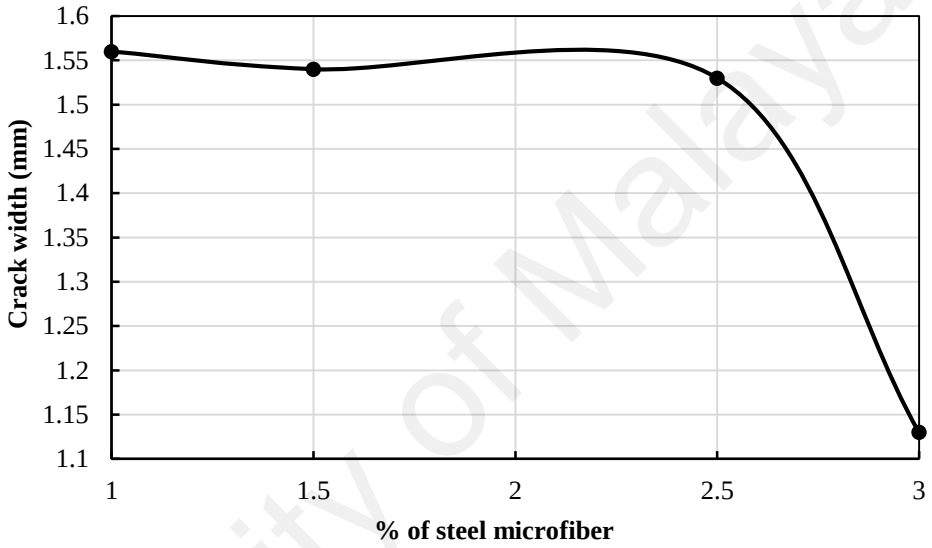

Figure 4.15: Effect of fiber on the reduction of crack width

Table 4.6: Mix proportions and results of fracture tests

Mixes	Steel microfiber (wt % of binder)	Compressive strength (MPa)	Maximum load (N)	Fracture energy (N/m)	Fracture toughness ($MPa.m^{1/2}$)
F0	0	47.85	382	276	-
F1	1	48.25	815	942	24.68
F1.5	1.5	48.50	820	1371	24.85
F2.5	2.5	49.45	1085	3194	32.88
F3	3	50.15	880	2715	26.66

4.4.3 Fracture energy and fracture toughness

Fracture energy of concrete plays a significant role to overcome the destructive consequence of dynamic loads such as; seismic, impact and blast on structures. The

properties of improved energy absorption capacity of mortar are greatly influenced by the incorporation of steel microfibers in mortar and these are reported by previous researchers (Pierre et al., 1999; Yi & Ostertag, 2001; Yoo, Shin, Yang, & Yoon, 2014). As shown in Table 4.7, the increase in compressive strength with the incorporation of steel microfiber is insignificant. The value of fracture energy is calculated from the area confined by the load-deflection curve. The fracture energy of the mixes F1, F1.5, F2.5 and F3 with the incorporation of 1%, 1.5%, 2.5% and 3% steel microfiber is 3.5, 5, 11.5 and 10 times higher respectively than the fracture energy of the mix with 0% microfiber. Fracture toughness of mortar increases up to the incorporation of 2.5% fiber and for 3% fiber it decreases. This phenomenon can be attributed to the fact that with the increase of fiber percentage, the probability of the fibers balling together and leaving more voids in the matrix which may reduce fracture toughness (Dias & Thaumaturgo, 2005). Same findings were found in the previous literature (F. Silva & Thaumaturgo, 2003). Figure 4.16 shows a generalised relationship between fracture energy and compressive strength.

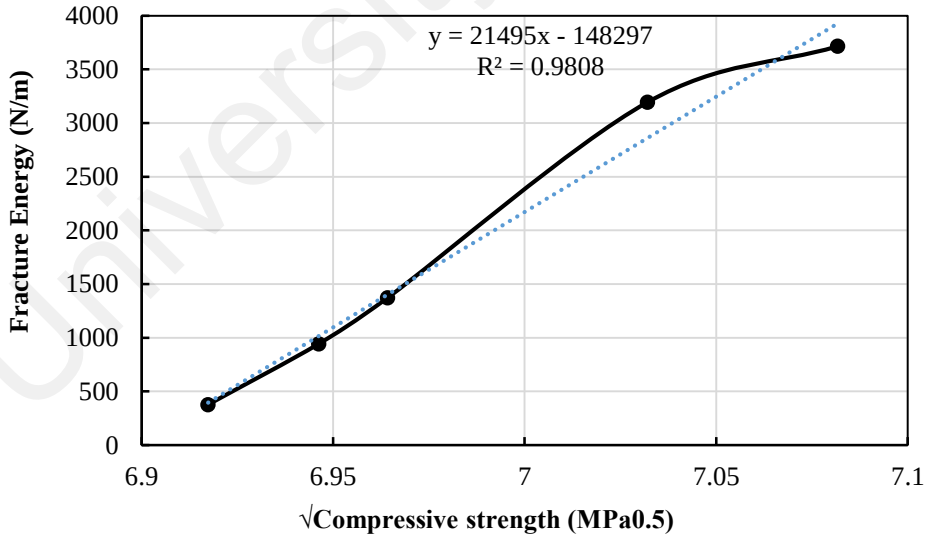

Figure 4.16: Normalized relationship between fracture energy and compressive strength

4.5 Engineering properties of concrete

4.5.1 General

This section depicts the results of oven dry density, compressive strength, splitting tensile strength, flexural strength, modulus of elasticity and ultrasonic pulse velocity tests on different mixes of concrete. A certain mix proportion of ternary binders found from the trial mixes of mortar as shown in section 4.2 was used for concrete. Workability test has been done on concrete but due to poor mixing, slump value was low. The lower value of slump test can be attributed to the use of GGBS content as half part of the total binder content. (Sugama, Brothers, & Van de Putte, 2005) and (Kumar et al., 2010) reported that GGBS content increased the setting time decreased in sodium silicate activated geopolymers. Figure 4.17 shows slump test of concrete.

Figure 4.17: Slump test of concrete

4.5.2 Oven dry density

The oven dry densities (ODD) of concrete at the age of 28-day are shown in Figure 4.18. The ODDs are varied between 1750 and 1930 kg/m^3 andbased on Euro-code 2 Part 1-1,

all the concrete mixes fall in the range of lightweight concrete (<2,200 kg/m^3). Since the quantities of binder, water and alkaline solution were kept constant for all mixes, the variation of hardened density depends on the resultant specific gravity of the aggregates. The increase in the density of the mixes with crushed granite at varying percentages (C2–C5) with the mix with 100% OPS (C1) was found to be between 1.5 and 10% for the increase of crushed granite from 20 to 100 %. So, the difference in density between OPS concrete and conventional crushed granite concrete was insignificant due to containing POC sand at percentage of 50% as light-weight fine aggregate. The ODD of OPS concrete (C1) was about 20% lighter than normal weight concrete of density 2200 kg/m^3 as per Eurocode. The substitution of OPS with crushed granite in percentages of 20%, 40%, 80% and 100% resulted in reduction of densities of 19%, 19%, 15% and 14.% lighter than normal weight concrete (NWC) of 2200 kg/m^3 as shown in Figure 4.19. Here, it was noticeable that crushed granite concrete with the use of as light-weight fine aggregate produced lower density as that of OPS concrete. Therefore, the decrease in the density was mainly attributed to the lower specific gravity of 1.97 for POC sand compared to 2.78 for M-sand.

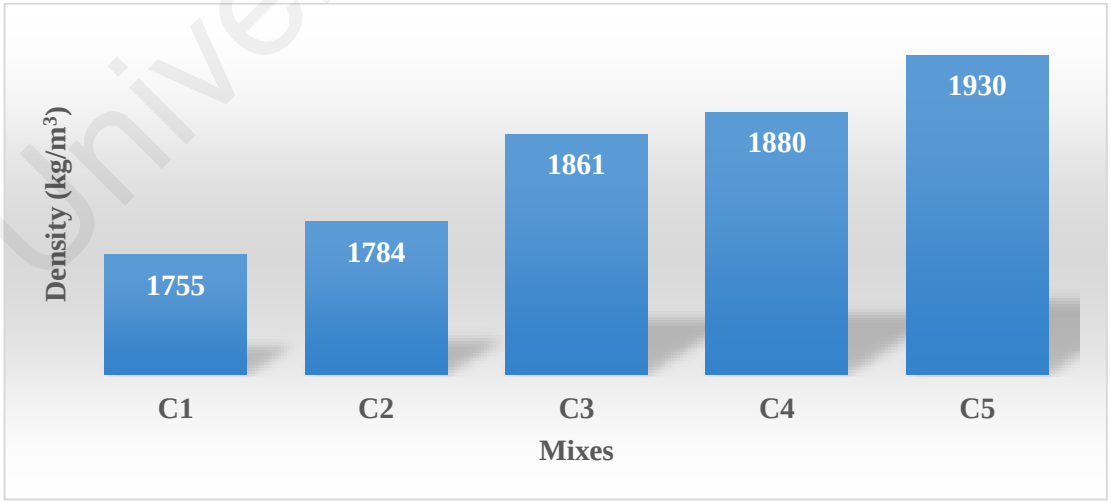

Figure 4.18: Oven dry density (ODD) of all mixes

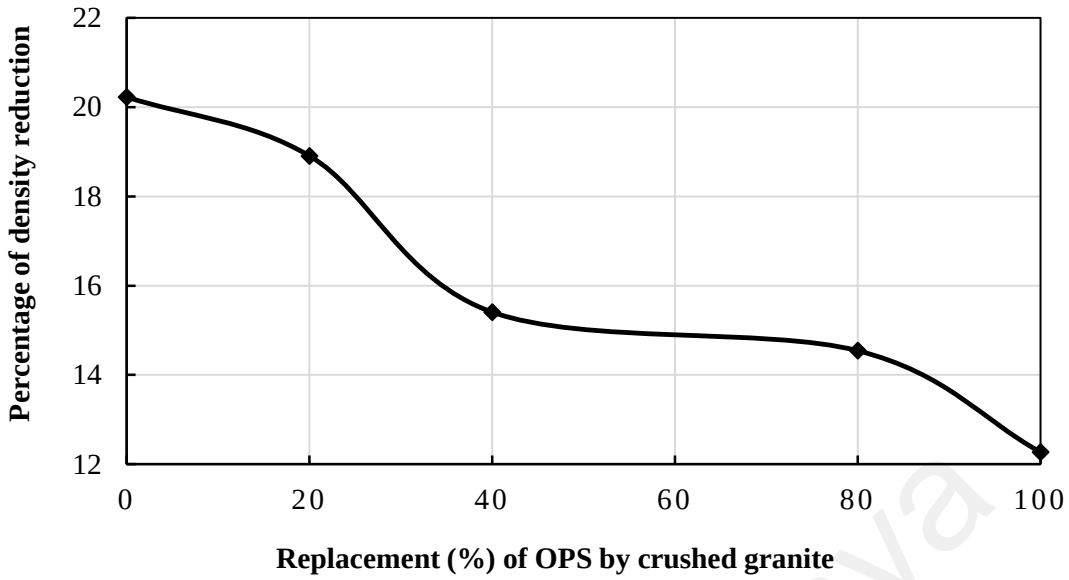

Figure 4.19: Density reduction (%) compared to the density of NWA (2200 kg/m^3)

Table 4.7: Mechanical properties of hardened concrete

Mixes	Compressive strength (MPa)			Splitting tensile strength (MPa)	Flexural strength (MPa)	Young's modulus of elasticity (GPa)	UPV (km/s)
	3-day	7-day	28-day	28-day			
C1 (100 OPS: 0 NWA)	24.0	24.3	25.0	1.40	2.40	5.00	2.80
C2 (80:20)	25.0	25.6	26.2	1.41	2.42	5.72	3.00
C3 (60:40)	29.0	29.0	30.4	1.52	3.03	7.50	3.00
C4 (20:80)	35.0	35.2	36.0	2.41	4.30	14.50	3.10
C5 (0:100)	37.0	37.6	38.0	2.60	4.50	18.00	3.30

*Parenthesis in the bracket indicate OPS and NWA contents

4.5.3 Compressive strength

The compressive strengths at the age of 3-, 7- and 28-day are presented in Table 4.7. The replacement of crushed granite by OPS (M1 – M4) exhibited lower compressive strength than the mix with 100% granite (M5). The strength gradually decreased with the increment of the quantity of OPS as shown in Figure 4.20. According to Eurocode 2, the minimum recommended cylinder compressive strength for structural grade lightweight concrete is 20 MPa (cube compressive strength 23 MPa) that is compiled by mixes M1 to M5.

As mentioned in the methodology, the increase in the quantity of OPS by weight proportion of total coarse aggregate from mixes M5 to M1 affected the strength. As the volume of OPS increased, the resulting compressive strength was decreased. Olanipekun, Olusola, and Ata (2006) also revealed that granite substitution by OPS decreased the compressive strength. This might be due to either the weaker bond interface between OPS surface and binder matrix (Okpala, 1990) and the low stiffness of the OPS (Alengaram, Muhit, & Jumaat, 2013). Mannan and Ganapathy ((2004)) noted the aggregate strength, thickness and density as the governing factors those could affect the compression strength of concrete. They also attributed the importance of both the contribution from aggregate strength and bond strength between aggregate and binder paste. This phenomena can be justified also by the fact that OPS concrete containing POC sand reduces compressive strength (Shafigh, Mahmud, Jumaat, Ahmmad, & Bahri, 2014). D. Teo, M. Mannan, and V. Kurian (2006) reported that the crack paths appeared between OPS surface and cement matrix at the earlier age.

The significance of shape, texture and particle size distribution is another important factor on the development of strength (Bashar et al., (2014); Quiroga & Fowler, 2004). The packing ability of fine particles also plays role that might have effect on the development

of compressive strength. The early age strength development was noticed for all the geopolymer concrete. As shown in Figure 4.21, the 3-day strength was found about 93% to 97% of 28-day compressive strength at the age of 3-day and it was about 94% to 99% at the age of 7-day. The rate of strength development was slowed down after the age of 7-day and the range was varied between 1 and 5% of 28-day compressive strength. This could be attributed to the lower SiO_2/ Al_2O_3 ratio (3.06) of the binder mix. The general range for SiO_2/ Al_2O_3 as reported by Islam et al. (2014a) was about 3.3-4.5. It has been reported that Al_2O_3 dissolves faster than SiO_2 and the reaction between aluminate and silicate species is faster than the reaction between only silicate species (P. D. Silva et al., 2007). Moreover, strength development is faster at high temperature curing in geopolymerization process (Islam et al., 2014a).

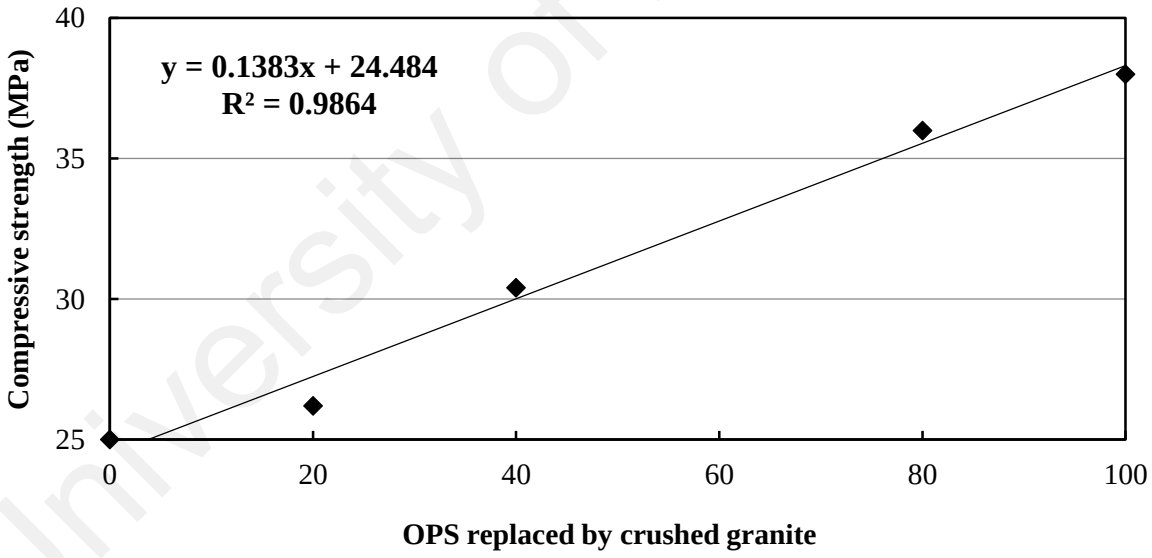

Figure 4.20: Increase of compressive strength with the crushed granite replacement level with OPS

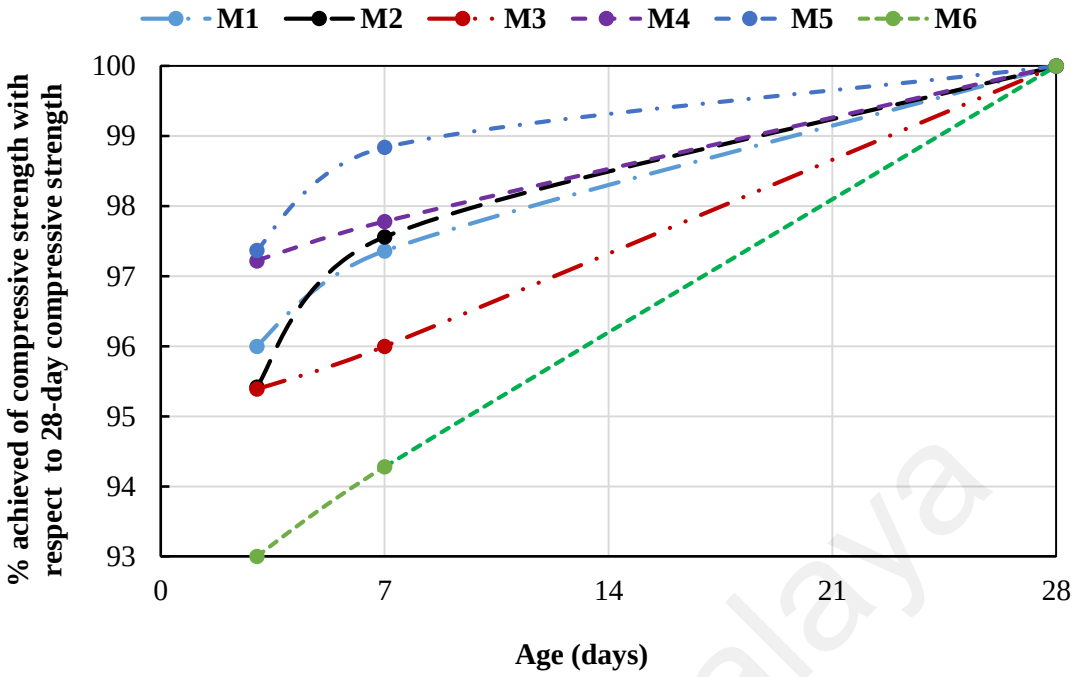

Figure 4.21: Development of compressive strength with respect to 28-day compressive strength

4.5.4 Splitting tensile strength

The tensile strength is a significant parameter to measure the vulnerability of concrete against cracking. The 28-day splitting tensile strength of geopolymer concrete was found in the range of 1.25–2.60 MPa as shown in Table 4.8. The increase in the splitting tensile strength of the mixes with 9 mm crushed granite aggregate at varying percentages from 20 to 100 in the mixes M2–M5 compared to the mix M1 (without crushed granite aggregate) was found to be between 0.7 and 85% . This could be attributed to poor mixing of large amount of POC due to low specific gravity of POC due to low specific gravity of POC that lead to weak bonding. This could be attributed to the porous characteristics of OPS (Alengaram, Mahmud, & Jumaat, 2011) which prepared spongy arrangement of lightweight aggregate and spread of micro-cracks under tensile loading (Shannag, 2011). The ratio of the splitting tensile to the compressive strength of concrete in this study ranged from 0.05 to 0.07 and this is comparable to 0.080 reported for lightweight concrete (Shafigh, Jumaat, Mahmud, & Hamid, 2012). However, these ratios are well below the

value of 0.10 reported for NWC (Shannag, 2011). Another reason for the decrease in the splitting tensile strength is the presence of high amount of GGBS content (50% of binder); A similar outcome was stated for GGBS-based concrete by (Güneyisi & Gesoğlu, 2008) and they established that the splitting tensile strength was decreased at a higher rate for higher percentages of GGBS. Figure 4.22 shows splitting tensile strength increases with the increase of OPS replacement (%) by crushed granite.

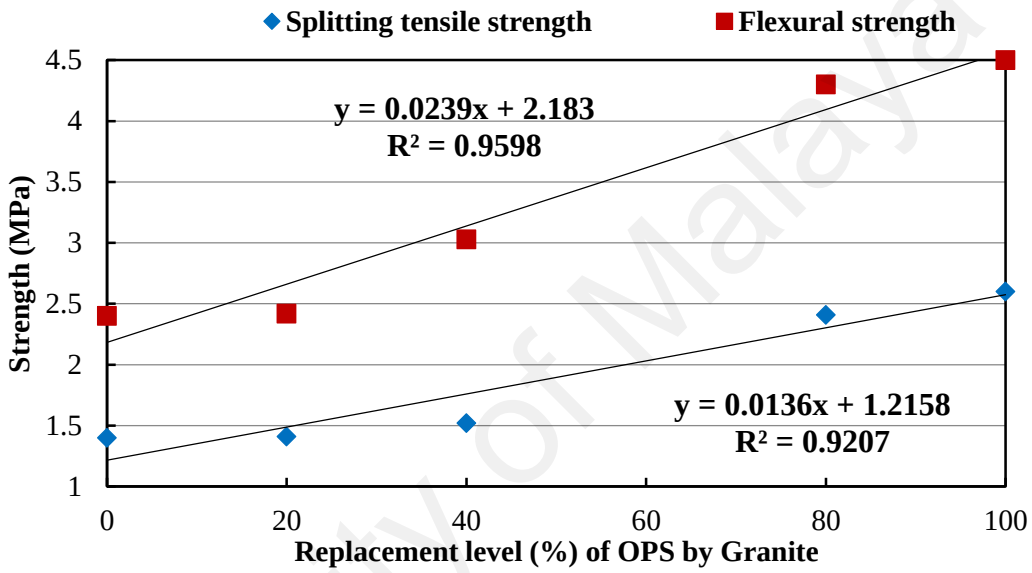

Figure 4.22: Comparison between the increase of splitting tensile strength and flexural strength for the replacement level (%) of OPS by granite

4.5.5 Flexural strength

The flexural strengths at 28-day age were found in the range of 2.0–4.5 MPa (Table 4.7) which are 10–12 % of their corresponding compressive strengths and these ratios are comparable to that of the published results of 8-14% by (D. C. L. TEO, M. A. MANNAN, & V. J. KURIAN, 2006). It was reported that bond failure occurs along the convex surfaces of OPS aggregates in the flexural specimens and this was evident in the present research work (U. Johnson Alengaram et al., 2011); further OPS aggregates might contribute to a more torturous path of crack transmission and delay the development of crack when exposed to flexural loads. Similar to the splitting tensile strength, the flexural strength was found to increase steadily with the increase of OPS replacement with granite

as shown in Figure 4.22. The decrease in the volume of OPS from 100 to 0 % led to an increase in the flexural strength by 0.83-87.5 %. This could be attributed to the stronger bond in the interfacial zone between the granite and binder matrix as large amount of OPS leads to weaker bond. The cracks formed by flexural load could be propagated within the weaker area at this interfacial zone and flexural failure occurred when sufficiently large crack was formed (U. Johnson Alengaram et al., 2011).

4.5.6 Static modulus of elasticity (MOE)

The static modulus of elasticity (MOE) is a material property which describes the stiffness of a material and critical load in the case of members susceptible to failure because of elastic instability. In this investigation, the highest MOE of 18 GPa was obtained for the control mix with granite of 100% (M5) while the MOE decreased from 14.5 to 5 GPa for the replacement of crushed granite with OPS from 20 to 100% as shown in Table 4.8. This could be justified by the lower stiffness of the OPS aggregates than for normal weight concrete (U. Johnson Alengaram et al., 2011) and the weak bond between the OPS and binder matrix containing large percentage of GGBS (50%) (U. Johnson Alengaram et al., 2011). The modulus of elasticity of lightweight aggregates is lower than normal weight aggregates, ranging mainly from 5 to 28 GPa (Mehta & Monteiro, 2006). In this investigation, the modulus of elasticity of OPS concrete containing 50% POC sand was found 5 GPa which was 42% lower than the findings of (Shafigh et al., 2014). (Shariq, Prasad, & Abbas, 2013) reported that the static modulus of elasticity of GGBS based concrete is lower than the cement concrete for all substitutions of cement by GGBS. This could be attributed to the use of a lower stiff material at high volume (Waehneldt, 1975). Figures 4.23 shows a direct relationship between the normalized compressive strength and static modulus of elasticity of the lightweight geopolymer concrete. As the increase in compressive strength of concrete means the increase in density of both the binder paste

and the interface, this in turn improved the elastic properties of binder paste matrix and aggregate and that results in higher modulus of elasticity of concrete (Sengul, Tasdemir, & Tasdemir, 2002). Equation 7 is proposed to relate the flexural strength with the square root of compressive strength.

$$Ec = 0.0036\sqrt{fc}^{4.5793} \ldots..7$$

Where Ec and fc are static modulus of elasticity in GPa and compressive strength in MPa, respectively.

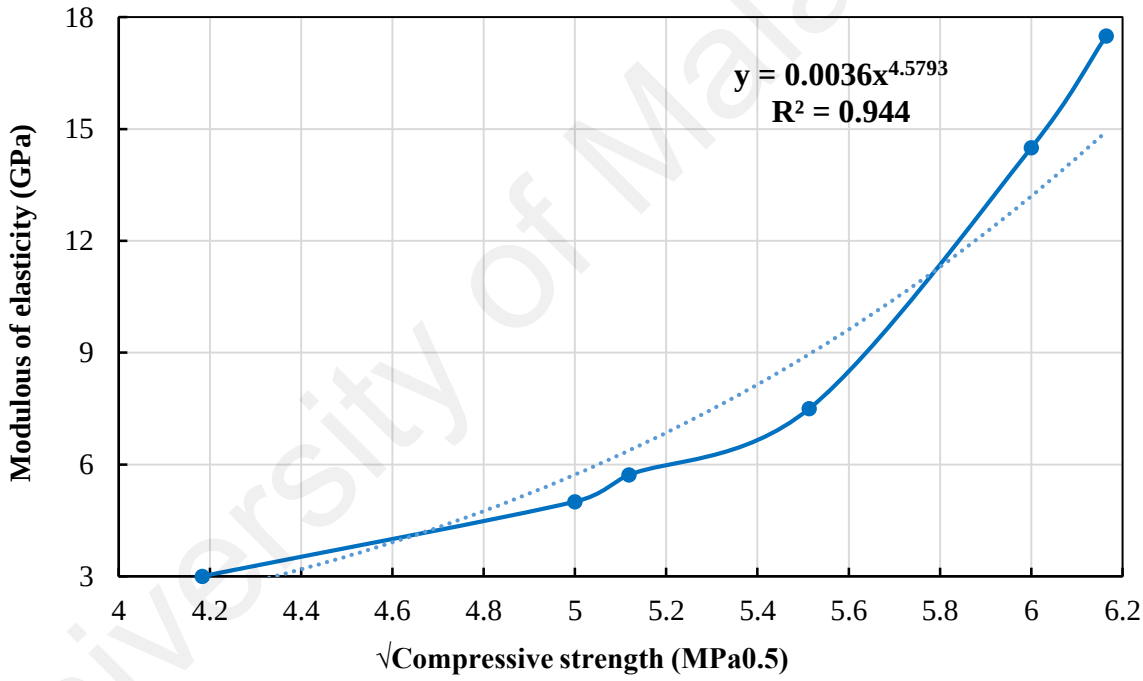

Figure 4.23: Relationship between square root of compressive strength and static modulus of elasticity

4.5.7 Ultrasonic pulse velocity (UPV)

The UPV test was a measure to perceive presence of voids and the consistency of concrete. The UPV values of all the mixes are presented in Table 4.8. The 28-day UPV of all the mixes was found in the range of 2.7-3.3 km/s. (Whitehurst, 1986) classified concretes as excellent, very good, good, poor and very poor for UPV values of 4.5 km/s and above, 3.5–4.5, 3.0–3.5, 2.0–3.0 km/s and below 2.0 km/s, respectively. The

replacement of OPS with crushed granite in the percentages of 20 to 100% (M3-M5) produced UPV of 3-3.3 km/s and it indicated that the replacement of M-sand with POC sand at 50% could be categorized as good quality concrete. The results in Table 4.8 showed that an increase in the replacement of OPS by crushed granite led to an increase in UPV values. This could be attributed to the well compacted mixes with crushed granite aggregate compared to 100% OPS aggregate mix. The presence of GGBS at high volume in the binder matrix would also reduce the UPV values of concrete as reported by previous researchers (Khan, 2012; Kou, Poon, & Agrela, 2011; Shariq, Prasad, & Masood, 2013).

CHAPTER 5: CONCLUSIONS AND RECOMMENDATIONS

5.1 Introduction

This chapter presents a summary of the present study, the major conclusions and some recommendations for future research. The main aim of the study was to develop appropriate mixture design for mortar and to utilize it for further mixes in concrete; the mechanical properties of the RHA-GGBS-POFA based geopolymer concrete was investigated. In addition, the effects of two different types of fine aggregate – manufactured sand (M-sand) and POC-sand, at the same time two different types of coarse aggregates- crushed OPS and crushed Granite were studied in oven-dry curing conditions. Another salient feature of the research was the determination of the effect of steel microfiber on the fracture properties of geopolymer mortar and microstructural analysis of geopolymer mortar.

5.1.1 Summary of Conclusions

Based on the variables investigated, the following conclusions were drawn:

Objective 1:

1. The mortar density increased with an increase in GGBS and MK due to the higher specific gravity and better packing ability of GGBS and MK than that for RHA.
2. The ability of flow of the mortar decreases for the mixes containing larger percentages of RHA and this could be attributed to higher value of LOI.
3. From 70% to 95% of the 28-day compressive strength was achieved at the age of 3 days due to fast geopolymerization during oven curing at 65^0C for 24 hours.
4. The mortar containing a high volume (>45%) of GGBS with a low volume of MK and RHA gained faster early age strength development at a temperature of 65ºC.

5. The gradual increment of the rate of geopolymerization until the age of 7 days was observed for the geopolymer matrix consisting of a SiO_2/Al_2O_3 ratio of 3.7 to 6.8.
6. The mixes with 14M alkali activator produced higher 28-day compressive strengths compared to mixes with 12M. The difference in compressive strength between the corresponding mixes with 14M and 12M was found lower for the mixes with high percentages of GGBS (>60%).
7. The development of the compressive strength is influenced by the binary/ternary combination of the binder. The ternary combination of RHA, GGBS and MK achieved higher strength than the binary combination of RHA and GGBS or RHA and MK.
8. The reduction in the compressive strength of the mortar containing a high volume of RHA (>25%), might be influenced by the unreactive additional solid particles of RHA.
9. The inclusion of MK above 25% in the ternary combination of RHA, GGBS and MK, reduced the compressive strength.

Objective 2 & 3:

10. The amorphorsity of the mortar increased with the increase in percentage of MK as binder. The formation of calcite ($CaCO_3$) in the diffractogram could have contributed to the highest 28-d compressive strength of mortar, the calcite was formed when the SiO_2/Al_2O_3 molar ratio was within 4.7 to 5.2. The formation of calcium silicate aluminium hydrate (C-A-S-H) was found when 30% MK was used in the synthesis.
11. A continuous dense microstructure with uniformly distributed pores was found for the mortar with highest 28-d compressive strength. Due to lack of alumina, the

pocket of C-S-H products formed with the C-A-S-H could be responsible for the decrease in the strength with MK in lower percentage.

Objective 4:

12. The incorporation of steel microfibers in geopolymer mortar at 1%, 1.5%, 2.5% and 3% improves its fracture energy 2.5, 4, 8.5 and 10 times higher respectively. Fracture toughness of mortar doesn't increase linearly with the incorporation of steel microfibers because the use of steel microfiber beyond 1.5% may increase porosity of the structure.

Objective 5:

13. The difference in density between OPS concrete and crushed granite concrete was found only 10% with both mixes contained 50% lightweight POC sand as replacement with M-sand and the concrete had a 28 days ODD below 2,000 kg/m^3 at all replacement levels of OPS with granite. The reduction in density was mainly due to the lower specific gravity of POC sand.
14. The 28-day compressive strength of about 24 to 38 MPa was achieved by a replacement of M-sand with 50% POC sand while lowest compressive strength was achieved for OPS concrete and highest compressive strength was achieved for granite concrete. So the findings suggest that the use of lightweight sand up to 50% can be used as based on the trial mixes, it was found that beyond this level, the strength was to decrease.
15. Up to 93 to 97% of the 28-day compressive strength was achieved at the age of 3 day and this could be attributed to the chemical composition and low SiO_2/Al_2O_3 ratio of binder materials.

16. The linear equation of the graph indicated that splitting tensile strength increased with the replacement of OPS by granite aggregate.
17. The flexural strength was increased with the increase of compressive strength. The rate of increase of flexural strength was higher than the rate of increase of splitting tensile strength with the replacement of OPS by granite.
18. The highest MOE of 18 GPa was achieved for 100% granite as coarse aggregate and 50% POC sand with M-sand as light-weight fine aggregate. The MOE increased with the increase of granite replacement level with OPS and the MOE of granite concrete was more than three times higher than the MOE of OPS concrete.
19. The replacement of OPS with crushed granite produced UPV of 3-3.3 km/s and it indicated that the replacement of M-sand with POC sand at 50% was suitable for geopolymer concrete based on the result of UPV test.

5.1.2 Future Recommendations

- Further investigation is necessary to increase the workability of concrete..
- Different curing conditions can be studied on RHA-GGBS-MK based geopolymer mortar and concrete.
- The effect of super-plasticizer needs to be investigated on the mix proportion of ternary blended geopolymer mortar.
- Microstructural investigations such as FESEM, FTIR, TGA can be done on RHA-GGBS-MK based geopolymer mortar.
- Effect of steel microfibers on fracture properties of geopolymer mortar specimens can be investigated on large scale specimens.
- Durability tests of ternary blended geopolymer concrete are very important to prove the actual usage of this kind of concrete.

- Thermal properties of the ternary blended geopolymer concrete have to be investigated.
- Fire resistant properties of fibre reinforced composites need to be checked.

REFERENCES

Abdullah, A. A. A. (1996). 10 - Palm oil shell aggregate for lightweight concrete. In S. Chandra (Ed.), *Waste Materials Used in Concrete Manufacturing* (pp. 624-636). Westwood, NJ: William Andrew Publishing.

Abu Bakar, B. H., Putrajaya, R., & Abdulaziz, H. (2010). Malaysian rice husk ash–improving the durability and corrosion resistance of concrete: pre-review. *Concrete Research Letters*, *1*(1), 6-13.

Ahmmad, R., Jumaat, M. Z., Bahri, S., & Islam, A. B. M. S. ((2014)). Ductility performance of lightweight concrete element containing massive palm shell clinker. *Construction and Building Materials*, *63*(0), 234-241. doi:http://dx.doi.org/10.1016/j.conbuildmat.2014.04.022

Alengaram, U. J., Jumaat, M. Z., & Mahmud, H. (2008). *Influence of sand content and silica fume on mechanical properties of palm kernel shell concrete.* Paper presented at the International conference on construction and building technology ICCBT.

Alengaram, U. J., Jumaat, M. Z., Mahmud, H., & Fayyadh, M. M. (2011). Shear behaviour of reinforced palm kernel shell concrete beams. *Construction and Building Materials*, *25*(6), 2918-2927.

Alengaram, U. J., Mahmud, H., & Jumaat, M. Z. (2011). Enhancement and prediction of modulus of elasticity of palm kernel shell concrete. *Materials & Design*, *32*(4), 2143-2148. doi:http://dx.doi.org/10.1016/j.matdes.2010.11.035

Alengaram, U. J., Muhit, B. A. A., & Jumaat, M. Z. (2013). Utilization of oil palm kernel shell as lightweight aggregate in concrete – A review. *Construction and Building Materials*, *38*, 161-172. doi:10.1016/j.conbuildmat.2012.08.026

Alengaram, U. J., Muhit, B. A. A., Jumaat, M. Z., & Jing, M. L. Y. (2013). A comparison of the thermal conductivity of oil palm shell foamed concrete with conventional materials. *Materials and Design*, *51*, 522-529. doi:http://dx.doi.org/10.1016/j.matdes.2013.04.078

Alhozaimy, A., Al-Negheimish, A., Alawad, O. A., Jaafar, M. S., & Noorzaei, J. (2012). Binary and ternary effects of ground dune sand and blast furnace slag on the compressive strength of mortar. *Cement and Concrete Composites*, *34*(6), 734-738. doi:http://dx.doi.org/10.1016/j.cemconcomp.2012.03.002

Alonso, S., & Palomo, A. (2001). Alkaline activation of metakaolin and calcium hydroxide mixtures: influence of temperature, activator concentration and solids ratio. *Materials Letters*, *47*(1), 55-62.

Appukutty, P., & Murugesan, R. (2009). Substitution of quarry dust to sand for mortar in brick masonry works. *International Journal on Design and Manufacturing Technologies*, *3*(1), 59-63.

Arellano Aguilar, R., Burciaga Díaz, O., & Escalante García, J. I. (2010). Lightweight concretes of activated metakaolin-fly ash binders, with blast furnace slag aggregates. *Construction and Building Materials, 24*(7), 1166-1175. doi:http://dx.doi.org/10.1016/j.conbuildmat.2009.12.024

Asavapisit, S., & Ruengrit, N. (2005). The role of RHA-blended cement in stabilizing metal-containing wastes. *Cement and Concrete Composites, 27*(7), 782-787.

Ashraf, M. A., Maah, M. J., Yusoff, I., Wajid, A., & Mahmood, K. (2011). Sand mining effects, causes and concerns: a case study from Bestari Jaya, Selangor, Peninsular Malaysia. *Scientific Research and Essays, 6*(6), 1216-1231.

Bakharev, T., Sanjayan, J., & Cheng, Y.-B. ((2001)). Resistance of alkali-activated slag concrete to alkali–aggregate reaction. *Cement and Concrete Research, 31*(2), 331-334.

Bamaga, S. O., Hussin, M. W., & Ismail, M. (2013). Palm Oil Fuel Ash: Promising supplementary cementing materials. *KSCE Journal of Civil Engineering, 17*(7), 1708-1713. doi:10.1007/s12205-013-1241-9

Barbosa, V. F. F., & MacKenzie, K. J. D. (2003). Thermal behaviour of inorganic geopolymers and composites derived from sodium polysalate. *Mater Res Bull, 38*(2), 319-331.

Barnett, S., Soutsos, M., Millard, S., & Bungey, J. (2006). Strength development of mortars containing ground granulated blast-furnace slag: Effect of curing temperature and determination of apparent activation energies. *Cement and Concrete Research, 36*(3), 434-440.

Basha, E., Hashim, R., Mahmud, H., & Muntohar, A. (2005). Stabilization of residual soil with rice husk ash and cement. *Construction and Building Materials, 19*(6), 448-453.

Bashar, I. I., Alengaram, U. J., Jumaat, M. Z., & Islam, A. ((2014)). The Effect of Variation of Molarity of Alkali Activator and Fine Aggregate Content on the Compressive Strength of the Fly Ash: Palm Oil Fuel Ash Based Geopolymer Mortar. *Advances in Materials Science and Engineering*. doi:10.1155/2014/245473

Bernal, S. A., Mejía de Gutiérrez, R., & Provis, J. L. (2012). Engineering and durability properties of concretes based on alkali-activated granulated blast furnace slag/metakaolin blends. *Construction and Building Materials, 33*, 99-108.

Bernal, S. A., Mejía de Gutiérrez, R., & Provis, J. L. (2012). Engineering and durability properties of concretes based on alkali-activated granulated blast furnace slag/metakaolin blends. *Construction and Building Materials, 33*(0), 99-108. doi:http://dx.doi.org/10.1016/j.conbuildmat.2012.01.017

Bernal, S. A., Provis, J. L., Rose, V., & Mejía de Gutierrez, R. (2011). Evolution of binder structure in sodium silicate-activated slag-metakaolin blends. *Cement and Concrete Composites, 33*(1), 46-54. doi:http://dx.doi.org/10.1016/j.cemconcomp.2010.09.004

Buchwald, A., Hilbig, H., & Kaps, C. (2007). Alkali-activated metakaolin-slag blends—performance and structure in dependence of their composition. *Journal of materials science, 42*(9), 3024-3032.

Burciaga-Diaz, O., Escalante-Garcia, J. I., & Gorokhovsky, A. (2012). Geopolymers based on a coarse low-purity kaolin mineral: Mechanical strength as a function of the chemical composition and temperature. *Cement and Concrete Composites, 34*(1), 18-24.

Caglar, B., Çırak, Ç., Tabak, A., Afsin, B., & Eren, E. (2013). Covalent grafting of pyridine-2-methanol into kaolinite layers. *Journal of Molecular Structure, 1032*, 12-22.

Chang, J. (2003). A study on the setting characteristics of sodium silicate-activated slag pastes. *Cement and Concrete Research, 33*(7), 1005-1011.

Chi, M., & Huang, R. (2013). Binding mechanism and properties of alkali-activated fly ash/slag mortars. *Construction and Building Materials, 40*, 291-298.

Chindaprasirt, P., De Silva, P., Sagoe-Crentsil, K., & Hanjitsuwan, S. (2012). Effect of SiO2 and Al2O3 on the setting and hardening of high calcium fly ash-based geopolymer systems. *Journal of materials science, 47*(12), 4876-4883.

Chindaprasirt, P., Jaturapitakkul, C., Chalee, W., & Rattanasak, U. (2009). Comparative study on the characteristics of fly ash and bottom ash geopolymers. *Waste management, 29*(2), 539-543.

Chindaprasirt, P., & Rukzon, S. (2008). Strength, porosity and corrosion resistance of ternary blend Portland cement, rice husk ash and fly ash mortar. *Construction and Building Materials, 22*(8), 1601-1606. doi:http://dx.doi.org/10.1016/j.conbuildmat.2007.06.010

Chindaprasirt, P., Rukzon, S., & Sirivivatnanon, V. (2008). Resistance to chloride penetration of blended Portland cement mortar containing palm oil fuel ash, rice husk ash and fly ash. *Construction and Building Materials, 22*(5), 932-938. doi:http://dx.doi.org/10.1016/j.conbuildmat.2006.12.001

Conradt, R., Pimkhaokham, P., & Leela-Adisorn, U. (1992). Nano-structured silica from rice husk. *Journal of Non-Crystalline Solids, 145*(0), 75-79. doi:http://dx.doi.org/10.1016/S0022-3093(05)80433-8

Coutinho, J. S. (2003). The combined benefits of CPF and RHA in improving the durability of concrete structures. *Cement and Concrete Composites, 25*(1), 51-59.

Damtoft, J. S., Lukasik, J., Herfort, D., Sorrentino, D., & Gartner, E. M. (2008). Sustainable development and climate change initiatives. *Cement and Concrete Research, 38*(2), 115-127. doi:http://dx.doi.org/10.1016/j.cemconres.2007.09.008

Davidovit, J. (2002). Inorganic polymeric new material.

Davidovits, J. (1991). Geopolymers. *Journal of Thermal Analysis and Calorimetry, 37*(8), 1633-1656.

Davidovits, J. (2005). *Geopolymer, Green Chemistry and Sustainable Development Solutions: Proceedings of the World Congress Geopolymer 2005*: Geopolymer Institute.

Davidovits, J. ((2008)). Chemistry and Applications Geopolymer Institute. *Saint-Quentin, France*.

Davidovits, J. ((2008)). *Geopolymer chemistry & application* (3rd ed.). 16 rule Galilee, F-02100 Saint-Quentin, France: Institute Géopolymèr.

de Gutiérrez, R. M., Díaz, L. N., & Delvasto, S. ((2005)). Effect of pozzolans on the performance of fiber-reinforced mortars. *Cement and Concrete Composites, 27*(5), 593-598. doi:http://dx.doi.org/10.1016/j.cemconcomp.2004.09.010

Della, V., Kühn, I., & Hotza, D. (2002). Rice husk ash as an alternate source for active silica production. *Materials Letters, 57*(4), 818-821.

Dhir, R. K., & Jappy, T. G. (1999). *Exploiting wastes in concrete: proceedings of the international seminar held at the University of Dundee, Scotland, UK on 7 September 1999*: Thomas Telford.

Dias, D. P., & Thaumaturgo, C. (2005). Fracture toughness of geopolymeric concretes reinforced with basalt fibers. *Cement and Concrete Composites, 27*(1), 49-54. doi:http://dx.doi.org/10.1016/j.cemconcomp.2004.02.044

Dinakar, P., Sethy, K. P., & Sahoo, U. C. (2013). Design of self-compacting concrete with ground granulated blast furnace slag. *Materials & Design, 43*, 161-169.

Donza, H., Cabrera, O., & Irassar, E. (2002). High-strength concrete with different fine aggregate. *Cement and Concrete Research, 32*(11), 1755-1761.

Duxson, P., Fernández-Jiménez, A., Provis, J., Lukey, G., Palomo, A., & Van Deventer, J. (2007). Geopolymer technology: the current state of the art. *Journal of materials science, 42*(9), 2917-2933.

Duxson, P., Lukey, G., Separovic, F., & Van Deventer, J. (2005). Effect of alkali cations on aluminum incorporation in geopolymeric gels. *Industrial & engineering chemistry research, 44*(4), 832-839.

Duxson, P., Provis, J. L., Lukey, G. C., Mallicoat, S. W., Kriven, W. M., & Van Deventer, J. S. (2005). Understanding the relationship between geopolymer composition, microstructure and mechanical properties. *Colloids and Surfaces A: Physicochemical and Engineering Aspects, 269*(1), 47-58.

Dvorkin, L., Bezusyak, A., Lushnikova, N., & Ribakov, Y. (2012). Using mathematical modeling for design of self compacting high strength concrete with metakaolin admixture. *Construction and Building Materials, 37*, 851-864.

Feng, J., Zhang, R., Gong, L., Li, Y., Cao, W., & Cheng, X. (2015). Development of porous fly ash-based geopolymer with low thermal conductivity. *Materials & Design, 65*(0), 529-533. doi:http://dx.doi.org/10.1016/j.matdes.2014.09.024

Fernández-Jiménez, A., Puertas, F., & Arteaga, A. (1998). Determination of kinetic equations of alkaline activation of blast furnace slag by means of calorimetric data. *Journal of Thermal Analysis and Calorimetry, 52*(3), 945-955.

Galau, D., & Ismail, M. (2010). *Characterization of Palm Oil Fuel Ash (POFA) from Different Mill as Cement Replacement Material.* Thesis, Faculty of Civil Engineering, Universiti Teknologi Malaysia, Johor, Malaysia.

Givi, A. N., Rashid, S. A., Aziz, F. N. A., & Salleh, M. A. M. ((2010)). Contribution of rice husk ash to the properties of mortar and concrete: a review. *Journal of American science, 6*(3), 157-165.

Güneyisi, E., & Gesoğlu, M. (2008). A study on durability properties of high-performance concretes incorporating high replacement levels of slag. *Materials and Structures, 41*(3), 479-493.

Guo, X., Shi, H., & Dick, W. A. (2010). Compressive strength and microstructural characteristics of class C fly ash geopolymer. *Cement and Concrete Composites, 32*(2), 142-147. doi:http://dx.doi.org/10.1016/j.cemconcomp.2009.11.003

Halstead, W. J. (1986). Use of fly ash in concrete. *NCHRP Synthesis of Highway Practice*(127).

Hardjito, D., Wallah, S. E., Sumajouw, D. M., & Rangan, B. V. (2005). Fly ash-based geopolymer concrete. *Australian Journal of Structural Engineering, 6*(1), 77-84.

Hardjito, D., Wallah, S. E., Sumajouw, D. M., & Rangan, B. V. ((2004)). On the development of fly ash-based geopolymer concrete. *ACI materials journal, 101*(6).

He, J., Jie, Y., Zhang, J., Yu, Y., & Zhang, G. (2013). Synthesis and characterization of red mud and rice husk ash-based geopolymer composites. *Cement and Concrete Composites, 37*, 108-118.

Isaia, G. C., Gastaldini, A. L. G., & Moraes, R. (2003). Physical and pozzolanic action of mineral additions on the mechanical strength of high-performance concrete. *Cement and Concrete Composites, 25*(1), 69-76. doi:http://dx.doi.org/10.1016/S0958-9465(01)00057-9

Islam, A., Alengaram, U. J., Jumaat, M. Z., & Bashar, I. I. (2014a). The development of compressive strength of ground granulated blast furnace slag-palm oil fuel ash-fly ash based geopolymer mortar. *Materials & Design, 56*(0), 833-841. doi:http://dx.doi.org/10.1016/j.matdes.2013.11.080

Islam, A., Alengaram, U. J., Jumaat, M. Z., & Bashar, I. I. (2014b). The development of compressive strength of ground granulated blast furnace slag-palm oil fuel ash-fly ash based geopolymer mortar. *Materials & Design, 56*, 833-841.

Joseph, B., & Mathew, G. (2012). Influence of aggregate content on the behavior of fly ash based geopolymer concrete. *Scientia Iranica, 19*(5), 1188-1194.

Kabir, S., Alengaram, U. J., Jumaat, M. Z., Sharmin, A., & Islam, A. ((2015)). Influence of Molarity and Chemical Composition on the Development of Compressive Strength in POFA Based Geopolymer Mortar. *Advances in Materials Science and Engineering, 2015*.

Kanadasan, J., & Abdul Razak, H. ((2015)). Engineering and sustainability performance of self-compacting palm oil mill incinerated waste concrete. *Journal of Cleaner Production, 89*(0), 78-86. doi:http://dx.doi.org/10.1016/j.jclepro.2014.11.002

Kanadasan, J., & Razak, H. A. (2013). Mix design for self-compacting palm oil clinker concrete based on particle packing. *Materials and Design*. doi:http://dx.doi.org/10.1016/j.matdes.2013.10.086

Kannan, V., & Ganesan, K. (2014). Chloride and chemical resistance of self compacting concrete containing rice husk ash and metakaolin. *Construction and Building Materials, 51*, 225-234.

Karim, M., Zain, M., Jamil, M., & Lai, F. (2013). Fabrication of a non-cement binder using slag, palm oil fuel ash and rice husk ash with sodium hydroxide. *Construction and Building Materials, 49*, 894-902.

Karim, M. R., Zain, M. F. M., Jamil, M., & Lai, F. C. ((2013)). Fabrication of a non-cement binder using slag, palm oil fuel ash and rice husk ash with sodium hydroxide. *Construction and Building Materials, 49*(0), 894-902. doi:http://dx.doi.org/10.1016/j.conbuildmat.2013.08.077

Khan, M. I. (2012). Evaluation of non-destructive testing of high strength concrete incorporating supplementary cementitious composites. *Resources, Conservation and Recycling, 61*(0), 125-129. doi:http://dx.doi.org/10.1016/j.resconrec.2012.01.013

Khana, M., Jamil, M., Karimc, M., & Zaind, M. (2014). Strength and Durability of Mortar and Concrete Containing Rice Husk Ash: A Review. *World Applied Sciences Journal, 32*(5), 752-765.

Klee, H., & Coles, E. (2004). The cement sustainability initiative–implementing change across a global industry. *Corporate Social Responsibility and Environmental Management, 11*(2), 114-120.

Kou, S.-c., Poon, C.-s., & Agrela, F. (2011). Comparisons of natural and recycled aggregate concretes prepared with the addition of different mineral admixtures. *Cement and Concrete Composites, 33*(8), 788-795. doi:http://dx.doi.org/10.1016/j.cemconcomp.2011.05.009

Kumar, S., Kumar, R., & Mehrotra, S. (2010). Influence of granulated blast furnace slag on the reaction, structure and properties of fly ash based geopolymer. *Journal of materials science, 45*(3), 607-615.

Kupaei, R. H., Alengaram, U. J., & Jumaat, M. Z. (2014). The effect of different parameters on the development of compressive strength of oil palm shell geopolymer concrete. *The Scientific World Journal, 2014*.

Kupaei, R. H., Alengaram, U. J., Jumaat, M. Z. B., & Nikraz, H. (2013). Mix design for fly ash based oil palm shell geopolymer lightweight concrete. *Construction and Building Materials*, *43*, 490-496.

Kusbiantoro, A., Nuruddin, M. F., Shafiq, N., & Qazi, S. A. (2012). The effect of microwave incinerated rice husk ash on the compressive and bond strength of fly ash based geopolymer concrete. *Construction and Building Materials, 36*(0), 695-703. doi:http://dx.doi.org/10.1016/j.conbuildmat.2012.06.064

Lawler, J. S. (2001). *Hybrid fiber-reinforcement in mortar and concrete*.

Lee, W., & Van Deventer, J. (2002). The effect of ionic contaminants on the early-age properties of alkali-activated fly ash-based cements. *Cement and Concrete Research*, *32*(4), 577-584.

Li, C., Sun, H., & Li, L. (2010). A review: The comparison between alkali-activated slag (Si+ Ca) and metakaolin (Si+ Al) cements. *Cement and Concrete Research, 40*(9), 1341-1349.

Li, Z., & Liu, S. (2007). Influence of slag as additive on compressive strength of fly ash-based geopolymer. *Journal of Materials in civil engineering, 19*(6), 470-474.

Liu, M. Y. J., Alengaram, U. J., Jumaat, M. Z., & Mo, K. H. (2014). Evaluation of thermal conductivity, mechanical and transport properties of lightweight aggregate foamed geopolymer concrete. *Energy and Buildings, 72*(0), 238-245. doi:http://dx.doi.org/10.1016/j.enbuild.2013.12.029

Liu, M. Y. J., Chua, C. P., Alengaram, U. J., & Jumaat, M. Z. (2014). Utilization of palm oil fuel ash as binder in lightweight oil palm shell geopolymer concrete. *Advances in Materials Science and Engineering, 2014*.

Lothenbach, B., Scrivener, K., & Hooton, R. (2011). Supplementary cementitious materials. *Cement and Concrete Research, 41*(12), 1244-1256.

Mahmud, H. B., Malik, M. F. A., Kahar, R. A., Zain, M. F. M., & Raman, S. N. (2009). Mechanical properties and durability of normal and water reduced high strength grade 60 concrete containing rice husk ash. *Journal of advanced concrete technology, 7*(1), 21-30.

Malagavelli, V., & Rao, P. (2010). High performance concrete with GGBS and ROBO sand. *International Journal of Engineering Science and Technology, 2*(10), 5107-5113.

Manmohan, D., & Mehta, P. (1981). Influence of pozzolanic, slag and chemical admixtures on pore size distribution and permeability of hardened cement pastes. *Cement, concrete, and aggregates, 3*(1), 63-67.

Mannan, M. A., & Ganapathy, C. ((2004)). Concrete from an agricultural waste-oil palm shell (OPS). *Building and Environment, 39*(4), 441-448. doi:http://dx.doi.org/10.1016/j.buildenv.2003.10.007

Maragkos, I., Giannopoulou, I. P., & Panias, D. (2009). Synthesis of ferronickel slag-based geopolymers. *Minerals Engineering, 22*(2), 196-203.

Mehta, P. K., & Monteiro, P. J. (2006). *Concrete: microstructure, properties, and materials* (Vol. 3): McGraw-Hill New York.

Mo, K. H., Yap, S. P., Alengaram, U. J., Jumaat, M. Z., & Bu, C. H. (2014). Impact resistance of hybrid fibre-reinforced oil palm shell concrete. *Construction and Building Materials, 50*(0), 499-507. doi:http://dx.doi.org/10.1016/j.conbuildmat.2013.10.016

Mohammed, B. S., Foo, W. L., & Abdullahi, M. ((2014)). Flexural strength of palm oil clinker concrete beams. *Materials & Design, 53*(0), 325-331. doi:http://dx.doi.org/10.1016/j.matdes.2013.07.041

Nematollahi, B., & Sanjayan, J. (2014). Effect of different superplasticizers and activator combinations on workability and strength of fly ash based geopolymer. *Materials & Design, 57*, 667-672.

Ng, T. S., & Foster, S. J. ((2013)). Development of a mix design methodology for high-performance geopolymer mortars. *Structural Concrete, 14*(2), 148-156.

Okpala, D. C. (1990). Palm kernel shell as a lightweight aggregate in concrete. *Building and Environment, 25*(4), 291-296. doi:http://dx.doi.org/10.1016/0360-1323(90)90002-9

Olanipekun, E., Olusola, K., & Ata, O. (2006). A comparative study of concrete properties using coconut shell and palm kernel shell as coarse aggregates. *Building and Environment, 41*(3), 297-301.

Ostertag, C., & Yi, C. (2007). Crack/fiber interaction and crack growth resistance behavior in microfiber reinforced mortar specimens. *Materials and Structures, 40*(7), 679-691.

Pierre, P., Pleau, R., & Pigeon, M. (1999). Mechanical properties of steel microfiber reinforced cement pastes and mortars. *Journal of Materials in civil engineering, 11*(4), 317-324.

Poon, C.-S., Lam, L., Kou, S., Wong, Y.-L., & Wong, R. (2001). Rate of pozzolanic reaction of metakaolin in high-performance cement pastes. *Cement and Concrete Research, 31*(9), 1301-1306.

Pui, Y. F. (2011). *Potential use of palm oil fuel ash as a construction material*. Universiti Teknologi Malaysia, Faculty of Civil Engineering.

Punmia, B., Jain, A. K., & Jain, A. K. (2003). *Basic Civil Engineering*: Firewall Media.

Quiroga, P. N., & Fowler, D. W. (2004). *The effects of aggregates characteristics on the performance of Portland cement concrete* (ICAR 104-1F). Retrieved from 1 University Station C1755, Austin, TX 78712-0277:

Ranjbar, N., Mehrali, M., Alengaram, U. J., Metselaar, H. S. C., & Jumaat, M. Z. ((2014)). Compressive strength and microstructural analysis of fly ash/palm oil fuel ash based geopolymer mortar under elevated temperatures. *Construction and Building Materials, 65*(0), 114-121. doi:http://dx.doi.org/10.1016/j.conbuildmat.2014.04.064

Ranjbar, N., Mehrali, M., Behnia, A., Alengaram, U. J., & Jumaat, M. Z. (2014). Compressive strength and microstructural analysis of fly ash/palm oil fuel ash based geopolymer mortar. *Materials & Design, 59*(0), 532-539. doi:http://dx.doi.org/10.1016/j.matdes.2014.03.037

Ranjbar, N., Mehrali, M., Behnia, A., Alengaram, U. J., & Jumaat, M. Z. ((2014)). Compressive strength and microstructural analysis of fly ash/palm oil fuel ash based geopolymer mortar. *Materials & Design, 59*(0), 532-539. doi:http://dx.doi.org/10.1016/j.matdes.2014.03.037

Rehan, R., & Nehdi, M. (2005). Carbon dioxide emissions and climate change: policy implications for the cement industry. *Environmental Science & Policy, 8*(2), 105-114. doi:http://dx.doi.org/10.1016/j.envsci.2004.12.006

Safiuddin, M., Abdus Salam, M., & Jumaat, M. Z. (2011). Utilization of palm oil fuel ash in concrete: a review. *Journal of civil engineering and management, 17*(2), 234-247.

Sakai, E., Hoshino, S., Ohba, Y., & Daimon, M. (1997). The fluidity of cement paste with various types of inorganic powders. *Proc. of the 10th Int'l Cong. on the Chemistry of Cement, Gothenburg, Sweden, 2*.

Sayed, M., & Zeedan, S. R. (2012). Green binding material using alkali activated blast furnace slag with silica fume. *HBRC Journal, 8*(3), 177-184.

Sengul, O., Tasdemir, C., & Tasdemir, M. A. (2002). Influence of aggregate type on mechanical behavior of normal-and high-strength concretes. *ACI materials journal, 99*(6).

Shafigh, P., Jumaat, M. Z., Mahmud, H. B., & Alengaram, U. J. (2013). Oil palm shell lightweight concrete containing high volume ground granulated blast furnace slag. *Construction and Building Materials, 40*(0), 231-238. doi:http://dx.doi.org/10.1016/j.conbuildmat.2012.10.007

Shafigh, P., Jumaat, M. Z., Mahmud, H. B., & Hamid, N. A. A. (2012). Lightweight concrete made from crushed oil palm shell: Tensile strength and effect of initial curing on compressive strength. *Construction and Building Materials, 27*(1), 252-258.

Shafigh, P., Mahmud, H. B., Jumaat, M. Z. B., Ahmmad, R., & Bahri, S. (2014). Structural lightweight aggregate concrete using two types of waste from the palm

oil industry as aggregate. *Journal of Cleaner Production, 80*(0), 187-196. doi:http://dx.doi.org/10.1016/j.jclepro.2014.05.051

Shannag, M. J. (2011). Characteristics of lightweight concrete containing mineral admixtures. *Construction and Building Materials, 25*(2), 658-662. doi:http://dx.doi.org/10.1016/j.conbuildmat.2010.07.025

Shariq, M., Prasad, J., & Abbas, H. (2013). Effect of GGBFS on age dependent static modulus of elasticity of concrete. *Construction and Building Materials, 41*(0), 411-418. doi:http://dx.doi.org/10.1016/j.conbuildmat.2012.12.035

Shariq, M., Prasad, J., & Masood, A. (2013). Studies in ultrasonic pulse velocity of concrete containing GGBFS. *Construction and Building Materials, 40*(0), 944-950. doi:http://dx.doi.org/10.1016/j.conbuildmat.2012.11.070

Sharma, J., & Chand, N. (2013). Dynamic mechanical analysis and dielectric studies of agro-waste rice husk/polypropylene composites with cenosphere. *Journal of Composite Materials, 47*(15), 1833-1842.

Shi, C., Jiménez, A. F., & Palomo, A. (2011). New cements for the 21st century: the pursuit of an alternative to Portland cement. *Cement and Concrete Research, 41*(7), 750-763.

Silva, F., & Thaumaturgo, C. (2003). Fibre reinforcement and fracture response in geopolymeric mortars. *Fatigue & Fracture of Engineering Materials & Structures, 26*(2), 167-172.

Silva, P. D., Sagoe-Crenstil, K., & Sirivivatnanon, V. (2007). Kinetics of geopolymerization: Role of Al< sub> 2</sub> O< sub> 3</sub> and SiO< sub> 2</sub>. *Cement and Concrete Research, 37*(4), 512-518.

Škvára, F., Kopecký, L., Nemecek, J., & Bittnar, Z. ((2006)). Microstructure of geopolymer materials based on fly ash. *Ceramics-Silikaty, 50*(4), 208-215.

Soroushian, P., Khan, A., & Hsu, J.-W. (1992). Mechanical properties of concrete materials reinforced with polypropylene or polyethylene fibers. *ACI materials journal, 89*(6).

Sugama, T., Brothers, L., & Van de Putte, T. (2005). Acid-resistant cements for geothermal wells: sodium silicate activated slag/fly ash blends. *Advances in Cement Research, 17*(2), 65-75.

Susan, B., Ruby, D. G., Silvio, D., & Erich, R. ((2006)). *Performance of geopolymeric concrete reinforced with steel fibers.* Paper presented at the 10th International Inorganic–Bonded Fibre Composites Conference, Brazil.

Talling, B., & Brandstetr, J. (1989). Present state and future of alkali-activated slag concretes. *ACI Special Publication, 114*.

Tamim, M. M., Dhar, A., & Hossain, M. S. (2013). Fly ash in Bangladesh-An Overview. *International Journal of Scientific & Engineering Research, 4*(6), 809-812.

Teo, D., Mannan, M., & Kurian, V. (2006). Structural concrete using oil palm shell (OPS) as lightweight aggregate. *Turk J Eng Environ Sci, 30*(4), 251-257.

TEO, D. C. L., MANNAN, M. A., & KURIAN, V. J. (2006). Structural concrete using oil palm shell (OPS) as lightweight aggregate. *Turkish Journal of Engineering and Environmental Sciences, 30*(4), 251-257.

Teoreanu, I., Volceanov, A., & Stoleriu, S. (2005). Non Portland cements and derived materials. *Cement and Concrete Composites, 27*(6), 650-660.

Waehneldt, T. (1975). Sodium dodecyl sulfate in protein chemistry. *Biosystems, 6*(3), 176-187.

Wang, J., Wu, X.-l., Wang, J.-x., Liu, C.-z., Lai, Y.-m., Hong, Z.-k., & Zheng, J.-p. (2012). Hydrothermal synthesis and characterization of alkali-activated slag–fly ash–metakaolin cementitious materials. *Microporous and Mesoporous Materials, 155*(0), 186-191. doi:http://dx.doi.org/10.1016/j.micromeso.2012.01.016

Wang, S.-D., Pu, X.-C., Scrivener, K., & Pratt, P. ((1995)). Alkali-activated slag cement and concrete: a review of properties and problems. *Advances in Cement Research, 7*(27), 93-102.

Warid Hussin, M., & Abdul Awal A. S, M. (1997). Palm oil fuel ash : A potential pozzolanic material in concrete construction. *Journal of Ferrocement, 27*(4), 321-327. Retrieved from http://www.refdoc.fr/Detailnotice?idarticle=14825089

Whitehurst, E. A. (1986). Evaluation of concrete properties from sonic tests. *ACI Monograph, 2*, 73.

Wood, S. A., & Marek, C. R. (1995). *Recovery and utilization of quarry by-products for use in highway construction*. Paper presented at the ICAR 3rd annual symposium.

Wu, H.-C., & Sun, P. (2007). New building materials from fly ash-based lightweight inorganic polymer. *Construction and Building Materials, 21*(1), 211-217.

Xu, H., & van Deventer, J. S. (2003). Effect of source materials on geopolymerization. *Industrial & engineering chemistry research, 42*(8), 1698-1706.

Yalçin, N., & Sevinç, V. (2001). Studies on silica obtained from rice husk. *Ceramics International, 27*(2), 219-224. doi:http://dx.doi.org/10.1016/S0272-8842(00)00068-7

Yang, K.-H., Song, J.-K., Ashour, A. F., & Lee, E.-T. (2008). Properties of cementless mortars activated by sodium silicate. *Construction and Building Materials, 22*(9), 1981-1989. doi:http://dx.doi.org/10.1016/j.conbuildmat.2007.07.003

Yao, X., Zhang, Z., Zhu, H., & Chen, Y. (2009). Geopolymerization process of alkali–metakaolinite characterized by isothermal calorimetry. *Thermochimica Acta, 493*(1), 49-54.

Yap, S. P., Bu, C. H., Alengaram, U. J., Mo, K. H., & Jumaat, M. Z. (2014). Flexural toughness characteristics of steel–polypropylene hybrid fibre-reinforced oil palm shell concrete. *Materials and Design, 57*, 652-659. doi:http://dx.doi.org/10.1016/j.matdes.2014.01.004

Yi, C., & Ostertag, C. (2001). Strengthening and toughening mechanisms in microfiber reinforced cementitious composites. *Journal of materials science, 36*(6), 1513-1522.

Yi, C., & Ostertag, C. ((2001)). Strengthening and toughening mechanisms in microfiber reinforced cementitious composites. *Journal of materials science, 36*(6), 1513-1522.

Yip, C. K., Lukey, G., & Van Deventer, J. (2005). The coexistence of geopolymeric gel and calcium silicate hydrate at the early stage of alkaline activation. *Cement and Concrete Research, 35*(9), 1688-1697.

Yip, C. K., Lukey, G. C., Provis, J. L., & van Deventer, J. S. (2008). Effect of calcium silicate sources on geopolymerisation. *Cement and Concrete Research, 38*(4), 554-564.

Yoo, D.-Y., Shin, H.-O., Yang, J.-M., & Yoon, Y.-S. (2014). Material and bond properties of ultra high performance fiber reinforced concrete with micro steel fibers. *Composites Part B: Engineering, 58*(0), 122-133. doi:http://dx.doi.org/10.1016/j.compositesb.2013.10.081

Yoo, D.-Y., Shin, H.-O., Yang, J.-M., & Yoon, Y.-S. ((2014)). Material and bond properties of ultra high performance fiber reinforced concrete with micro steel fibers. *Composites Part B: Engineering, 58*(0), 122-133. doi:http://dx.doi.org/10.1016/j.compositesb.2013.10.081

Yusuf, M. O., Johari, M. A. M., Ahmad, Z. A., & Maslehuddin, M. (2014). Effects of addition of Al(OH)3 on the strength of alkaline activated ground blast furnace slag-ultrafine palm oil fuel ash (AAGU) based binder. *Construction and Building Materials, 50*(0), 361-367. doi:http://dx.doi.org/10.1016/j.conbuildmat.2013.09.054

Yusuf, M. O., Megat Johari, M. A., Ahmad, Z. A., & Maslehuddin, M. ((2014)-a). Effects of H2O/Na2O molar ratio on the strength of alkaline activated ground blast furnace slag-ultrafine palm oil fuel ash based concrete. *Materials & Design, 56*(0), 158-164. doi:http://dx.doi.org/10.1016/j.matdes.2013.09.078

Yusuf, M. O., Megat Johari, M. A., Ahmad, Z. A., & Maslehuddin, M. ((2014)-b). Strength and microstructure of alkali-activated binary blended binder containing palm oil fuel ash and ground blast-furnace slag. *Construction and Building Materials, 52*(0), 504-510. doi:http://dx.doi.org/10.1016/j.conbuildmat.2013.11.012

Zhu, Y., & Xu, S. Fracture properties of cement paste and mortar: an experimental investigation.

Abdullah, A. A. A. (1996). 10 - Palm oil shell aggregate for lightweight concrete. Waste Materials Used in Concrete Manufacturing. S. Chandra. Westwood, NJ, William Andrew Publishing**:** 624-636.

Abu Bakar, B. H., Putrajaya, R. and Abdulaziz, H. (2010). "Malaysian rice husk ash–improving the durability and corrosion resistance of concrete: pre-review." Concrete Research Letters **1**(1): 6-13.

Ahmmad, R., Jumaat, M. Z., Bahri, S. and Islam, A. B. M. S. ((2014)). "Ductility performance of lightweight concrete element containing massive palm shell clinker." Construction and Building Materials **63**(0): 234-241.

Alengaram, U. J., Jumaat, M. Z. and Mahmud, H. (2008). Influence of sand content and silica fume on mechanical properties of palm kernel shell concrete. International conference on construction and building technology ICCBT.

Alengaram, U. J., Jumaat, M. Z., Mahmud, H. and Fayyadh, M. M. (2011). "Shear behaviour of reinforced palm kernel shell concrete beams." Construction and Building Materials **25**(6): 2918-2927.

Alengaram, U. J., Mahmud, H. and Jumaat, M. Z. (2011). "Enhancement and prediction of modulus of elasticity of palm kernel shell concrete." Materials & Design **32**(4): 2143-2148.

Alengaram, U. J., Muhit, B. A. A. and Jumaat, M. Z. (2013). "Utilization of oil palm kernel shell as lightweight aggregate in concrete – A review." Construction and Building Materials **38**: 161-172.

Alengaram, U. J., Muhit, B. A. A., Jumaat, M. Z. and Jing, M. L. Y. (2013). "A comparison of the thermal conductivity of oil palm shell foamed concrete with conventional materials." Materials and Design **51**: 522-529.

Alonso, S. and Palomo, A. (2001). "Alkaline activation of metakaolin and calcium hydroxide mixtures: influence of temperature, activator concentration and solids ratio." Materials Letters **47**(1): 55-62.

Appukutty, P. and Murugesan, R. (2009). "Substitution of quarry dust to sand for mortar in brick masonry works." International Journal on Design and Manufacturing Technologies **3**(1): 59-63.

Arellano Aguilar, R., Burciaga Díaz, O. and Escalante García, J. I. (2010). "Lightweight concretes of activated metakaolin-fly ash binders, with blast furnace slag aggregates." Construction and Building Materials **24**(7): 1166-1175.

Asavapisit, S. and Ruengrit, N. (2005). "The role of RHA-blended cement in stabilizing metal-containing wastes." Cement and Concrete Composites **27**(7): 782-787.

Ashraf, M. A., Maah, M. J., Yusoff, I., Wajid, A. and Mahmood, K. (2011). "Sand mining effects, causes and concerns: a case study from Bestari Jaya, Selangor, Peninsular Malaysia." Scientific Research and Essays **6**(6): 1216-1231.

Bakharev, T., Sanjayan, J. and Cheng, Y.-B. ((2001)). "Resistance of alkali-activated slag concrete to alkali–aggregate reaction." Cement and Concrete Research **31**(2): 331-334.

Bamaga, S. O., Hussin, M. W. and Ismail, M. (2013). "Palm Oil Fuel Ash: Promising supplementary cementing materials." KSCE Journal of Civil Engineering **17**(7): 1708-1713.

Barbosa, V. F. F. and MacKenzie, K. J. D. (2003). "Thermal behaviour of inorganic geopolymers and composites derived from sodium polysalate." Mater Res Bull **38**(2): 319-331.

Barnett, S., Soutsos, M., Millard, S. and Bungey, J. (2006). "Strength development of mortars containing ground granulated blast-furnace slag: Effect of curing temperature and determination of apparent activation energies." Cement and Concrete Research **36**(3): 434-440.

Basha, E., Hashim, R., Mahmud, H. and Muntohar, A. (2005). "Stabilization of residual soil with rice husk ash and cement." Construction and Building Materials **19**(6): 448-453.

Bashar, I. I., Alengaram, U. J., Jumaat, M. Z. and Islam, A. ((2014)). "The Effect of Variation of Molarity of Alkali Activator and Fine Aggregate Content on the Compressive Strength of the Fly Ash: Palm Oil Fuel Ash Based Geopolymer Mortar." Advances in Materials Science and Engineering.

Bernal, S. A., Mejía de Gutiérrez, R. and Provis, J. L. (2012). "Engineering and durability properties of concretes based on alkali-activated granulated blast furnace slag/metakaolin blends." Construction and Building Materials **33**(0): 99-108.

Bernal, S. A., Mejía de Gutiérrez, R. and Provis, J. L. (2012). "Engineering and durability properties of concretes based on alkali-activated granulated blast furnace slag/metakaolin blends." Construction and Building Materials **33**: 99-108.

Bernal, S. A., Mejía de Gutiérrez, R. and Provis, J. L. ((2012)). "Engineering and durability properties of concretes based on alkali-activated granulated blast furnace slag/metakaolin blends." Construction and Building Materials **33**: 99-108.

Bernal, S. A., Provis, J. L., Rose, V. and Mejía de Gutierrez, R. (2011). "Evolution of binder structure in sodium silicate-activated slag-metakaolin blends." Cement and Concrete Composites **33**(1): 46-54.

Buchwald, A., Hilbig, H. and Kaps, C. (2007). "Alkali-activated metakaolin-slag blends—performance and structure in dependence of their composition." Journal of materials science **42**(9): 3024-3032.

Burciaga-Diaz, O., Escalante-Garcia, J. I. and Gorokhovsky, A. (2012). "Geopolymers based on a coarse low-purity kaolin mineral: Mechanical strength as a function of the chemical composition and temperature." Cement and Concrete Composites **34**(1): 18-24.

Caglar, B., Çırak, Ç., Tabak, A., Afsin, B. and Eren, E. (2013). "Covalent grafting of pyridine-2-methanol into kaolinite layers." Journal of Molecular Structure **1032**: 12-22.

Chang, J. (2003). "A study on the setting characteristics of sodium silicate-activated slag pastes." Cement and Concrete Research **33**(7): 1005-1011.

Chi, M. and Huang, R. ((2013)). "Binding mechanism and properties of alkali-activated fly ash/slag mortars." Construction and Building Materials **40**: 291-298.

Chindaprasirt, P., De Silva, P., Sagoe-Crentsil, K. and Hanjitsuwan, S. (2012). "Effect of SiO2 and Al2O3 on the setting and hardening of high calcium fly ash-based geopolymer systems." Journal of materials science **47**(12): 4876-4883.

Chindaprasirt, P., Jaturapitakkul, C., Chalee, W. and Rattanasak, U. (2009). "Comparative study on the characteristics of fly ash and bottom ash geopolymers." Waste management **29**(2): 539-543.

Chindaprasirt, P. and Rukzon, S. (2008). "Strength, porosity and corrosion resistance of ternary blend Portland cement, rice husk ash and fly ash mortar." Construction and Building Materials **22**(8): 1601-1606.

Chindaprasirt, P., Rukzon, S. and Sirivivatnanon, V. (2008). "Resistance to chloride penetration of blended Portland cement mortar containing palm oil fuel ash, rice husk ash and fly ash." Construction and Building Materials **22**(5): 932-938.

Conradt, R., Pimkhaokham, P. and Leela-Adisorn, U. (1992). "Nano-structured silica from rice husk." Journal of Non-Crystalline Solids **145**(0): 75-79.

Coutinho, J. S. (2003). "The combined benefits of CPF and RHA in improving the durability of concrete structures." Cement and Concrete Composites **25**(1): 51-59.

Damtoft, J. S., Lukasik, J., Herfort, D., Sorrentino, D. and Gartner, E. M. (2008). "Sustainable development and climate change initiatives." Cement and Concrete Research **38**(2): 115-127.

Davidovit, J. ((2002)). "Inorganic polymeric new material."

Davidovits, J. (1991). "Geopolymers." Journal of Thermal Analysis and Calorimetry **37**(8): 1633-1656.

Davidovits, J. (2005). Geopolymer, Green Chemistry and Sustainable Development Solutions: Proceedings of the World Congress Geopolymer 2005, Geopolymer Institute.

Davidovits, J. ((2008)). "Chemistry and Applications Geopolymer Institute." Saint-Quentin, France.

Davidovits, J. ((2008)). Geopolymer chemistry & application. 16 rule Galilee, F-02100 Saint-Quentin, France, Institute Géopolymèr.

de Gutiérrez, R. M., Díaz, L. N. and Delvasto, S. ((2005)). "Effect of pozzolans on the performance of fiber-reinforced mortars." Cement and Concrete Composites **27**(5): 593-598.

Della, V., Kühn, I. and Hotza, D. (2002). "Rice husk ash as an alternate source for active silica production." Materials Letters **57**(4): 818-821.

Dhir, R. K. and Jappy, T. G. (1999). Exploiting wastes in concrete: proceedings of the international seminar held at the University of Dundee, Scotland, UK on 7 September 1999, Thomas Telford.

Dinakar, P., Sethy, K. P. and Sahoo, U. C. (2013). "Design of self-compacting concrete with ground granulated blast furnace slag." Materials & Design **43**: 161-169.

Donza, H., Cabrera, O. and Irassar, E. (2002). "High-strength concrete with different fine aggregate." Cement and Concrete Research **32**(11): 1755-1761.

Duxson, P., Fernández-Jiménez, A., Provis, J., Lukey, G., Palomo, A. and Van Deventer, J. (2007). "Geopolymer technology: the current state of the art." Journal of materials science **42**(9): 2917-2933.

Duxson, P., Lukey, G., Separovic, F. and Van Deventer, J. (2005). "Effect of alkali cations on aluminum incorporation in geopolymeric gels." Industrial & engineering chemistry research **44**(4): 832-839.

Duxson, P., Provis, J. L., Lukey, G. C., Mallicoat, S. W., Kriven, W. M. and Van Deventer, J. S. (2005). "Understanding the relationship between geopolymer composition, microstructure and mechanical properties." Colloids and Surfaces A: Physicochemical and Engineering Aspects **269**(1): 47-58.

Dvorkin, L., Bezusyak, A., Lushnikova, N. and Ribakov, Y. (2012). "Using mathematical modeling for design of self compacting high strength concrete with metakaolin admixture." Construction and Building Materials **37**: 851-864.

Feng, J., Zhang, R., Gong, L., Li, Y., Cao, W. and Cheng, X. (2015). "Development of porous fly ash-based geopolymer with low thermal conductivity." Materials & Design **65**(0): 529-533.

Fernández-Jiménez, A., Puertas, F. and Arteaga, A. (1998). "Determination of kinetic equations of alkaline activation of blast furnace slag by means of calorimetric data." Journal of Thermal Analysis and Calorimetry **52**(3): 945-955.

Galau, D. and Ismail, M. (2010). Characterization of Palm Oil Fuel Ash (POFA) from Different Mill as Cement Replacement Material, Thesis, Faculty of Civil Engineering, Universiti Teknologi Malaysia, Johor, Malaysia.

Givi, A. N., Rashid, S. A., Aziz, F. N. A. and Salleh, M. A. M. ((2010)). "Contribution of rice husk ash to the properties of mortar and concrete: a review." Journal of American science **6**(3): 157-165.

Güneyisi, E. and Gesoğlu, M. ((2008)). "A study on durability properties of high-performance concretes incorporating high replacement levels of slag." Materials and Structures **41**(3): 479-493.

Guo, X., Shi, H. and Dick, W. A. (2010). "Compressive strength and microstructural characteristics of class C fly ash geopolymer." Cement and Concrete Composites **32**(2): 142-147.

Halstead, W. J. (1986). "Use of fly ash in concrete." NCHRP Synthesis of Highway Practice(127).

Hardjito, D., Wallah, S. E., Sumajouw, D. M. and Rangan, B. V. (2005). "Fly ash-based geopolymer concrete." Australian Journal of Structural Engineering **6**(1): 77-84.

Hardjito, D., Wallah, S. E., Sumajouw, D. M. and Rangan, B. V. ((2004)). "On the development of fly ash-based geopolymer concrete." ACI materials journal **101**(6).

He, J., Jie, Y., Zhang, J., Yu, Y. and Zhang, G. (2013). "Synthesis and characterization of red mud and rice husk ash-based geopolymer composites." Cement and Concrete Composites **37**: 108-118.

Isaia, G. C., Gastaldini, A. L. G. and Moraes, R. (2003). "Physical and pozzolanic action of mineral additions on the mechanical strength of high-performance concrete." Cement and Concrete Composites **25**(1): 69-76.

Islam, A., Alengaram, U. J., Jumaat, M. Z. and Bashar, I. I. (2014). "The development of compressive strength of ground granulated blast furnace slag-palm oil fuel ash-fly ash based geopolymer mortar." Materials & Design **56**(0): 833-841.

Islam, A., Alengaram, U. J., Jumaat, M. Z. and Bashar, I. I. (2014). "The development of compressive strength of ground granulated blast furnace slag-palm oil fuel ash-fly ash based geopolymer mortar." Materials & Design **56**: 833-841.

Joseph, B. and Mathew, G. (2012). "Influence of aggregate content on the behavior of fly ash based geopolymer concrete." Scientia Iranica **19**(5): 1188-1194.

Kabir, S., Alengaram, U. J., Jumaat, M. Z., Sharmin, A. and Islam, A. ((2015)). "Influence of Molarity and Chemical Composition on the Development of Compressive Strength in POFA Based Geopolymer Mortar." Advances in Materials Science and Engineering **2015**.

Kanadasan, J. and Abdul Razak, H. ((2015)). "Engineering and sustainability performance of self-compacting palm oil mill incinerated waste concrete." Journal of Cleaner Production **89**(0): 78-86.

Kanadasan, J. and Razak, H. A. (2013). "Mix design for self-compacting palm oil clinker concrete based on particle packing." Materials and Design.

Kannan, V. and Ganesan, K. (2014). "Chloride and chemical resistance of self compacting concrete containing rice husk ash and metakaolin." Construction and Building Materials **51**: 225-234.

Kannan, V. and Ganesan, K. ((2014)). "Chloride and chemical resistance of self compacting concrete containing rice husk ash and metakaolin." Construction and Building Materials **51**: 225-234.

Karim, M., Zain, M., Jamil, M. and Lai, F. ((2013)). "Fabrication of a non-cement binder using slag, palm oil fuel ash and rice husk ash with sodium hydroxide." Construction and Building Materials **49**: 894-902.

Karim, M. R., Zain, M. F. M., Jamil, M. and Lai, F. C. ((2013)). "Fabrication of a non-cement binder using slag, palm oil fuel ash and rice husk ash with sodium hydroxide." Construction and Building Materials **49**(0): 894-902.

Khan, M. I. (2012). "Evaluation of non-destructive testing of high strength concrete incorporating supplementary cementitious composites." Resources, Conservation and Recycling **61**(0): 125-129.

Khana, M., Jamil, M., Karimc, M. and Zaind, M. (2014). "Strength and Durability of Mortar and Concrete Containing Rice Husk Ash: A Review." World Applied Sciences Journal **32**(5): 752-765.

Klee, H. and Coles, E. (2004). "The cement sustainability initiative–implementing change across a global industry." Corporate Social Responsibility and Environmental Management **11**(2): 114-120.

Kou, S.-c., Poon, C.-s. and Agrela, F. (2011). "Comparisons of natural and recycled aggregate concretes prepared with the addition of different mineral admixtures." Cement and Concrete Composites **33**(8): 788-795.

Kumar, S., Kumar, R. and Mehrotra, S. (2010). "Influence of granulated blast furnace slag on the reaction, structure and properties of fly ash based geopolymer." Journal of materials science **45**(3): 607-615.

Kupaei, R. H., Alengaram, U. J. and Jumaat, M. Z. (2014). "The effect of different parameters on the development of compressive strength of oil palm shell geopolymer concrete." The Scientific World Journal **2014**.

Kupaei, R. H., Alengaram, U. J., Jumaat, M. Z. B. and Nikraz, H. (2013). "Mix design for fly ash based oil palm shell geopolymer lightweight concrete." Construction and Building Materials **43**: 490-496.

Kusbiantoro, A., Nuruddin, M. F., Shafiq, N. and Qazi, S. A. (2012). "The effect of microwave incinerated rice husk ash on the compressive and bond strength of fly ash based geopolymer concrete." Construction and Building Materials **36**(0): 695-703.

Lawler, J. S. ((2001)). Hybrid fiber-reinforcement in mortar and concrete.

Lee, W. and Van Deventer, J. (2002). "The effect of ionic contaminants on the early-age properties of alkali-activated fly ash-based cements." Cement and Concrete Research **32**(4): 577-584.

Li, C., Sun, H. and Li, L. (2010). "A review: The comparison between alkali-activated slag (Si+ Ca) and metakaolin (Si+ Al) cements." Cement and Concrete Research **40**(9): 1341-1349.

Li, Z. and Liu, S. (2007). "Influence of slag as additive on compressive strength of fly ash-based geopolymer." Journal of Materials in civil engineering **19**(6): 470-474.

Liu, M. Y. J., Alengaram, U. J., Jumaat, M. Z. and Mo, K. H. (2014). "Evaluation of thermal conductivity, mechanical and transport properties of lightweight aggregate foamed geopolymer concrete." Energy and Buildings **72**(0): 238-245.

Liu, M. Y. J., Chua, C. P., Alengaram, U. J. and Jumaat, M. Z. (2014). "Utilization of palm oil fuel ash as binder in lightweight oil palm shell geopolymer concrete." Advances in Materials Science and Engineering **2014**.

Lothenbach, B., Scrivener, K. and Hooton, R. (2011). "Supplementary cementitious materials." Cement and Concrete Research **41**(12): 1244-1256.

Mahmud, H. B., Malik, M. F. A., Kahar, R. A., Zain, M. F. M. and Raman, S. N. (2009). "Mechanical properties and durability of normal and water reduced high strength grade 60 concrete containing rice husk ash." Journal of advanced concrete technology **7**(1): 21-30.

Malagavelli, V. and Rao, P. (2010). "High performance concrete with GGBS and ROBO sand." International Journal of Engineering Science and Technology **2**(10): 5107-5113.

Manmohan, D. and Mehta, P. (1981). "Influence of pozzolanic, slag and chemical admixtures on pore size distribution and permeability of hardened cement pastes." Cement, concrete, and aggregates **3**(1): 63-67.

Mannan, M. A. and Ganapathy, C. ((2004)). "Concrete from an agricultural waste-oil palm shell (OPS)." Building and Environment **39**(4): 441-448.

Maragkos, I., Giannopoulou, I. P. and Panias, D. (2009). "Synthesis of ferronickel slag-based geopolymers." Minerals Engineering **22**(2): 196-203.

Mehta, P. K. and Monteiro, P. J. (2006). Concrete: microstructure, properties, and materials, McGraw-Hill New York.

Mo, K. H., Yap, S. P., Alengaram, U. J., Jumaat, M. Z. and Bu, C. H. (2014). "Impact resistance of hybrid fibre-reinforced oil palm shell concrete." Construction and Building Materials **50**(0): 499-507.

Mohammed, B. S., Foo, W. L. and Abdullahi, M. ((2014)). "Flexural strength of palm oil clinker concrete beams." Materials & Design **53**(0): 325-331.

Nematollahi, B. and Sanjayan, J. (2014). "Effect of different superplasticizers and activator combinations on workability and strength of fly ash based geopolymer." Materials & Design **57**: 667-672.

Ng, T. S. and Foster, S. J. ((2013)). "Development of a mix design methodology for high-performance geopolymer mortars." Structural Concrete **14**(2): 148-156.

Okpala, D. C. (1990). "Palm kernel shell as a lightweight aggregate in concrete." Building and Environment **25**(4): 291-296.

Olanipekun, E., Olusola, K. and Ata, O. (2006). "A comparative study of concrete properties using coconut shell and palm kernel shell as coarse aggregates." Building and Environment **41**(3): 297-301.

Ostertag, C. and Yi, C. (2007). "Crack/fiber interaction and crack growth resistance behavior in microfiber reinforced mortar specimens." Materials and Structures **40**(7): 679-691.

Pierre, P., Pleau, R. and Pigeon, M. (1999). "Mechanical properties of steel microfiber reinforced cement pastes and mortars." Journal of Materials in civil engineering **11**(4): 317-324.

Poon, C.-S., Lam, L., Kou, S., Wong, Y.-L. and Wong, R. (2001). "Rate of pozzolanic reaction of metakaolin in high-performance cement pastes." Cement and Concrete Research **31**(9): 1301-1306.

Pui, Y. F. (2011). Potential use of palm oil fuel ash as a construction material, Universiti Teknologi Malaysia, Faculty of Civil Engineering.

Punmia, B., Jain, A. K. and Jain, A. K. (2003). Basic Civil Engineering, Firewall Media.

Quiroga, P. N. and Fowler, D. W. (2004). The effects of aggregates characteristics on the performance of Portland cement concrete. 1 University Station C1755, Austin, TX 78712-0277, International Centre for Aggregates Research (ICAR), The University of Texas at Austin.

Ranjbar, N., Mehrali, M., Alengaram, U. J., Metselaar, H. S. C. and Jumaat, M. Z. ((2014)). "Compressive strength and microstructural analysis of fly ash/palm oil fuel ash based geopolymer mortar under elevated temperatures." Construction and Building Materials **65**(0): 114-121.

Ranjbar, N., Mehrali, M., Behnia, A., Alengaram, U. J. and Jumaat, M. Z. (2014). "Compressive strength and microstructural analysis of fly ash/palm oil fuel ash based geopolymer mortar." Materials & Design **59**(0): 532-539.

Ranjbar, N., Mehrali, M., Behnia, A., Alengaram, U. J. and Jumaat, M. Z. ((2014)). "Compressive strength and microstructural analysis of fly ash/palm oil fuel ash based geopolymer mortar." Materials & Design **59**(0): 532-539.

Rehan, R. and Nehdi, M. (2005). "Carbon dioxide emissions and climate change: policy implications for the cement industry." Environmental Science & Policy **8**(2): 105-114.

Safiuddin, M., Abdus Salam, M. and Jumaat, M. Z. (2011). "Utilization of palm oil fuel ash in concrete: a review." Journal of civil engineering and management **17**(2): 234-247.

Sakai, E., Hoshino, S., Ohba, Y. and Daimon, M. (1997). "The fluidity of cement paste with various types of inorganic powders." Proc. of the 10th Int'l Cong. on the Chemistry of Cement, Gothenburg, Sweden **2**.

Sayed, M. and Zeedan, S. R. ((2012)). "Green binding material using alkali activated blast furnace slag with silica fume." HBRC Journal **8**(3): 177-184.

Sengul, O., Tasdemir, C. and Tasdemir, M. A. (2002). "Influence of aggregate type on mechanical behavior of normal-and high-strength concretes." ACI materials journal **99**(6).

Shafigh, P., Jumaat, M. Z., Mahmud, H. B. and Alengaram, U. J. (2013). "Oil palm shell lightweight concrete containing high volume ground granulated blast furnace slag." Construction and Building Materials **40**(0): 231-238.

Shafigh, P., Jumaat, M. Z., Mahmud, H. B. and Hamid, N. A. A. (2012). "Lightweight concrete made from crushed oil palm shell: Tensile strength and effect of initial curing on compressive strength." Construction and Building Materials **27**(1): 252-258.

Shafigh, P., Mahmud, H. B., Jumaat, M. Z. B., Ahmmad, R. and Bahri, S. ((2014)). "Structural lightweight aggregate concrete using two types of waste from the palm oil industry as aggregate." Journal of Cleaner Production **80**(0): 187-196.

Shannag, M. J. (2011). "Characteristics of lightweight concrete containing mineral admixtures." Construction and Building Materials **25**(2): 658-662.

Shariq, M., Prasad, J. and Abbas, H. ((2013)). "Effect of GGBFS on age dependent static modulus of elasticity of concrete." Construction and Building Materials **41**(0): 411-418.

Shariq, M., Prasad, J. and Masood, A. (2013). "Studies in ultrasonic pulse velocity of concrete containing GGBFS." Construction and Building Materials **40**(0): 944-950.

Sharma, J. and Chand, N. (2013). "Dynamic mechanical analysis and dielectric studies of agro-waste rice husk/polypropylene composites with cenosphere." Journal of Composite Materials **47**(15): 1833-1842.

Shi, C., Jiménez, A. F. and Palomo, A. (2011). "New cements for the 21st century: the pursuit of an alternative to Portland cement." Cement and Concrete Research **41**(7): 750-763.

Silva, F. and Thaumaturgo, C. (2003). "Fibre reinforcement and fracture response in geopolymeric mortars." Fatigue & Fracture of Engineering Materials & Structures **26**(2): 167-172.

Silva, P. D., Sagoe-Crenstil, K. and Sirivivatnanon, V. (2007). "Kinetics of geopolymerization: Role of Al< sub> 2</sub> O< sub> 3</sub> and SiO< sub> 2</sub>." Cement and Concrete Research **37**(4): 512-518.

Škvára, F., Kopecký, L., Nemecek, J. and Bittnar, Z. ((2006)). "Microstructure of geopolymer materials based on fly ash." Ceramics-Silikaty **50**(4): 208-215.

Soroushian, P., Khan, A. and Hsu, J.-W. (1992). "Mechanical properties of concrete materials reinforced with polypropylene or polyethylene fibers." ACI materials journal **89**(6).

Sugama, T., Brothers, L. and Van de Putte, T. (2005). "Acid-resistant cements for geothermal wells: sodium silicate activated slag/fly ash blends." Advances in Cement Research **17**(2): 65-75.

Susan, B., Ruby, D. G., Silvio, D. and Erich, R. ((2006)). Performance of geopolymeric concrete reinforced with steel fibers. 10th International Inorganic–Bonded Fibre Composites Conference, Brazil.

Talling, B. and Brandstetr, J. (1989). "Present state and future of alkali-activated slag concretes." ACI Special Publication **114**.

Tamim, M. M., Dhar, A. and Hossain, M. S. (2013). "Fly ash in Bangladesh-An Overview." International Journal of Scientific & Engineering Research **4**(6): 809-812.

Teo, D., Mannan, M. and Kurian, V. ((2006)). "Structural concrete using oil palm shell (OPS) as lightweight aggregate." Turk J Eng Environ Sci **30**(4): 251-257.

TEO, D. C. L., MANNAN, M. A. and KURIAN, V. J. ((2006)). "Structural concrete using oil palm shell (OPS) as lightweight aggregate." Turkish Journal of Engineering and Environmental Sciences **30**(4): 251-257.

Teoreanu, I., Volceanov, A. and Stoleriu, S. (2005). "Non Portland cements and derived materials." Cement and Concrete Composites **27**(6): 650-660.

Waehneldt, T. (1975). "Sodium dodecyl sulfate in protein chemistry." Biosystems **6**(3): 176-187.

Wang, J., Wu, X.-l., Wang, J.-x., Liu, C.-z., Lai, Y.-m., Hong, Z.-k. and Zheng, J.-p. (2012). "Hydrothermal synthesis and characterization of alkali-activated slag–fly ash–metakaolin cementitious materials." Microporous and Mesoporous Materials **155**(0): 186-191.

Wang, S.-D., Pu, X.-C., Scrivener, K. and Pratt, P. ((1995)). "Alkali-activated slag cement and concrete: a review of properties and problems." Advances in Cement Research **7**(27): 93-102.

Warid Hussin, M. and Abdul Awal A. S, M. (1997). "Palm oil fuel ash : A potential pozzolanic material in concrete construction." Journal of Ferrocement **27**(4): 321-327.

Whitehurst, E. A. ((1986)). "Evaluation of concrete properties from sonic tests." ACI Monograph **2**: 73.

Wood, S. A. and Marek, C. R. (1995). Recovery and utilization of quarry by-products for use in highway construction. ICAR 3rd annual symposium. **10**.

Wu, H.-C. and Sun, P. (2007). "New building materials from fly ash-based lightweight inorganic polymer." Construction and Building Materials **21**(1): 211-217.

Xu, H. and van Deventer, J. S. (2003). "Effect of source materials on geopolymerization." Industrial & engineering chemistry research **42**(8): 1698-1706.

Yalçin, N. and Sevinç, V. (2001). "Studies on silica obtained from rice husk." Ceramics International **27**(2): 219-224.

Yang, K.-H., Song, J.-K., Ashour, A. F. and Lee, E.-T. (2008). "Properties of cementless mortars activated by sodium silicate." Construction and Building Materials **22**(9): 1981-1989.

Yao, X., Zhang, Z., Zhu, H. and Chen, Y. (2009). "Geopolymerization process of alkali–metakaolinite characterized by isothermal calorimetry." Thermochimica Acta **493**(1): 49-54.

Yap, S. P., Bu, C. H., Alengaram, U. J., Mo, K. H. and Jumaat, M. Z. (2014). "Flexural toughness characteristics of steel–polypropylene hybrid fibre-reinforced oil palm shell concrete." Materials and Design **57**: 652-659.

Yi, C. and Ostertag, C. ((2001)). "Strengthening and toughening mechanisms in microfiber reinforced cementitious composites." Journal of materials science **36**(6): 1513-1522.

Yip, C. K., Lukey, G. and Van Deventer, J. (2005). "The coexistence of geopolymeric gel and calcium silicate hydrate at the early stage of alkaline activation." Cement and Concrete Research **35**(9): 1688-1697.

Yip, C. K., Lukey, G. C., Provis, J. L. and van Deventer, J. S. (2008). "Effect of calcium silicate sources on geopolymerisation." Cement and Concrete Research **38**(4): 554-564.

Yoo, D.-Y., Shin, H.-O., Yang, J.-M. and Yoon, Y.-S. ((2014)). "Material and bond properties of ultra high performance fiber reinforced concrete with micro steel fibers." Composites Part B: Engineering **58**(0): 122-133.

Yusuf, M. O., Johari, M. A. M., Ahmad, Z. A. and Maslehuddin, M. (2014). "Effects of addition of Al(OH)3 on the strength of alkaline activated ground blast furnace slag-ultrafine palm oil fuel ash (AAGU) based binder." Construction and Building Materials **50**(0): 361-367.

Yusuf, M. O., Megat Johari, M. A., Ahmad, Z. A. and Maslehuddin, M. ((2014)). "Effects of H2O/Na2O molar ratio on the strength of alkaline activated ground blast furnace slag-ultrafine palm oil fuel ash based concrete." Materials & Design **56**(0): 158-164.

Yusuf, M. O., Megat Johari, M. A., Ahmad, Z. A. and Maslehuddin, M. ((2014)). "Strength and microstructure of alkali-activated binary blended binder containing palm oil fuel ash and ground blast-furnace slag." Construction and Building Materials **52**(0): 504-510.

Zhu, Y. and Xu, S. "Fracture properties of cement paste and mortar: an experimental investigation."

LIST OF PUBLICATIONS AND PAPERS PRESENTED

Journal Papers

1. Sharmin, A., Alengaram, U. J., Mohd Zamin Jumaat, S. M., & Bashar, I. Engineering properties of lightweight geopolymer concrete with oil palm shell and palm oil clinker. (Published).

2. Kabir, S. M., Alengaram, U. J., Jumaat, M. Z., Sharmin, A., & Islam, A. (2015). Influence of Molarity and Chemical Composition on the Development of Compressive Strength in POFA Based Geopolymer Mortar. Advances in Materials Science and Engineering, 2015. (Published).

3. Sharmin, A., Alengaram, U. J., Mohd Zamin Jumaat, S. M., & Bashar, I. Roles of oxide compositions on the performance of ternary blended geopolymer mortars. Construction & Building Materials. Ref. No.: CONBUILDMAT-D-15-02469 (Under review).

Conference Papers

1. Sharmin, A., Alengaram, U. J., Mohd Zamin Jumaat, S. M., (2015, 16th June). Fine and coarse aggregates from local wastes for Geopolymer Concrete. Paper has been presented at the International Conference on Engineering Tachnology and Management (ICETM) held in Kuala Lumpur, Malaysia.

2. Kabir, S. M., Alengaram, U. J., Jumaat, M. Z., Sharmin, A. (2015, 16th June). Fine and coarse aggregates from local wastes for Geopolymer Concrete. Paper has been presented at the International Conference on Engineering Tachnology and Management (ICETM) held in Kuala Lumpur, Malaysia.